AUTOHYDROLYSIS OF *MISCANTHUS X GIGANTEUS* FOR THE PRODUCTION OF XYLOOLIGOSACCHARIDES

BY

MING-HSU CHEN

DISSERTATION

Submitted in partial fulfillment of the requirements
for the degree of Doctor of Philosophy in Agricultural and Biological Engineering
in the Graduate College of the
University of Illinois at Urbana-Champaign, 2015

Urbana, Illinois

Doctoral Committee:

Professor Vijay Singh, Chair
Associate Professor Kent D. Rausch
Professor Kelly S. Swanson
Professor Emeritus M. E. Tumbleson
Biochemical Engineer Bruce S. Dien, NCAUR, ARS, USDA
Researcher Esha Khullar, Dow AgroSciences

Abstract

Miscanthus x giganteus (MxG) is considered a potential bioenergy crop due to its high yield and ecological properties. Xylooligosaccharides (XOS) are sugar oligomers made of xylose units. Due to their prebiotic functionality and other health promoting effects, XOS can be a value added coproduct for the cellulosic ethanol industry. There is lack of information on the production of XOS in conjunction with cellulosic ethanol processes, especially with MxG. The objective of this study was to investigate the production, purification, characterization and biological activity of XOS from MxG.

To determine the optimal condition for producing XOS from MxG, autohydrolysis was performed in a steel pipe reactor submerged in a fluidized sand bath. The water/solid ratio was set at 9:1. Temperatures and times were tested from 140°C to 220°C and 0 to 60 min. The XOS could be produced efficiently at 160°C, 60 min or 180°C, 20 min or 200°C, 5 min. Conversions of 13.5% (w/w) initial biomass and 69.2% (w/w) initial xylan into XOS were obtained. Compositions of XOS from three reaction conditions were similar.

Soluble XOS were recovered using activated carbon adsorption coupled with ethanol/water elution. The highest recovery of 47.9% (w/w) XOS was recovered by using 10% activated carbon (w/v) and eluted sequentially with 5, 30, 50, 70 and 95% ethanol/water solution. Most XOS were eluted at 30 and 50% ethanol/water solution. Further tests were conducted using gel permeation chromatography (GPC) measuring the molecular weight (MW) distribution in each XOS fraction. Higher ethanol solution recovered higher DP oligomers. Recoveries of 91.8% xylobiose, 86.9% xylotriose, 66.3% xylotetraose, 56.2% xylopentaose and 48.9% xylohexaose from ethanol elution were observed.

To separate DP2 to DP6 oligomers into individual fractions, crude XOS hydrolyzate was fractionated by centrifugal partition chromatography (CPC) using a butanol:methanol:water (4:1:4) solvent system. CPC fractions were consolidated and five fractions rich in DP2 to DP6 were collected with recoveries of 90.2% DP2, 64.5% DP3, 71.2% DP4, 61.9% DP5 and 68.9% DP6. Purities of DP2 to DP6 fractions were 61.9, 63.2, 44.5, 31.5, and 51.3%, respectively. DP2

and DP3 fractions were analyzed by ESI-MS; pentobiose and pentotriose were verified as the primary components.

The ethanol eluted XOS fractions were combined and further purified. With a combination of different ion exchange resins, most of the impurities and colorants were removed. The end product, MxG XOS, had 76.6% xylose oligomers, 1.5% arabinose oligomers, 4.4% glucose oligomers and 6.9% bound acetyl groups. Total substituted oligosaccharides were 89.3% (w/w). The MxG XOS had 1.7% xylose (X1), 8.9% xylobiose (X2), 11.3% xylotriose (X3), 8.8% xylotetraoase (X4), 9.0% xylopentaose (X5) and 5.8% xylohexaose (X6).

Purified MxG XOS were cultured with health beneficial bacteria *Bifidobacterium adolescentis* and *Bifidobacterium catenulatum*. Both *Bifidobacteria* were able to utilize MxG XOS as a carbon source for proliferation while *B. adolescentis* grew faster than *B. catenulatum* with specific growth rates of 0.69 to 0.33 (h^{-1}). The substrate utilization was 84.1% by *B. adolescentis* and 76.9% by *B. catenulatum*. There are substrate preferences of xylobiose, xylotriose and xylotetraose.

Purified MxG XOS were cultured with human fecal microbiota to simulate digestion in the colon. A medium pH drop, from 7.1 to 5.0, was indicative of the utilization of MxG XOS. During 12 h of fermentation, 1 g MxG XOS was metabolized into 466 mg acetic acid, 75 mg propionic acid and 84 mg butyric acid. The short chain fatty acid produced from MxG XOS was the highest amount among three tested substrates. The qPCR was adopted to enumerate bacteria populations. With MxG XOS used as the substrate, the *Bifidobacteria* spp. and *Lactobacillus* spp. increased, in addition, there was no significant growth in *Clostridium perfringens* .

We explored the feasibility of producing XOS from MxG in combination with pretreatment, direct purification of XOS from crude hydrolyzate, separation mono DP out of complex XOS oligomers and the biological activities of MxG XOS. The xylose oligomers have application potential to be a coproduct for a cellulosic ethanol plant. The procedure developed in this research can apply to other bioenergy crops with modifications depending upon material property.

Acknowledgements

First and foremost, I wish to thank to my advisor Dr. Vijay Singh wholeheartedly. It is very lucky to have a PhD advisor who is patient, open minded and always encouraging students with positive thinking. In Dr. Singh's lab, it is like a step by step training to become a professional. Dr. Singh ever told me: Let's do it, even if it is not working, it is science. With this spirit, I can test, learn, improve and eventually present these results.

I would like to express my gratitude to Dr. Kent Rausch and Dr. Mike Tumbleson for their precious instructions. I will always remember those great trips we had and the concepts and attitude you taught me. It was very fortunate to have Dr. Bruce Dien, Dr. Kelly Swanson and Dr. Esha Khullar in my committee. I am very grateful for Dr. Dien's guidance to lead me through the area of cellulosic ethanol and oligosaccharide research. I would like to thank Dr. Kelly Swanson, who initiated the adventure of gut microbiota. Thanks to Dr. Khullar's kindly advice from my first day of PhD study. The frame of this thesis was based on Dr. Khullar's previous achievements in *Miscanthus*.

The research was kindly supported by National Center for Agricultural Utilization Research, Agricultural Research Service, USDA. I would like to thank Drs. Michael Cotta, Terence Whitehead, and Rhonda Zeltwanger for conducting the *Bifidobacteria* fermentations and total xylose quantification; Dr. Michael Bowman for the HPAEC-PAD analysis of oligomer DP and consumption; Patricia O'Brian for the GPC and HPLC analysis; Loren Iten for the scale up of autohydrolysis.

The oligomer separation would not have been possible without the help from Dr. Julie Carrier and Kalavathy Rajan. It was a great pleasure to visit the University of Arkansas at Fayetteville. Thank you for your hospitality and offering this previous chance.

I especially wish to thank Dr. George Fahey and Dr. Swanson's group from Department of Animal Sciences for the prebiotic test. Thanks to Laura Bauer for conducting anaerobic fermentation, medium pH monitoring and SCFA analysis and Dr. Alison Beloshapka for the anaerobic fermentation, qPCR and cell counting.

I am happy to be a member of our ABE family and thanks to Dr. K. C. Ting, Ronda Sullivan, Robin Fonner, Mary Schultze, Jennifer Black, Jana Lenz, Heather Crump, Tracy Wikoff for your guidance and assistance since I stepped in this department. It is an honor to work with many brilliant fellows in the Food and Bioprocess Engineering Division. Thanks to Wei Liu, Li Xu, Dr. Haibo Huang, Dr. Ravi Challa, Divya Ramchandran, Sun Min Kim, Pavel Somavat, Song Li, Gurshagan Kandhola, Zhaoqin Wang, Bruno Guagliano and Bruce Zhang for their helps and excellent teamwork. Thanks to Dr. Zewei Miao and Timothy Mies from Energy Bioscience Institution for the *Miscanthus* samples. I am also grateful to Brian Jacobson from IBRL for nitrogen analysis and Parr reactor operation.

Finally, I would like to thank my parents and sister for their encouragement and support through my study. Thanks to my master thesis advisor Dr. Wen-Hsiung Liu and all laboratory colleagues from National Taiwan University. With your exact training during my master study that I could stand on a solid base and start to explore the engineering disciplines in UIUC. I would like to thank my friends Dr. Shih-Fang Chen, Yun Yin, Susan, Jeannie, Po-Liang Chen, Sabrina Tseng, Zoey Ho for your invaluable friendships. A PhD dissertation is made possible by many people's efforts, I wish to thank everyone who have helped and contributed to this work. I am somehow sure the printed dissertation may stay on the bookshelves for a long time, but with all these enjoyable interactions, my PhD days and memories became colorful. Thank you.

Table of Contents

Chapter 1. Introduction

Production of ethanol from cellulosic material promises to expand the supply of renewable transportation fuel in the near future (Balat and Balat, 2009). Benefits from using cellulosic material are based on its abundance, diversity and small carbon footprint (Hill, 2007). However, commercialization has been slower than anticipated (Brown and Brown, 2013).

A scarcity of coproducts is a commercial barrier to producing cellulosic ethanol. Kaylen (2000) reported a facility solely producing cellulosic ethanol will be unprofitable. In other technoeconomic studies regarding cellulosic ethanol investigation (Huang et al., 2009; Kazi et al., 2010; Bals et al., 2011; Humbird et al., 2011), they found minimum ethanol selling prices (MESP) were estimated to be $1.50 to $4.00/gal. This range overlaps with the current ethanol price $1.70/gal (Dec, 2014). Potential candidates for the coproduct production include the hemicelluloses and lignin fractions, which represent the majority of plant material aside from cellulose. Presently, related studies on producing coproducts from cellulosic ethanol plants are limited.

The focus of this study is xylooligosaccharides (XOS) that are short, soluble carbohydrates with xylose backbones and possible side groups of sugar monomers or organic acids. They can be produced by partial hydrolysis of hemicellulose (Vázquez et al., 2000). There is growing interest in production of XOS based on their beneficial health effects including prebiotic effects in gastroenteritis, functional properties as a soluble fiber and ability to lower cholesterol blood levels (Rastall et al, 2002). They can be used as food ingredients, symbiotic food, pharmaceuticals or fertilizer (Moure et al., 2006). The current market price for XOS is relatively high at $22 to 50/kg, based on product purity (Otieno and Ahring, 2012).

The hydronium catalyzed process, autohydrolysis, involves treating biomass with hot water or steam (140 to 200°C) to partially hydrolyze and extract hemicellulose. At high temperatures, water acts as a weak acid and acetyl groups released from the hemicelluloses are a further source of acid. The hydronium ions catalyze cleavage of glycosidic bonds within the xylan resulting in the liberation of XOS into the liquid phase. Autohydrolysis avoids chemical use, is efficient in producing XOS and maintains its solubility for further processing.

Furthermore, the pretreated solid residue is enriched in cellulose, and can be processed to ethanol. This creates an opportunity to combine both products (XOS and ethanol) in the same procedure.

Miscanthus x giganteus (MxG) is a warm season perennial grass that has gained attention as a bioenergy crop; it is a leading candidate because it produces high biomass yields and has low input requirements (Lewandowski et al., 2000). MxG grows rapidly, reaches up to 4 m in height and contains greater than 50% structural carbohydrates (Eitzinger and Kossler, 2002). Recently, MxG has been tested in central Illinois and has been reported to attain an average yield of 36 MT/ha/year (Khanna et al., 2008). MxG was used as raw material in this study.

For developing XOS into a coproduct from cellulosic ethanol plants, we started the research focusing on XOS production, characterization, purification and biological activity. To produce XOS from MxG, the reaction condition of autohydrolysis needed to be optimized because XOS are intermediate products. An anticipated reaction condition should provide higher extraction of xylan, lower formation of free monosaccharides and inhibitors. The partial degradation of the xylan resulting in XOS fall into a range of oligomers with chain lengths of 2 to 10. Only a small number of investigations have characterized the distribution of degree of polymerization (DP), even though the DP played an important role in the physical, chemical and biological properties of XOS. There were sugar oligomers, lignin degraded products, proteins and reaction derivatives coexisted in pretreated liquid. Previously scientists used multiple steps of membrane filtration, solvent extraction, vacuum evaporation and ion exchange chromatography to obtain a 90% purity XOS. In this study, a carbon adsorption coupled with ethanol solution method was investigated to replace the energy intensive membrane filtration and problematic solvent extraction. With the combination of ion exchange chromatography in the purification process, an alternative procedure for XOS purification from biomass autohydrolyzate was expected. Furthermore, it was laborious to produce high purity xylose oligomers with mono DP. A centrifugal partition chromatography (CPC) was tested to fractionate the mono DP oligomers from biomass crude hydrolyzate.

The purified MxG XOS was evaluated for biological activity with *Bifidobacterium* spp. and human fecal microbiota *in vitro*. With XOS cultured with pure strain probiotics, the relation between bacterial growth and substrate consumption could be clarified. Oligomer consumption in each DP was monitored by HPAEC-PAD. Since the pure culture fermentation could not

represent the complex metabolism in the colon, MxG XOS were cultured with human fecal microbiota. The pH change and short chain fatty acid (SCFA) produced were measured and quantified. The quantitative polymerase chain reaction (qPCR) was used to enumerate the health beneficial bacteria: *Bifidobacterium* spp. and *Lactobacillus* spp. and potential pathogens: *Escherichia coli* and *Clostridium perfringens* during utilization of XOS.

The objective of this study was to investigate XOS production, characterization, purification, oligomer separation and biological activity from MxG. Specific objectives were to

1. Determine XOS production conditions using autohydrolysis. (Chapter 3)
2. Determine molecular weight and degree of polymerization of XOS. (Chapter 4)
3. Investigate XOS recovery by carbon adsorption and ethanol elution. (Chapter 5)
4. Evaluate XOS separation by centrifugal partition chromatography. (Chapter 6)
5. Investigate high purity MxG XOS refining. (Chapter 7)
6. Evaluate MxG XOS fermentation with *Bifidobacterium* spp. (Chapter 8)
7. Evaluate MxG XOS fermentation with human fecal microbiota. (Chapter 9)

Chapter 2. Literature review

2.1 Overview of cellulosic ethanol development

Ethanol has been used in automotive fuel for more than 100 years. In the late 19th century, engineers Henry Ford and Nicholas Otto designed their engines running with ethanol (Kovarik, 1998). As one of the oxygenated additives to petroleum gasoline, ethanol aids in the completion of octane burning in internal combustion engine and reduces the emission of carbon monoxide to the environment (Dias de Oliveira et al., 2005). Since tetraethyl lead (TEL) was phased out of gasoline market because of neurotoxicity and damage to catalytic converters, the interest in using ethanol as octane booster increased. Rapid growth of ethanol usage in gasoline started in 2002 when the methyl tert-butyl ether (MTBE) was restricted and banned in many states and cities (Solomon et al., 2007). MTBE as a replacement for TEL was blamed for contaminating ground water and soil, resulting in potential health risk from environment (Finneran and Lovley, 2001). The Energy Policy Act of 2005, which established the goal of using ethanol to replace MTBE as gasoline additives, further supported the growth of fuel ethanol production (Solomon et al., 2007). Today, more than 13 billion gallons of fuel ethanol is produced each year in US (Chum et al., 2013).

Fuel ethanol can be produced either from biological fermentation, the major process route, or chemical synthesis from ethylene (Subramani and Gangwal, 2008). There are different options for carbohydrate sources, depending upon climates and crops. In Brazil, where the tropical climate is optimum for planting sugarcane, direct conversion of cane sugar into ethanol became feasible. In 2012, 5.7 billion gallons of fuel ethanol was produced (Chum et al., 2013). On the contrary, in US, where the temperate climate is optimal for planting maize, corn starch became the major material for conversion. Today, 95% of fuel ethanol in US is produced from corn kernel and 5% from barley, beverage residue, cheese whey, milo, wheat or other starches (Solomon et al., 2007). Use of cane sugar or cereal starch for ethanol conversion overlap with food supply chain. This arouses social issues such as using food material for fuel production. Therefore, to shift fuel production out of food crop and fulfill yearly demand of 140 billion

gallons of gasoline in US, researchers are investigating using alternative carbohydrate sources and converting them into ethanol such as from cellulosic material (Carroll and Somerville, 2009).

Cellulosic material is the most abundant carbohydrate source on earth; the annual production potential is estimated to be 1×10^{10} MT worldwide (Sánchez and Cardona, 2008). Though the detailed composition varies from species to species, most cellulosic material is composed of cellulose, hemicellulose, lignin and other lesser components such as pectin and minerals. For decades, there has been an extensive research on converting cellulosic material into fuel ethanol. Conversion generally includes three steps: (1) pretreatment of biomass to loosen recalcitrant bindings between cell wall polymers, (2) hydrolysis of carbohydrate polymers such as cellulose and hemicellulose into fermentable sugars and (3) microbial conversion of sugars into ethanol. The hydrolysis can be performed using enzyme cocktails or chemical methods (Sun and Cheng, 2002). For cellulosic ethanol fermentation, several microorganisms such as *Saccharomyces* sp. (Gupta et al., 2009), *Pichia* sp. (Gupta et al., 2009), *Zymomonas* sp. (Vasan et al., 2011) or *Escherichia coli* (Lau et al., 2010) can be used. Genetically modified microbial strains are able to utilize five carbon sugars and are more tolerant to toxic chemicals from the process. According to joint DOE and USDA study, published by Oak Ridge National Laboratory, the United States would have the capacity of producing 1.3 billion dry tons of cellulosic material yearly by 2030 (Perlack et al., 2005). Estimating a fuel conversion yield of 90 gal of ethaol per ton of biomass, 1.3 billion tons of biomass can produce 117 billion gallons of ethanol, which is expected to become an important fuel supply source for US (Carroll and Somerville, 2009).

Although cellulosic ethanol is a promising technology and may be the solution to searching a clean energy source, recent progress on large scale production is behind schedule (Brown and Brown, 2013). According to Renewable Fuel Standard (RFS), cellulosic ethanol was targeted at 100 million gallons in 2010. The Environmental Protection Agency (EPA) lowered the goal to 5 million gallons. Cellulosic ethanol projects are at least three years behind schedule though several commercial scale plants are announcing to join the market in a short time. Wyman (2007) made several suggestions on the cellulosic ethanol project; he suggested only focusing on several research topics such as commercialization, risk analysis, cost reductions, overcoming recalcitrance of cellulosic structure, advancing biological processing and breeding better feedstock to overcome the obstacles in mass production of cellulosic ethanol.

2.2 Pretreatment of cellulosic material

Cellulosic ethanol is produced by converting component sugars into ethanol. Although plant cells can be categorized into 35 different functional types with different composition and structure (Cosgrove, 2005), all cells have a thick cell wall structure for support and protection (Chundawat et al., 2011). Plant cell walls are composed primarily of cellulose, hemicellulose and lignin. Among them, cellulose and hemicellulose which comprise 30 to 60% (Balat, 2011) and 15 to 35% (Girio et al., 2010), respectively, of plant biomass are hydrolyzed into fermentable sugars. Compositions of different cellulosic materials are shown in Table 2.1.

Table 2.1. Composition of some prospective energy crops (Brosse et al., 2009; Carroll and Somerville, 2009).

Source	Extractives	Lignin	Uronic Acids	Arabinan	Xylan	Mannan	Galactan	Cellulose
Sugarcane bagasse	3.8	23.1	2.2	2.1	22.1	0.4	0.5	39.0
Corn stover	5.6	18.6	3.0	2.4	21.6	0.4	0.9	37.7
Wheat straw	13.0	16.9	2.2	2.4	19.2	0.3	0.8	32.6
Monterey pine	2.7	25.9	2.5	1.6	5.9	10.7	2.4	41.7
Hybrid poplar	6.9	25.2	4.3	0.9	13.1	1.8	0.9	39.2
Eucalyptus	4.2	26.9	4.1	0.3	10.4	1.2	0.7	48.1
Switchgrass (alamo)	17.0	17.6	1.2	2.8	20.4	0.3	0.9	31.0
Switchgrass (cave-in-rock)	13.8	17.5	No data	3.0	20.9	0.3	1.0	33.1
Sweet sorghum	22.0	16.1	1.1	1.7	14.1	0.2	0.5	34.0
Miscanthus	No data	26.3	No data	2.5	29.7	0.1	0.5	33.9

Cellulose is a linear polysaccharide comprised of D-glucose subunits. Within the structure, glucose monomers are linked by β-1,4 glycosidic bonds and form D-anhydroglucopyranose units. Depending on the sources, the degree of polymerization (DP) can range from 100 to 10,000 (Somerville et al., 2004). Several linear cellulose chains are packed together into microfibrils (3 to 5 nm in diameter). The microfibrils further bundle together to form the cellulose fibers. The whole cellulose structure is stabilized and tightened by covalent bonds, hydrogen bonds and Van der Waals forces resulting from pyranose ring stacking and hydroxyl groups. Because of the strong fiber packing, some of the cellulose fibers form a crystalline morphology that contribute to low saccharification yields (Zhou et al., 2009). Recently, the research focus went further to explore the cellulose polymorph and enzymatic digestion at a molecular level (Chundawat et al., 2011).

Hemicellulose is a branched chain polysaccharide comprised of pentoses (D-xylose, L-arabinose), hexoses (D-mannose, D-glucose, D-galactose) and uronic acids (D-glucuronic acid, D-galacturonic acid) (Girio et al., 2010). Unlike cellulose, many types of glycosidic bonds and side chain modifications such as α-1,2; α-1,3; α-1,6 and β-1,2-6 appear in the structure (Table 2.2). Based on the backbone sugars, these complex heteropolysaccharides can be divided into four groups: (a) xylans (β-1,4 xylosyl backbone), (b) mannans (β-1,4 mannosyl or glucosyl-mannosyl backbone), (c) β-glucans (β-1,3-1,4-glucosyl backbone) and (d) xyloglucans (β-1,4-glucosyl backbone) (Chundawat et al., 2011). Xylan is the most abundant polymer in hemicellulose. The actual sugar composition and DP vary with plant species and tissue type (Table 2.3). Due to an amorphous and branched structure, hemicellulose is sensitive to thermal or chemical treatment (Saha, 2003). The xylan portion can be extracted by acid or alkaline solution (Girio et al., 2010). Glucuronoarabinoxylans and galactoglucomannans are two major hemicelluloses present in monocots and dicots (Chundawat et al., 2011). Hemicellulose is a polysaccharide waste in most cellulosic ethanol demonstration plants, which is worthy of further investigation for utilization and application (Girio et al., 2010).

Table 2.2. Main types of polysaccharides present in hemicellulose (Girio et al., 2010).

Polysaccharide type	Biological origin	Amount (%)	Units			DP
			Backbone	Side chains	Linkage	
Arabinogalactan	Softwoods	1 to 3; 35	β-D-Gal*p*	β-D-Gal*p*	β-(1→6)	100 to 600
				α-L-Ara*f*	α-(1→3)	
				β-L-Ara*p*	β-(1→3)	
Xyloglucan	Hardwoods, grasses	2 to 25	β-D-Glu*p*	β-D-Xyl*p*	β-(1→4)	
			β-D-Xyl*p*	β-D-Gal*p*	α-(1→3)	
				α-L-Ara*f*	β-(1→2)	
				α-L-Fuc*p*	α-(1→2)	
				Acetyl	α-(1→2)	
Galactoglucomannan	Softwoods	10 to 25	β-D-Man*p*	β-D-Galp	α-(1→6)	40 to 100
			β-D-Glc*p*	Acetyl		
Glucomannan	Softwoods and hardwoods	2 to 5	β-D-Man*p*			40 to 70
			β-D-Glu*p*			
Glucuronoxylan	Hardwoods	15 to 30	β-D-Xyl*p*	4-*o*-Me-α-D-Glc*p*A	α-(1→2)	100 to 200
				Acetyl		
Arabinoglucuronoxylan	Grasses and cereals, softwoods	5 to 10	β-D-Xyl*p*	4-*o*-Me-α-D-GlcpA*β*-$_L$-Ara*f*	α-(1→2)	50 to 185
					α-(1→3)	
Arabinoxylans	Cereals	0.15 to 30	β-D-Xyl*p*	α-$_L$-Ara*f*Feruloy	α-(1→2)	
					α-(1→3)	
Glucuronoarabinoxylans	Grasses and cereals	15 to 30	β-D-Xyl*p*	α-$_L$-Ara*f*	α-(1→2)	
				4-*o*-Me-α-D-Glc*p*A	α-(1→3)	
				Acetyl		
Homoxylans	Algae		β-D-Xyl*p*			

Table 2.3. Hemicellulose composition of various lignocellulosic materials (Girio et al., 2010).

Raw material	Xyl	Ara	Man	Gal	Rha	UA	AcG	References[d]
Softwoods								
Douglas fir	6.0	3.0	–	3.7	–	–	–	(1)
Pine	5.3–10.6	2.0–4.2	5.6–13.3	1.9–3.8	–	2.5–6.0	1.2–1.9	(2, 3)
Spruce	5.3–10.2	1.0–1.2	9.4–15.0	1.9–4.3	0.3	1.8–5.8	1.2–2.4	(2, 4–7)
Hardwoods								
Aspen	18–27.3	0.7–4.0	0.9–2.4	0.6–1.5	0.5	4.8–5.9	4.3	(1, 2, 4, 8)
Birch	18.5–24.9	0.3–0.5	1.8–3.2	0.7–1.3	0.6	3.6–6.3	3.7–3.9	(2, 4)
Black locust	16.7–18.4	0.4–0.5	1.1–2.2	0.8	–	4.7	2.7–3.8	(2, 9)
Eucalypt	14–19.1	0.6–1	1–2.0	1–1.9	0.3–1	2	3–3.6	(10–13)
Maple	18.1–19.4	0.8–1	1.3–3.3	1.0	–	4.9	3.6–3.9	(2, 9)
Oak	21.7	1.0	2.3	1.9	–	3	3.5	(14)
Poplar	17.7–21.2	0.9–1.4	3.3–3.5	1.1	–	2.3–3.7	0.5–3.9	(2, 15)
Sweet gum	19.9	0.5	0.4	0.3	–	2.6	2.3	(16)
Sycamore	18.5	0.7	1.0	–	–	–	3.6	(9)
Willow	11.7–17.0	2.1	1.8–3.3	1.6–2.3	–	–	–	(4, 17)
Agricultural and agro-industrial materials								
Almond shells	34.3	2.5	1.9	0.6	–	–	–	(18)
Barley straw	15	4.0	–	–	–	–	–	(19)
Brewery's spent grain	15	8	0	1	0	2	0.8	(12)
Cardoon	26.0	2.5	3.7	1.4	0.9	–	–	(20)
Corn cobs	28–35.3	3.2–5.0	–	1–1.2	1	3	1.9–3.8	(9, 13, 21, 22)
Corn fibre	21.6	11.4	–	4.4	–	–	–	(23)
Corn stalks	25.7	4.1	<3.0	<2.5	–	–	–	(24)
Corn stover	14.8–25.2	2–3.6	0.3–0.4	0.8–2.2	–	–	1.7–1.9	(9, 25, 26)
Olive stones	2.0–3.7	1.1–1.2	0.2–0.3	0.5–0.7	0.3–0.5	1.2–2.2	–	(27)
Rice husks	17.7	1.9	–	–	–	–	1.62	(28)
Rice straw	14.8–23	2.7–4.5	1.8	0.4	–	–	–	(23, 26)
Sugar cane bagasse	20.5–25.6	2.3–6.3	0.5–0.6	1.6	–	–	–	(29–31)
Wheat bran	16	9	0	1	0	2	0.4	(13)
Wheat straw	19.2–21.0	2.4–3.8	0–0.8	1.7–2.4	–	–	–	(8, 26)

[a] Non-glycosidic units.
[b] Expressed as g/100 g of dry material.
[c] The percentages of oses were, in some cases, calculated from the corresponding "polymers". Xyl, xylose; Ara, arabinose; Man, mannose; Gal, galactose; Rha, rhamnose; UA, uronic acids; AcG, acetyl groups.

Lignin is an amorphous heteropolymer made of aromatic units. The main function of lignin is to strengthen cell wall and defend against microbial attack. Three basic monolignols: hydroxyphenyls (H), guaicyls (G) and syringyls (S) comprise the lignin net structure. Percentages of H, G and S vary depending on species and cell types. Hardwood lignin is composed mainly of G and S. Softwood lignin is mainly G. Monocot lignin consists of almost equal amounts of G and S with more H compared with hardwood and softwood (Chundawat et al., 2011). Lignin synthesis starts with using a free radical reaction to connect two monolignols to form a dimer (Pandey and Kim, 2010). The β-*o*-4-aryl ether bond is the most frequent binding type in polymerization; nevertheless, other types of linkage are observed (Table 2.4). Lignin is insoluble in water and optically inactive. As shown in Table 2.5, there are many specific names for quantification of lignin with different wet chemistry methods (Tuomela et al., 2000).

Table 2.4. Proportion of major linkages in lignin (Panday and Kim, 2011).

Linkage type	Softwood (spruce) [%]	Hardwood (birch) [%]
β-*o*-4-Aryl ether	46	60
β-*o*-4-Ary ether	6 to 8	6 to 8
4-*o*-5-Diary ether	3.5 to 4	6.5
β-5-Phenylcoumaran	9 to12	6
5-5-Biphenyl	9.5 to11	4.5
β-1-(1,2-Diarypropane)	7	7
β-β-(Resinol)	2	3
Others	13	5

The major plant cell wall components, cellulose, hemicellulose and lignin are connected to form a polymer matrix structure. Hemicellulose in plant cell walls is thought to be a coating on cellulose fibers (Agbor et al., 2011). The unbranched hemicellulose forms hydrogen bonds with the surface of cellulose microfibrils. Hemicellulose side chain groups, such as uronic acids

and arabinose, form covalent bonds with hemicellulose or lignin. Lignin is described as the “glue” that connects cellulose fibers and hemicellulose to form a lignin carbohydrate complex (LCC). The polymer matrix forms a net structure with a pore size less than 10 nm (Chundawat et al., 2011). For the above reasons, the crystal structure of cellulose, form a physical barrier for enzyme access and are called “recalcitrance”. To have an efficient enzyme hydrolysis, 50% of hemicellulose should be removed from biomass; therefore, pretreatment is essential (Agbor et al., 2011).

Pretreatments are utilized to loosen the bindings among cellulose, hemicellulose and lignin, decrystallize the cellulose structure and increase pore size and surface area for enzymatic reaction. Based on methods, pretreatments can be categorized into biological, chemical, physical and physical chemical (Table 2.6).

Biological pretreatments use mircroorganims such as brown, white and soft rot fungi to degrade biomass (Alvira et al., 2010). Fungi secrete extracellular enzymes such as lignin peroxidases, polyphenol oxidases, maganesse dependent peroxidases and laccases to hydrolyze lignin. Many basidiomycetes strains such as *Phanerochaete chrysosporium*, *Phelebia radiate*, *Dichmitus squalens*, *Rigidosporus lignosus* and *Jungua separabilima* perform selective degradation of lignin (Agbor et al., 2011). The biological pretreatment is environmentally friendly, low cost, low energy and low chemical requirement. However, the whole degradation takes weeks to be effective and results in the following enzymatic reactions to be less comparable to other pretreatment methods which limit the utilization of biological pretreatments to industrial scale (Wyman et al., 2005).

In chemical pretreatments, acids, alkalis, organic solvents and ionic liquids are used to alter the structure and composition of cellulosic material. Among these methods, the use of acids and alkali is employed. Concentrated and diluted acid such as sulfuric acid or hydrochloric acid are used in acid pretreatments. Benefit of using concentrated acids is that they are effective in breaking down cell wall polymers, but the drawbacks are toxicity, corrosiveness and production of inhibitors such as furfural and hydroxymethylfurfural (HMF). Also reactors are required to be resistant to strong acids (Sun and Cheng, 2002). The dilute acid pretreatment is more attractive in industrial scale pretreatment. Pretreatment generally combines acid with thermal treatment on biomass. The acid conditions lead to the breaking down of hemicellulose into xylose oligomers.

Many cellulosic materials, such as switchgrass, corn stover, spruce, poplar and rice straw have been tested in dilute acid pretreatment. Bases such as sodium hydroxide (NaOH), potassium hydroxide (KOH), calcium hydroxide ($Ca(OH)_2$) and ammonia (NH_3) are used in alkaline pretreatment. Under alkaline conditions, the intermolecular ester bonds between hemicellulose and cellulose or lignin are saponified and result in the separation of hemicellulose and swelling of biomass. Some percentage of lignin also is removed during alkaline treatment. The ammonia which is a mild alkaline solvent has less severe effect on cellulosic material. Minimal sugar release or breakdown of polymers is detected during ammonia pretreatment but the structure of the biomass is opened.

One major treatment used in physical pretreatment is comminution. The process of chipping, shredding, grinding and milling reduces the particle size, increases the surface area and reduces the crystallinity of cellulose and DP. During processing, biomass could be chipped into 10 to 30 mm and the grinding and milling further reduce the particle size to 0.2 to 2 mm (Agbor et al., 2011). Khullar et al. (2013) demonstrated that with particle size reduced to less than 0.08 mm, enzymatic hydrolysis increased. Ball, disk and hammer mills are three possible choices for grinding. One major drawback of the comminution is energy consumption, dependent upon material property, during size reduction. Hendrick and Zeeman (2009) suggested that due to high energy consumption, comminution is unlikely to be an economically feasible option. However, Zhu et al. (2010) indicated the energy required for comminution performed after chemical pretreatment was reduced.

Several methods, such as steam explosion, autohydrolysis (hydronium catalyzed, liquid hot water) and wet oxidation can be classified into physical chemical pretreatment. Autohydrolysis is a term sometimes used for both steam explosion and liquid hot water pretreatment. The main difference between steam explosion and liquid hot water is that steam explosion includes a sudden release of pressure. For autohydrolysis, the process involves treating biomass with superheated steam (140 to 200°C) to partially hydrolyze and extract hemicellulose. The released acetyl groups from hemicellulose acts as weak acid and forms hydronium ions. The hydronium ions catalyze cleavage of glycosidic bonds within the xylan and result in the release of XOS into the liquid phase.

Table 2.5. Commonly utilized methods for analyzing, isolating and synthesizing lignin (Tuomela et al., 2000).

Name	Principle of the method	Advantages	Disadvantages
Quantitative measurement of lignin			
Klason lignin Acid-insoluble lignin	Residue after treatment of sample with 72% sulphuric acid	Suitable for a wide range of samples	Structure different from that of lignin
Acetyl bromide method	Lignin is dissolved in acetyl bromide-acetic acid, the amount of lignin measured from the absorbance at 280 nm	Rapid, simple, adaptable for small amounts of sample, minimal chemical modification of sample	Solubility of bleached pulps can be incomplete, oxidation during bleaching of the pulp can change the spectral absorption characteristics of the lignin
Kappa number	The amount of oxidant (potassium permanganate) consumed by sample corresponds to the amount of residual lignin	Rapid, simple	Used mainly in quality control in commercial pulping
Isolation of lignin			
Milled wood lignin (MWL = Björkman lignin)	Ultramilling of wood and extraction with neutral solvents followed by precipitation in water and ethyl ether	Best representation of native lignin, macromolecular	Low yield, preparation time-consuming and cumbersome, some contaminating sugars
Cellulase enzyme lignin (CEL)	Cellulase enzyme treatment	Good representation of native lignin, macromolecular	Low yield, contains protein impurities
Kraft lignin	Cooking in the presence of NaOH and Na_2SO_4	Easy availability	Structure far from native lignin, not entirely macromolecular, contaminating sugars
Brauns' lignin	Extraction with ethanol	Easier preparation compared to MWL	Low molecular weight
Synthetic lignin			
Dehydrogenation polymer (DHP)	Synthesized from its precursors, usually from coniferyl alcohol	Good representation of native lignin, macromolecular	Laborious synthesis

Table 2.6. Summary of advantages and disadvantages with different methods for pretreating lignocellulosic biomass (Alvira et al., 2010).

Pretreatment method	Advantages	Disadvantages
Biological	– Degrades lignin and hemicellulose – Low energy consumption	– Low rate of hydrolysis
Milling	– Reduces cellulose crystallinity	– High power and energy consumption
Steam explosion	– Causes lignin transformation and hemicellulose solubilization – Cost-effective – Higher yield of glucose and hemicellulose in the two-step method	– Generation of toxic compounds – Partial hemicellulose degradation
AFEX	– Increases accessible surface area – Low formation of inhibitors	– Not efficient for raw materials with high lignin content – High cost of large amount of ammonia
CO_2 explosion	– Increases accessible surface area – Cost-effective – Do not imply generation of toxic compounds	– Does not affect lignin and hemicelluloses – Very high pressure requirements
Wet oxidation	– Efficient removal of lignin – Low formation of inhibitors – Minimizes the energy demand (exothermic)	– High cost of oxygen and alkaline catalyst
Ozonolysis	– Reduces lignin content – Does not imply generation of toxic compounds	– High cost of large amount of ozone needed
Organosolv	– Causes lignin and hemicellulose hydrolysis	– High cost – Solvents need to be drained and recycled
Concentrated acid	– High glucose yield – Ambient temperatures	– High cost of acid and need to be recovered – Reactor corrosion problems – Formation of inhibitors
Diluted acid	– Less corrosion problems than concentrated acid – Less formation of inhibitors	– Generation of degradation products – Low sugar concentration in exit stream

Pretreatment of cellulosic material is essential for successful subsequent enzyme hydrolysis, but it is regarded as one of the most expensive steps in processing cellulosic material into ethanol. Methods like concentrated acids, wet oxidation, solvents and metal complexes are effective, but the overall cost is too high compared with glucose price (Hendricks and Zeeman, 2009). To make the pretreatment more economically feasible in the future, sugar loss should be minimized; solid loading needs to be increased and the associated equipment cost lowered. More detailed information on molecular level of pretreatment may contribute to improved efficiencies (Alvira et al., 2010).

2.3 *Miscanthus x giganteus* as a potential bioenergy crop

MxG, a perennial rhizomatous grass, is a leading candidate energy crop for fuel conversion (Somerville et al., 2010). Bred by crossing *M. sinesis* and *M. sacchariflorus*, MxG is a triploid hybrid and cannot reproduce in field. An efficient C4 photosynthetic pathway is adapted by MxG resulting in the ability to convert 1 to 2% of solar energy into biomass (Heaton et al., 2008). Compared to other crops, MxG grows fast and could grow up to 3.5 m tall (Lewandowski et al., 2000). The total biomass is 60% more than a well fertilized maize and can reach 30 MT/ha/year (Somerville et al., 2010). High carbohydrate contents are observed in MxG cell walls from biomass generated for biofuel and chemical productions (Brosse et al., 2012).

2.4 Xylooligosaccharide production

XOS are sugar oligomers with xylose backbones (Fig 2.1). Structures consist of xylose units connected by β-1,4 glycosidic bonds and decorated with α-1,2- or α-1,3- glycosidic bonds connecting other sugars or glucuronic acids. The hydroxyl group on C2 and C3 often are replaced by acetyl groups (Oteino and Ahring, 2012). The branching and substituted acids determine the solubility of XOS in water and the structure varies depending upon the soure of biomass and method used to extract the xylan. The term “oligosaccharide” generally refers to a DP of from 3 -10, but for XOS the definition is broadened to include from 2 - 20 (Moure et al., 2006).

XOS appear naturally at low concentration in most plants, honey and milk. They are nontoxic, noncarcinogenic and have a mild sweet taste. The sweetness of xylobiose is equal to 30% of sucrose. Because enzymes from human digestion system cannot hydrolyze β-1,4 glycosidic bonds, XOS are a natural, noncariogenic sweetener and can be utilized in antiobesity foods. Compared with other food oligosaccharides such as fructooligosaccharides, XOS are stable over a wide pH range (2.5 to 8.0) and when heated (up to 100°C). Owing to their technologic and health promoting benefits, XOS have been used in many food products (Vázquez et al., 2000).

Large scale production of XOS is industrially produced by partially hydrolyzing hemicellulose using either chemical enzyme or the hydronium catalyzed routes (Vázquez et al., 2000). XOS can be produced from almond shells, barley husk, bamboo, birchwood, corncobs, corn stover, rice straw, wood and many other resources (Table 2.7; Moure et al., 2006).With the chemical enzyme method, xylan is extracted with caustic chemicals (alkali, acid or oxidizing agent) followed by limited enzymatic hydrolysis of the xylan into XOS. The hydronium catalyzed process simulatneously extracts and partially hydrolyzes xylan. A disadvantage of the chemical enzyme method is that it removes the acetic and uronic acid side groups, thereby lowering solubility (Nabarlatz et al., 2005). Benefits of autohydrolysis include fewer chemical inputs and retaining side-groups that increase solubility of longer XOS chains. The pretreated solid residue, which is enriched for cellulose, can be subsequently used for ethanol production.

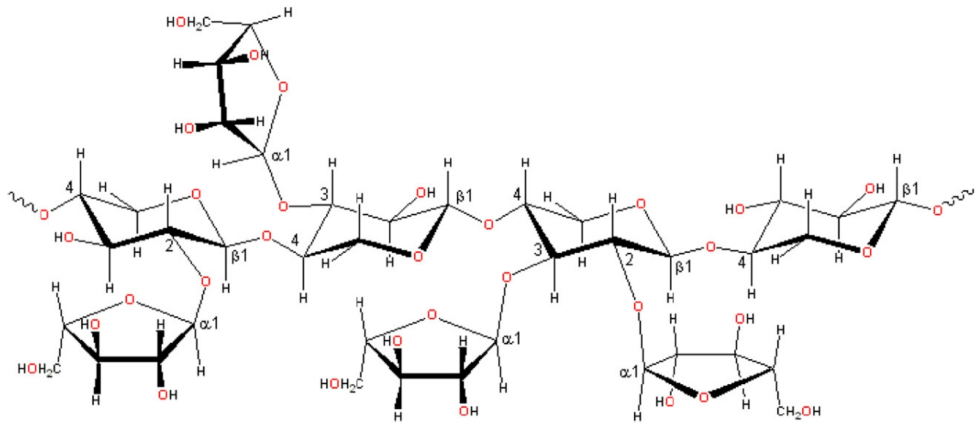

Fig. 2.1. Xylooligosaccharides structure showing different intermolecular bonds (Otieno and Ahring, 2012).

Table 2.7. Comparative studies of xylooligosaccharides synthesized in batch process from 100 g of xylan (Otieno and Ahring, 2012).

Biomass	Pretreatment process	% XOS yield
Panicum virgatum	0.1% H_2SO_4 + 145 °C (1 h)	84.15 ± 2.29
Miscanthus sinensis	0.1% H_2SO_4 + 145 °C (1 h)	64.95 ± 2.12
Calamagrostis acutiflora	0.1% H_2SO_4 + 145 °C (1 h)	87.88 ± 1.19
Bagasse	0.1% H_2SO_4 + 145 °C (1 h)	92.28 ± 3.25
Tobacco stalk (*Nicotiana* sp.)	2.5% H_2SO_4 + 40 °C (0.5 h)	13.00 ± 0.02
Corncobs	0.1% H_2SO_4 + 140 °C (0.5) + xylanase	67.70 ± 0.04
Tobacco stalk (*Nicotiana* sp.)	*A. niger* xylanase (40 °C, 24 h, pH5.5)	11.40 ± 0.02
Corncobs (CC)	Autohydrolysis (179 °C, 23 min)	59.40 ± 0.04
Almond shells (AS)	Autohydrolysis (179 °C, 23 min)	61.20 ± 0.02
Olive stones (OS)	Autohydrolysis (179 °C, 23 min)	53.50 ± 0.04
Wheat straw (WS)	Autohydrolysis (179 °C , 23 min)	41.20 ± 0.03
Barley straw (BS)	Autohydrolysis (179 °C, 23 min)	47.10 ± 0.05
Rice husks (RH)	Autohydrolysis (179 °C, 23 min)	42.80 ± 0.06
Corncobs	15% Ammonia solution	54.80 ± 0.05
Barley husks	Autohydrolysis (145–190 °C)	27.10 ± 0.04
Corncobs	Autohydrolysis (145–190 °C)	24.80 ± 0.05
Rice husks	Autohydrolysis (145–190 °C)	18.00 ± 0.06
Eucalyptus wood	Autohydrolysis (145–190 °C)	15.40 ± 0.03
Corncobs	Autohydrolysis (180–225 °C)	25.10 ± 0.03
Oat spelt xylan	Autohydrolysis (180 °C, 30 min)	50.17 ± 0.06
Oat spelt xylan	Autohydrolysis (200 °C, 10 min)	48.52 ± 0.03
Cornhusks	Rapidase Pomaliq enzyme (50 °C, 4 h, pH5.0)	8.21 ± 0.16
Corncobs	Rapidase Pomaliq enzyme (50 °C, 4 h, pH5.0)	9.90 ± 0.03
Oat spelt xylan	Rapidase Pomaliq enzyme (50 °C, 4 h, pH5.0)	18.27 ± 0.21
Oat spelt xylan	Endoxylanase (*T. fusca*, 60 °C, 24 h, pH7.0)	40.10 ± 0.25
Corncob	Endoxylanase (*T. fusca*, 60 °C, 24 h, pH7.0)	29.50 ± 0.16
Bagasse	Endoxylanase (*T. fusca*, 60 °C, 24 h, pH7.0)	23.70 ± 0.11
Wheat bran	Endoxylanase (*T. fusca*, 60 °C, 24 h, pH7.0)	7.60 ± 0.09
Peanut shell	Endoxylanase (*T. fusca*, 60 °C, 24 h, pH7.0)	10.10 ± 0.11
Corncob	Endoxylanase (*Trichoderma* sp.)(50 °C, 12 h, pH7.0)	46.50 ± 0.27
Brewers spent grain	Autohydrolysis (190 °C, 5 min)	61.00 ± 0.25
Wheat bran insoluble fiber	Xylanase (*B. subtilis*, 50 °C, 16 h, pH 5.0)	31.22 ± 0.21
Corncob	Endoxylanase (*A. oryzae*, 50 °C, 6 h, pH 5.0)	86.70 ± 3.51
Corncob	Endoxylanase (*A. oryzae*, 50 °C, 12 h, pH 5.0)	80.40 ± 2.93
Corncob	Alkali + endoxylanase (*A. oryzae*, 50 °C,14 h, pH 5.0)	81.20 ± 1.51
Corncob	Alkali + endoxylanase (*A. oryzae*, 50 °C,42 h, pH 5.0)	69.62 ± 3.34
Corncob	Autohydrolysis (Steam cooked)	77.20 ± 1.81
Corncob	Acid pretreatment	52.20 ± 3.24

Means in (% w/w of xylan) ± SD) per dry weight
SD – standard deviation, and ranges from 4 to 6 for each measurement.

2.5 Xylooligosaccharide purification

XOS are produced primarily for use in foods and therefore an emphasis is put on high purity mixtures. Purity of 75 to 95% is considered marketable. The XOS rich mixture obtained from chemical enzyme method is easier to purify because the xylan has been selectively recovered in the chemical step (Moure et al., 2006). In contrast, XOS extracted with autohydrolysis cotain a complex mixture of components, which substantially complicates purification (Vázquez et al., 2000).

Besides the XOS as the major component, the liquid phase of autohydrolysis contains a variety of undesirable components such as monosaccharides, acetic acid, water extractives, acid soluble lignin, inorganic material and degradation products from sugars and protein (Gullón et al., 2010). Multiple stages of separation are needed to eliminate these other components. Vacuum evaporation and freeze drying can be used prior to concentrate the crude solution and remove volatile compounds including acetic acid (Vázquez et al., 2005). Solvent extraction is used to remove nonsaccharide solubles (Vegas et al., 2005). The adsorption by surface active materials, such as activated charcoal, clay, silica, aluminum hydroxide and porous synthetic material, can be used to separate XOS from pretreated liquids based on affinity binding (Vázquez et al., 2000). Charcoal adsorption is favored by industry because of its higher loading capacity compared to other absorbants. Chromatography methods, including ion exchange and size exclusion chromatography, are used to acquire high purity fractions (Moure et al., 2006). Membrane separations, including ultrafiltration and nanofiltration, are alternatives to chromatography methods (Nabarlatz et al., 2007).

Besides purification of the whole XOS mixture, it is important to develop the technique to separate XOS molecules based on degree of polymerization (DP). XOS with different DP and side groups have different biological functions (Van Laere et al., 2000). Centrifugal partition chromatography (CPC) is a separation method developed from countercurrent chromatography. The special liquid, liquid system uses two immiscible solvents as stationary phase and mobile phase. Density and solubility are two main factors for separation (Marchal et al., 2003). Sample separations are achieved by rotation at a constant centrifugal force and difference in the partition between two solvents. Advantages of CPC are the ability to separate compounds in a wide molecular weight range and have high recovery during separation (Berthod et al., 1988). Lau et

al. (2011) used CPC for xylose oligomers separation from hydrolyzed birch wood xylan; the solvent system was selected as tetrahydrofuran:dimethyl sulfoxide:water at 6:1:3 ratio. The purity of xylobiose (DP2), xylotriose (DP3), xylotetraose (DP4) and xylopentaose (DP5) were 85, 55, 38 and 30%, respectively. Lau et al. (2013) further improved the solvent system used in CPC to butanol:methanol:water at 5:1:4 ratio. The purity of xylobiose to xylopentaose improved to 95, 90, 89 and 68%, respectively.

2.6 The human gut microbiota, probiotics and prebiotics

The gut microbiota represents a group of symbiotic microorganisms including bacteria, viruses and eukaryotes that are resided in the gastrointestinal (GI) tract. In humans, the gut microbiota is dominated by bacteria. Total bacteria in the human GI tract can range from 10^{13} to 10^{14} cells with more than 1,000 different species. The microbiota is a dynamic microbial ecosystem that starts to develop after birth and becomes relatively stable by five years of age. Each person has a unique microbiota profile as a "bacteria fingerprint", but there are around 57 species that are universal to all humans (Aureli et al., 2011). Lozupone et al. (2012) analyzed the gut microbiota of four adults (A, B, C and D) from the US, revealing a diversified bacterial phylum across healthy adults (Fig. 2.2). Primary bacterial genera in human gut microbiota are *Bacteroides* spp., *Bifidobacterium* spp., *Clostridium* spp., *Eubacterium* spp., *Fusobacterium* spp. and *Lactobacillus* spp. in higher cell numbers and *Enterococcus* spp., methanogens and sulfur reducing bacteria in lower numbers (Wallace et al., 2011).

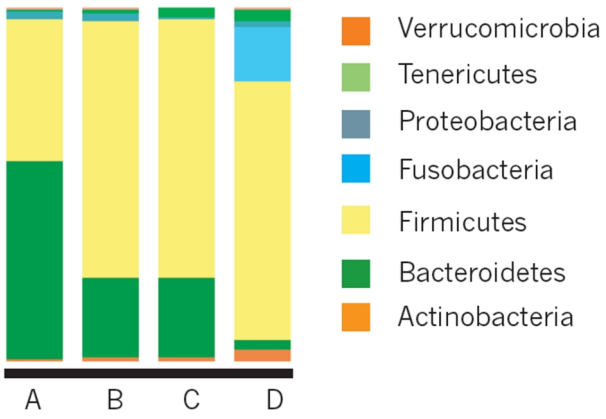

Fig. 2.2. Diversity of human microbiota (Lozupone et al., 2012).

The gut microbiota is related closely to human health. The microbiota attaches to mucosa and forms a mucosal barrier on the inner surface of the GI tract. The mucosal barrier is an important defense mechanism to separate food residues and pathogens from direct contact with lymphatic tissue. The imbalance of gut microbiota has been shown to be associated with many health disorders. Researchers found during allergies, the population of *Lactobacillus*. spp and *Bifidobacterium adolescentis* decreased; during type II diabetes, the population of *Firmicutes* and *Clostridia* declined while *Bacteroidetes* and *Betaproteobacteria* increased. Therefore, maintaining a balanced microbiota becomes an important issue for health (Clemente et al., 2012).

Some strains of *Clostridium* spp., sulfur reducing and amino acid metabolizing bacteria, are related to carcinogen and toxin production; some strains of *Escherichia coli* are associated with toxin production and diarrhea. Therefore, these bacteria are classified as potentially pathogens (Picard et al., 2005). On the other hand, *Bifidobacterium* spp. and *Lactobacillus* spp. are regarded as examples of health promoting bacteria. Both genera do not include pathogenic strains, and they can aid in lactose digestion, alleviate constipation and diarrhea, and reduce infection. These health promoting bacteria are named as "probiotics" which must be safe for food usage and the definition from World Health Organization (WHO) is "Live microorganisms which when administered in adequate amount confer a health benefits effect on host". Typical probiotic strains can be found in *Bifidobacterium* spp., *Lactobacillus* spp., *Bacillus coagulans* and *Saccharomyces boulardii* (Aureli et al., 2011).

Some proposed probiotic functions are shown in Fig. 2.3. Probiotics can inhibit pathogen growth by secreting bacteriocins and organic acids. Bacteriocins are protein based toxins that can inhibit the growth of gram positive bacteria such as *Streptococcus*, *Staphylococcus*, *Listeria* and *Mycobacteria*. Organic acids such as acetic, propionic and lactic acids reduce the pH in GI system and lead to an unfavorable low pH environment for gram negative pathogens such as *Salmonella enterica*. Probiotic competitively block the receptors on the surface of enterocytes to prevent pathogen adherence and enterotoxin binding. The released bacteria components from probiotics such as lipopolysaccharides (LPS) and peptidoglycan can be detected by intestinal cells and initiate a series of signal transduction pathways to modulate host immune responses (Fujiya and Kohgo, 2010).

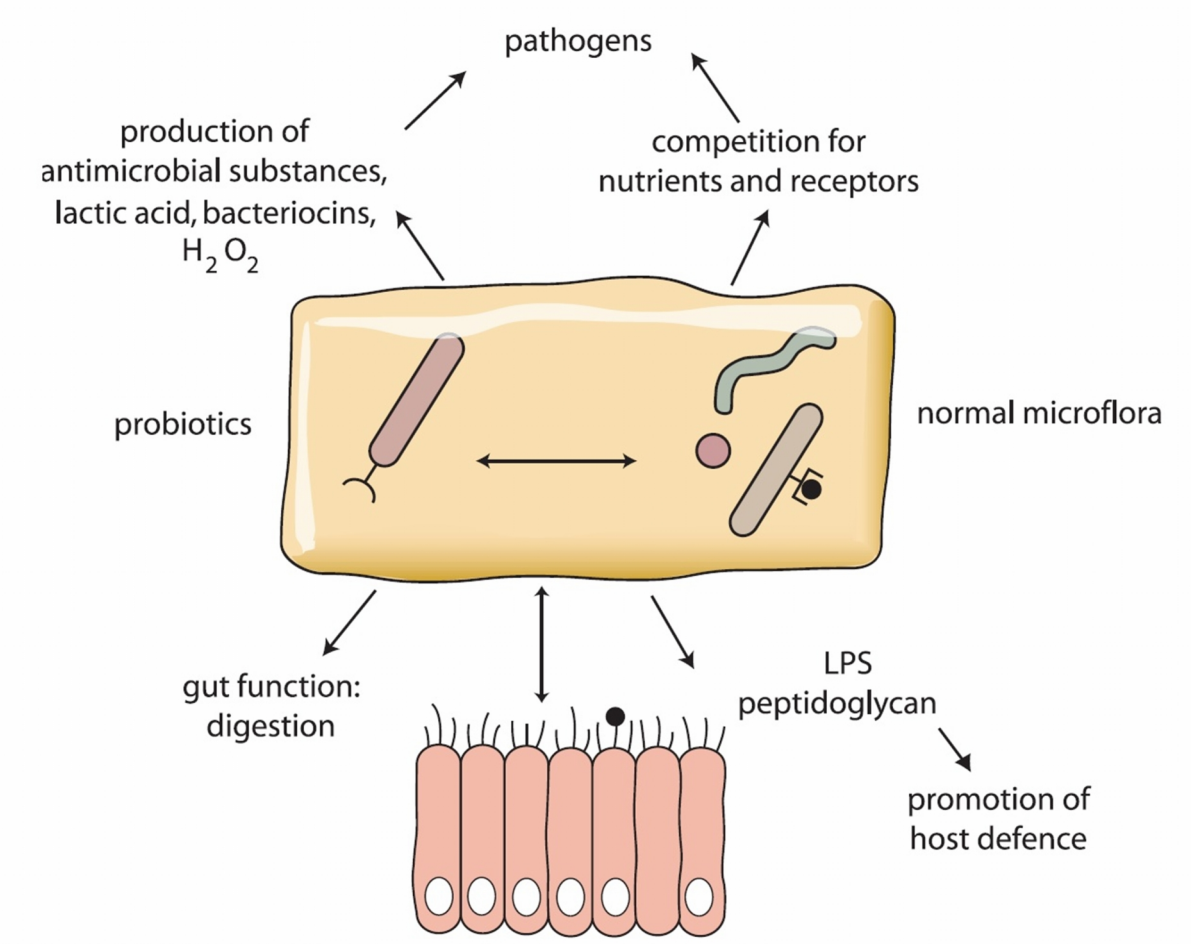

Fig 2.3. Mechanisms of probiotic function (Sullivan and Nord, 2005).

The gut microbiota is affected primarily by diet. The probiotics population in microbiota can be increased by feeding host with particular dietary supplement that is called “prebiotics” (Brüssow and Parkinson. 2014). A formal definition for prebiotics is “a nondigestible food ingredient that beneficially affects the host by selectively stimulating the growth and/or activity of one or a limited number of bacteria in the colon and thus improves the host’s health” (Gibson and Roberfroid, 1995). Most of the prebiotics are nondigestible carbohydrates; typical candidates are inulin, fructooligosaccharides, soya oligosaccharides, xylooligosaccharides and isomaltoligosaccharides (Table 2.8).

Table 2.8. Properties of prebiotic candidates (Macfarlane et al., 2006).

Name	Composition	Method of manufacture	DP
Inulin	β(2–1) fructans	Extraction from chicory root	11–65
Fructo-oligosaccharides	β(2–1) fructans	Tranfructosylation from sucrose, or hydrolysis of chicory inulin	2–10 3–5
Galacto-oligosaccharides	Oligo-galactose (85%), with some glucose and lactose	Produced from lactose by β-galactosidase	2–5
Soya-oligosaccharides	Mixture of raffinose (F-Gal-G) and stachyose (F-Gal-Gal-G)	Extracted from soya bean whey	3–4
Xylo-oligosaccharides	β(1–4)-linked xylose	Enzymic hydrolysis of xylan	2–4
Pyrodextrins	Mixture of glucose-containing oligosaccharides	Pyrolysis of potato or maize starch	Various
Isomalto-oligosaccharides	α(1–4) glucose and branched α(1–6) glucose	Transgalactosylation of maltose	2–8

DP, degree of polymerization; F, fructose; Gal, galactose; G, glucose.

Fermentation of nondigestible fibers in the colon results in production of short chain fatty acid (SCFA) which are organic acids with 1 to 6 carbons such as acetic, propionic and butyric. Daily production of SCFA in adult is 100 to 200 mM, and the majority are absorbed in the colon. SCFA are reported to participate in many physiological functions and exert different effects (Cook and Sellin, 1998). As shown in Fig. 2.4, acetic acid is the most abundant SCFA and is the substrate for muscle cells, hepatic *de novo* lipogenesis and cholesterol synthesis; propionic acid can enter the blood stream and regulate hepatic gluconeogenesis; butyric acid can be used directly by enterocytes as an energy source or promote intestinal gluconeogenesis by activating relative gene in enterocytes (Brüssow and Parkinson, 2014). All three SCFA can induce selective apoptosis in cancer cells, and butyric acid is reported with higher efficiency (Cook and Sellin, 1998).

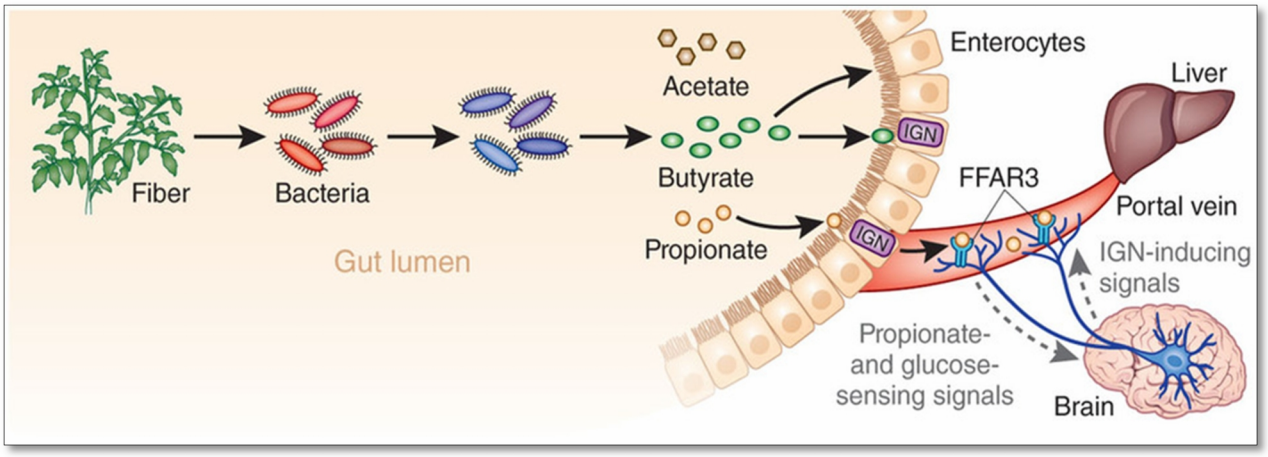

Fig. 2.4. SCFA produced by microbial fermentation improve glucose regulation (Brüssow and Parkinson, 2014).

2.7 Quantitative polymerase chain reaction for microbial analysis

Quantitative polymerase chain reaction (qPCR) is an efficient method to enumerate specific bacteria numbers in fecal samples. A DNA extraction step is required to prepare fecal DNA mixture. The typical PCR reaction amplifies template DNA sequence with two oligonucleotide primers (forward and reverse), dNTPs, DNA polymerase, magnesium ion and buffer. The quantity of DNA was doubled after each cycle. For qPCR, a fluorescence dye SYBR Green I is used to reflect the amount of DNA in solution. SYBR Green I is an asymmetric cyanine dye that emits green light (520 nm) when binds with DNA. The intensity of the fluorescence is proportional to DNA amount in the reaction mixture and recorded to form a response curve. The amplification cycles needed to reach a particular fluorescence signal level is called CT value. Different CT values reflect the difference in the initial amount of DNA templates (Kubista et al., 2006). Standard curves of CT vs. bacteria colony forming unit (CFU) can be prepared to quantify the number of specific bacteria in samples (Fig. 2.5).

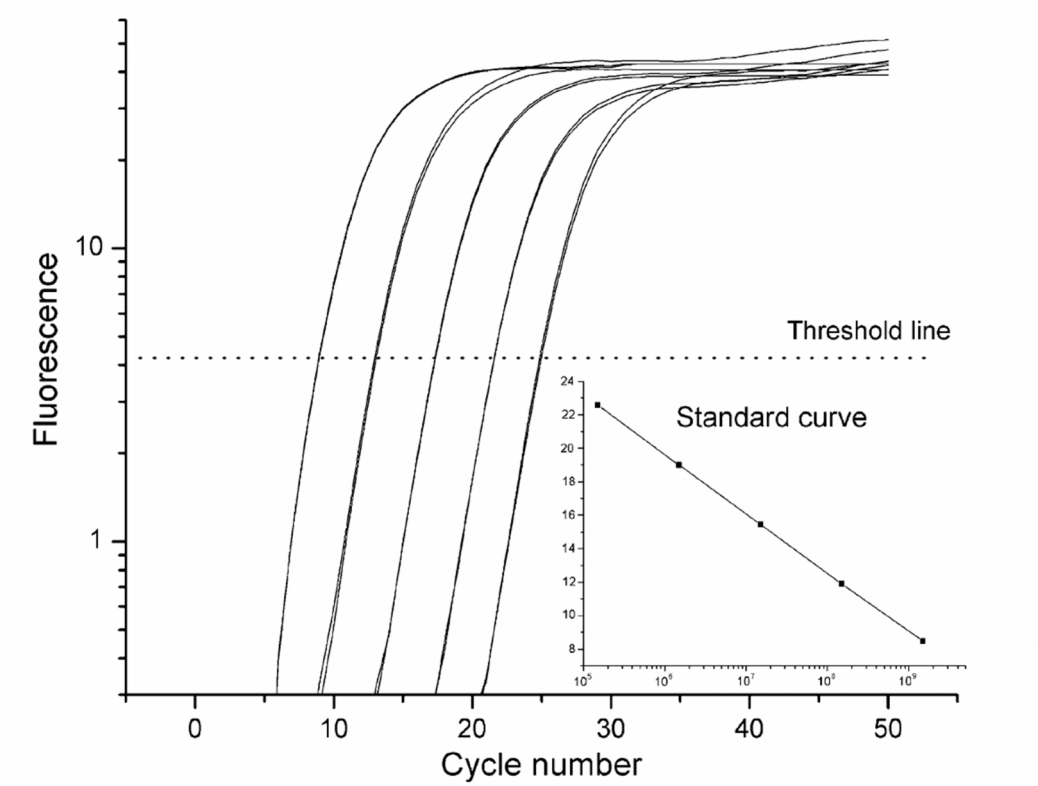

Fig. 2.5. qPCR response curves, CT values and standard curve (Kubista et al., 2006).

2.8 Biological activity of xylooligosaccharides

The interest of producing XOS from lignocellulosic material originates from their health benefits, including selective utilization by probiotic microorganisms, improvement in gastrointestinal function, production of SCFA, lower blood cholesterol concentration, reduction of ulcer lesions in stomach and prevention of colorectal cancer (Carvalho et al., 2013). From a nutritional point of view, XOS act as nondigestible oligosaccharides (NDO), which are not digested by gastrointestinal enzymes or low pH gastric fluids, but can be metabolized by microbiota in the large bowel. XOS can stimulate growth of *Bifidobacterium* spp. and *Lactobacillus* spp. which are considered beneficial. Potential pathogens, such as *Escherichia coli*, *Enterococci* spp., *Clostridium difficile* or *Clostridium perfringers*, are unable to use XOS. The utilization of XOS *in vivo* is a complex process because different microorganisms consume XOS at different metabolic stages; the end product from one microorganism may be the nutrient for other microorganisms (Moure et al., 2006). XOS with DP of 2 to 10 are able to be fermented *in*

vitro by *Bifidobacterium* spp. Linear and lower DP XOS have faster consumption rates (Kabel et al., 2002). For branched and larger DP XOS, digestion is slower but leads to higher butyric acid production. The difference in consumption rate can be improved by adaptation. Once the microorganism adapts to specific substrates, there is no difference in consumption between linear form, acetylated form, substituted with uronic acid or arabinose (Kabel et al., 2002). XOS utilization has two stages, the first stage leads to the formation of acetic and lactic acids. The formed acetic and lactic acids can be further utilized in second stage and results in the production of propionic and butyric acids. SCFA could be utilized by nearby cells and play an important role in regulating cell metabolism. SCFA can improve bowel function, mineral absorption, lipid metabolism and reduce colon cancer risk (Scheppach et al., 2001).

Food products containing health promoting ingredients such as prebiotics or probiotics can be classified as functional foods. Since 2000, the market has grown at a rate of 10% per year; it was estimated to reach US $155.41 billion after 2010 (Otieno and Ahring, 2012). XOS can be an important ingredient for functional foods. Mumtaz et al. (2008) claimed the addition of XOS, up to 3.5% (w/w), did not influence the taste or overall acceptability of product. A representative XOS product called Xylooligo™ is marketed by Suntory located in Japan. The Xylooligo™ is produced from corn cobs and composed mainly of xylobiose and xylotriose (Broekaert et al., 2011). From 1994 to 1996, Suntory increased their production of XOS from 70 to 300 ton. In 2006, Japan represented one half of the world market in XOS, which were added to multiple food products such as soya milk, soft drinks, yogurts, cakes, pastries, puddings, jam and sold as healthy foods. There were more than 100 products mixed with XOS from 60 companies (Vázquez et al., 2000).

Chapter 3. Autohydrolysis of *Miscanthus x giganteus* for the production of xylooligosaccharides*

3.1 Introduction

Producing XOS using autohydrolysis, five temperatures 140, 160, 180, 200 and 220°C, were tested from 0 to 60 min and sampled every 10 min. After 4% sulfuric acid hydrolysis, XOS were quantified by HPLC. To obtain a more detailed kinetics curve, more sampling points were selected near the maximum XOS time points at each temperature. The objectives were to locate times and temperatures for the maximum production of XOS and observe inhibitor concentrations and degraded products during the reaction.

3.2 Materials and Methods

3.2.1 Raw material

In 2011, MxG was harvested from the University of Illinois Energy farm. It was oven dried at 49°C, sliced and ground in a hammer mill (model MHM4, Glen Mills, Clifton, NJ) equipped with a 250 μm screen. The 8.2% (w/w) moisture ground MxG was stored at 4°C (NREL/TP-510-42621). All chemicals and laboratory reagents, unless stated otherwise, were of analytical quality and were supplied by Fisher Scientific (Springfield, NJ).

3.2.2 Reactor systems and autohydrolysis

Custom fabricated 25 mL tubular batch mini reactors were cut from 0.75 inch OD x 0.065 inch thick, 316 stainless steel tubing (SS-T12-S-065-20, Swagelok, Chicago Fluid System Technologies, Chicago, IL). Reactor lengths were 4.125 inch and ends were covered using 0.75 inch, 316 stainless steel Swagelok caps (SS-1210-C, Swagelok, Chicago Fluid System Technologies, Chicargo, IL). A thermocouple (39105K212, Penetration/Immersion Thermocouple Probe Mini Conn, McMaster-Carr, Robbinsville, NJ) was inserted into one of the

* Published in Bioresource Technology 155 (2014) 359-365.

reactors for *in situ* temperature measurements. A data logger (HH306/306A, Datalogger Thermometer, Omega, Stamford, CT) was connected to the thermocouple for recording temperature profiles. Fast heating of loaded reactors was achieved using a fluidizing sand bath (IFB-51 Industrial Fluidized Bath, Techne Inc., Burlington, NJ). Pretreatment reactions were quenched by immersing the reactors in room temperature water.

Autohydrolysis was performed at a water:solid ratio of 9:1 g/g and a reaction temperature of 140, 160, 180, 200 or 220°C. Liquids and solids were separated by centrifugation (2600 x *g*, 5 min). The solid residue pellet was washed three times, dried and used for compositional analysis (NREL). Aliquots of the liquids, the source of XOS, were filtered through 0.2 μm membranes (Syringe filter, 13 mm Nylon, Waters, Ann Arbor, MI) and analyzed for sugars and organic acid concentrations. A second aliquot of the liquid was subjected to a quantitative posthydrolysis with 4% H_2SO_4 at 121°C for 60 min (NREL-LAP-014), for end hydrolysis of the XOS. Increases in concentrations of monosaccharides and acetic acid following end hydrolysis were used to calculate XOS yield and composition.

3.2.3 Analytical methods

Liquid phases were analyzed for arabinose, galactose, glucose, xylose, acetic acid, furfural, hydroxymethylfurfural (HMF), levulinic acid and formic acid using high performance liquid chromatography (HPLC) coupled with a refractive index detector (Model 2414, Waters Corporation, Milford, MA). It was not possible to separate all of these chemicals with a single column, so each sample was analyzed using two different ion exclusion columns (Bio-Rad Aminex HPX-87H and HPX-87P, Biorad, Hercules, CA). The HPLC samples were eluted with 0.005 M H_2SO_4 at 50°C with a flow rate of 0.6 mL/min through the HPX-87H column and with B-pure purified water (Barnstead Thermolyne Corp., Dubuque, IA) at 85°C with a flow rate of 0.6 mL/min through the HPX-87P column.

Compositional analysis of raw and pretreated MxG was conducted by following "Determination of extractives in biomass (TP-510-42619; Sluiter et al., 2008)", "Determination of structural carbohydrates and lignin in biomass (TP-510-42618; Sluiter et al., 2010)" and "Determination of ash in biomass (NREL/TP-510-42622; Sluiter et al., 2008)" procedures

developed and published by NREL (website: http://www.nrel.gov/biomass/analytical_procedures.html, accessed June 29, 2013). Individual samples were wrapped in a filter bag (XT4, Ankom Technology, Macedon, NY) and extracted using distilled water and 95% ethanol in a Soxhlet extractor for 6 and 16 h, respectively. Weight loss after 49°C oven drying was determined as extractives. The dried extractive free samples were analyzed for carbohydrate content and acid soluble and insoluble lignin. Analyses were performed using two step acid hydrolysis methods. Samples were hydrolyzed in 72% w/w sulfuric acid at 30°C for 2 h and diluted into 4% sulfuric acid before heating in an autoclave (121°C) for 1 h. The autoclaved solutions were filtered through crucibles. One aliquot of filtrate was for HPLC analysis for sugar determination. The second aliquot of filtrate was for acid soluble lignin measurement using a spectrophotometer (Evolution array, Thermo Scientific, Waltham, MA) set at 240 nm. The crucibles with acid insoluble portion were dried at 105°C for 4 h to determine dry weights followed by ashing at 575°C for 4 h.

3.3 Results and Discussion

3.3.1 *Miscanthus x giganteus* composition

MxG used in this study had 35.9% glucan, 19.5% xylan, 1.1% acid soluble lignin, 18.5% acid insoluble lignin, 11.3% extractives, and 0.5% total nitrogen (Table 3.1); mannan and galactan were below detectable limits (Table 3.1). Compositional results corresponded to previous reports regarding MxG (Le Ngoc Huyen et al., 2010; Otieno and Ahring, 2012; Timilsena et al., 2013). Le Ngoc Huyen et al. (2010) demonstrated that MxG from early and late harvest may change the amount of cell wall fractions which were attributed to leaf loss. However, glucan content remained consistent.

Table 3.1. Compositions of MxG.

Component	Amount (%w/w, db)
Extractives	11.3 ± 1.1
Glucan[a]	35.9 ± 0.2
Xylan[a]	19.5 ± 0.5
Acid soluble lignin	1.1 ± *
Acid insoluble lignin	18.5 ± 0.3
Total nitrogen	0.5 ± *

Mean ± standard deviation from triplicates.
[a]Anhydrous monosaccharides.
*Standard deviation was less than 0.05.

3.3.2 Xylooligosaccharides (XOS) production by autohydrolysis

As a preliminary experiment, MxG was pretreated at five temperatures ranging from 140 to 220°C. XOS production data are depicted in Fig. 3.1. Neither 140 nor 220°C was effective for extracting XOS (Fig. 3.1). Therefore, 160, 180 and 200°C were used in the kinetic study (Fig. 3.1). Temperatures profiles of the heating curves during autohydrolysis are shown in Fig. 3.2.

Kinetic profiles for XOS and side product formation at 160, 180 and 200°C are shown in Figs. 3.3, 3.4 and 3.5, respectively. For 160°C, XOS increased with reaction time and reached the highest peak of 11.8% (w/w % of initial dry weight) at 60 min. Maximums of 1.4% xylose, 0.8% glucose, 0.3% arabinose and 1.2% acetic acid were produced during the process (Fig. 3.3; Table 3.2). Furfural was observed after 50 min and reached 0.5% at 60 min. Formic acid was observed after 40 min and neither HMF nor levulinic acid was detected (data not shown). After 70 min, 12.9% xylan remained in pretreated biomass (Fig. 3.3; Table 3.4). For 180°C, XOS increased with reaction time and reached the highest peak of 13.0% (w/w % of initial dry weight) at 20 min. Maximums of 3.0% xylose, 0.7% glucose, 0.7% arabinose and 1.8% acetic acid were produced during the process (Fig.3.4; Table 3.2). Furfural was observed after 15 min and reached 0.6% at 20 min. Formic acid was observed after 10 min and neither HMF nor levulinic acid was detected (data not shown). After 30 min, 6.8% xylan remained in pretreated biomass (Fig. 3.4; Table 3.4). For 200°C, the highest quantity of XOS (13.5% w/w % of initial dry weight) appeared at 5 min and started to reduce rapidly. Maximums of 3.8% xylose, 0.7% glucose, 0.5%

arabinose and 3.5% acetic acid were produced during the process (Fig. 3.5; Table 3.2). Furfural was observed after 5 min and increased to 5.6% at 30 min. Formic acid and HMF were observed after 5 to 10 min and each reached 0.6% at 30 min (data not shown). Levulinic acid was observed at 30 min of reaction at 0.1% (data not shown). Xylan was degraded much faster at 200°C. After 20 min, no residual xylan was detected in pretreated biomass (Fig. 3.5; Table 3.4).

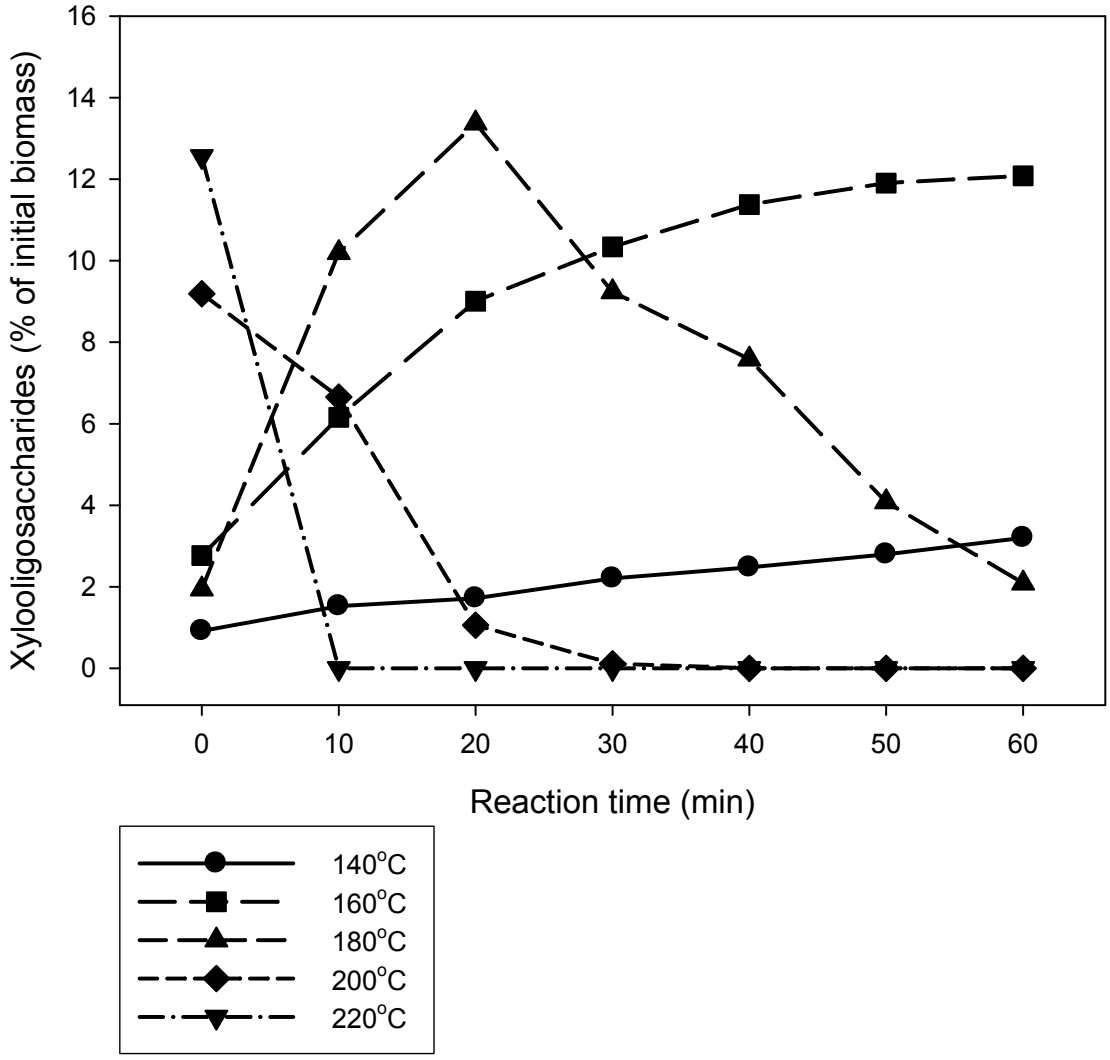

Fig. 3.1. Preliminary results for XOS production at 140, 160, 180, 200 and 220°C.

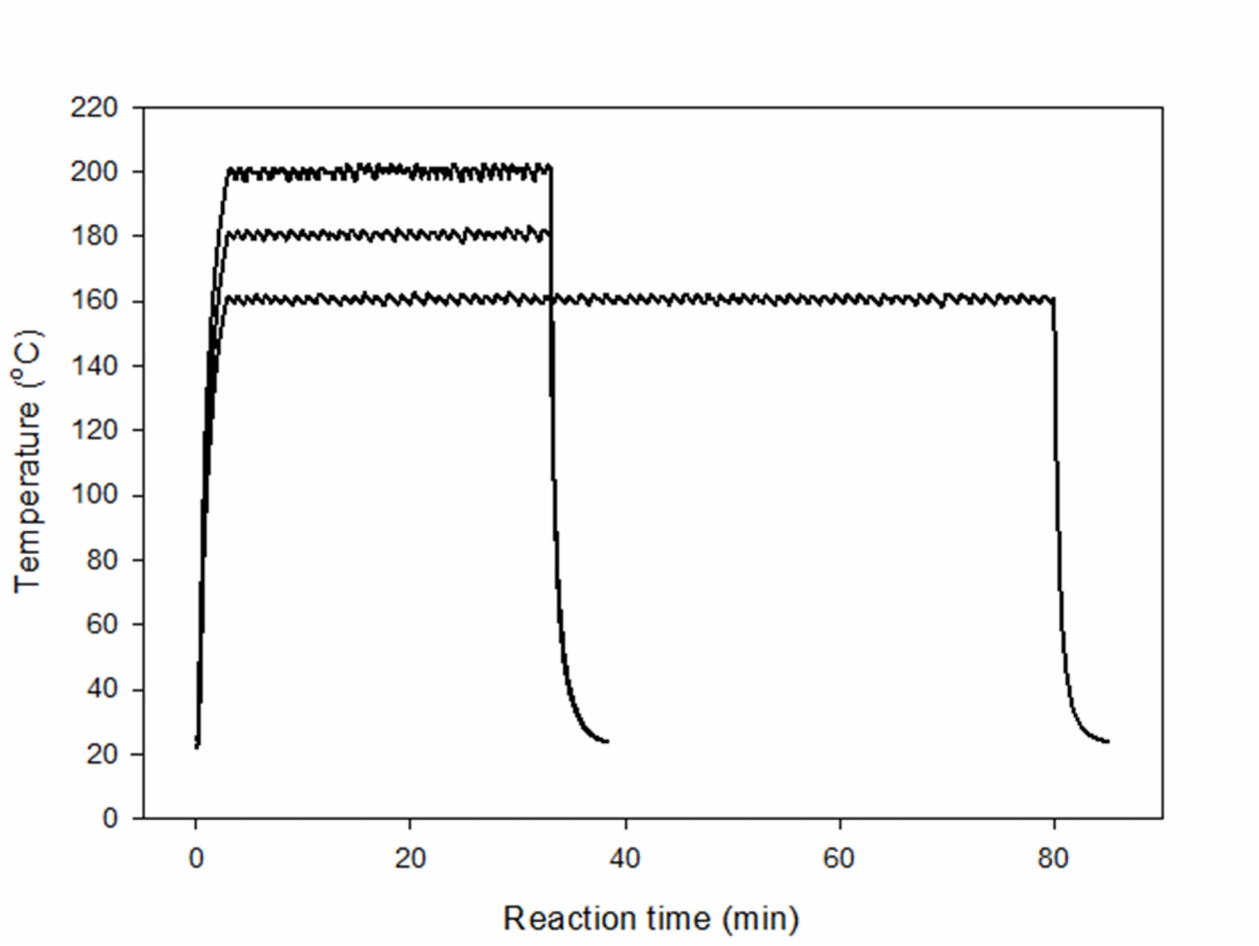

Fig. 3.2. Representative temperature profiles for autohydrolysis at 160, 180 and 200°C.

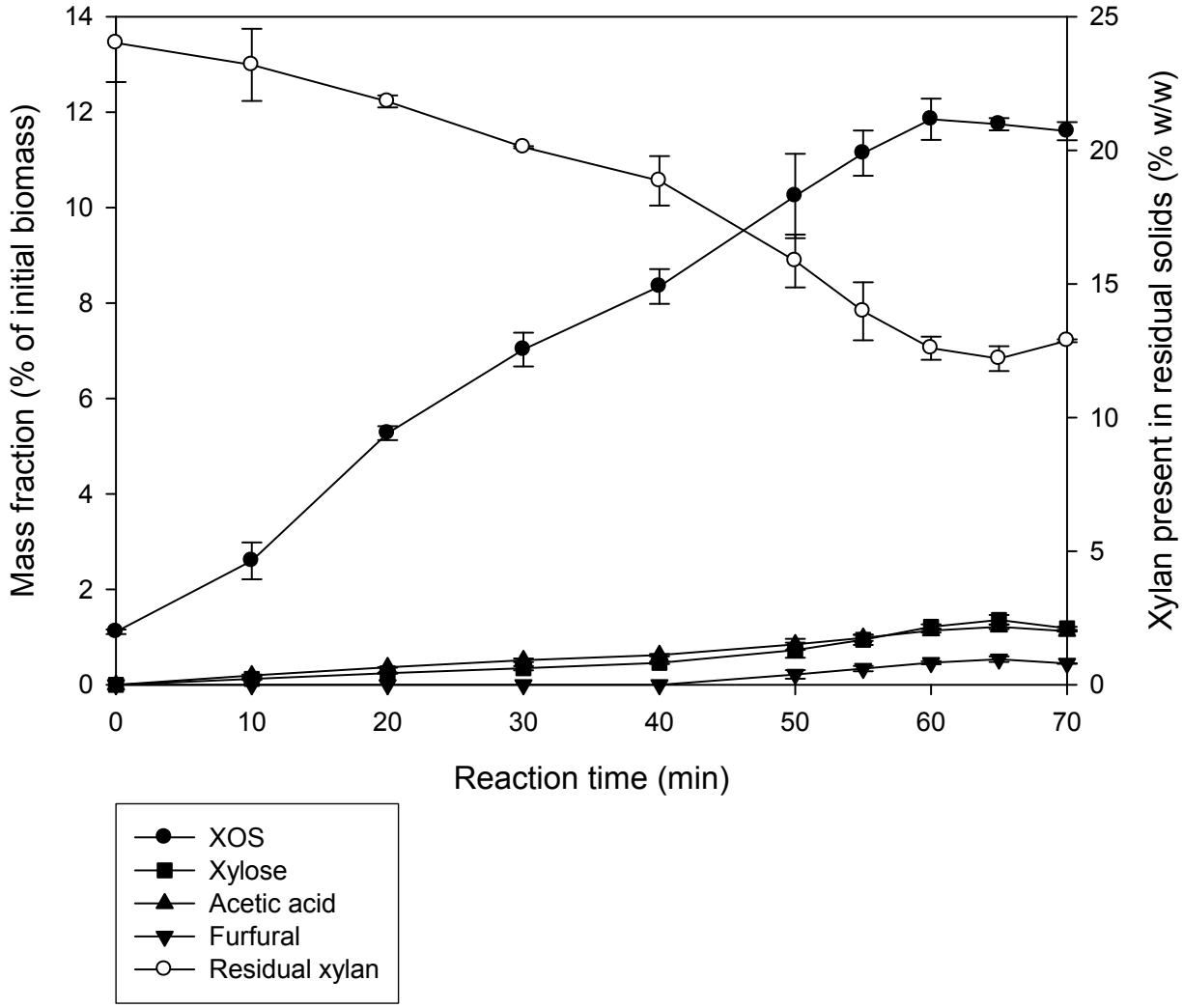

Fig. 3.3. Time course of MxG conversion into XOS, xylose, acetic acid, furfural and the residual xylan in pretreated biomass at 160°C.

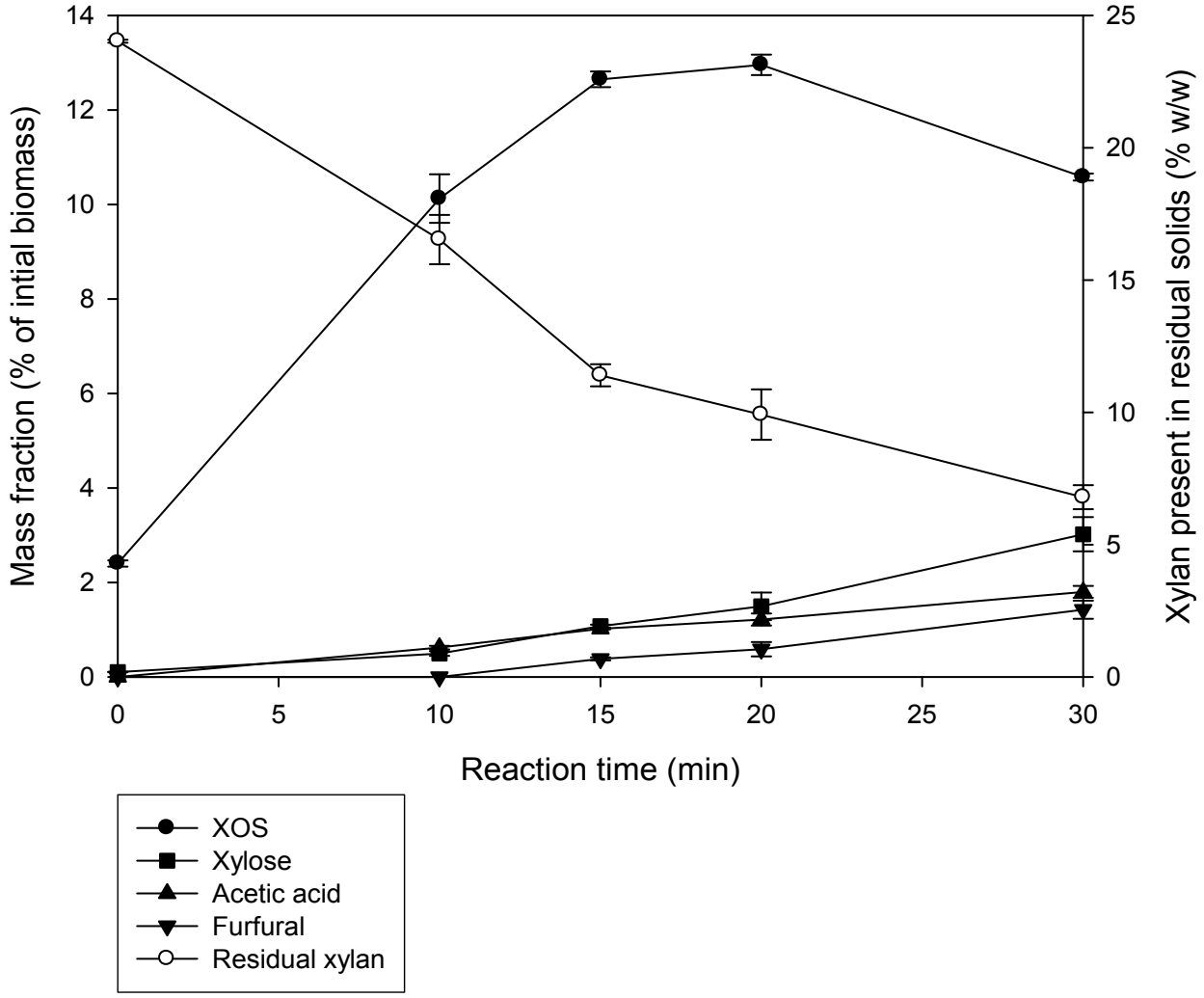

Fig. 3.4. Time course of MxG conversion into XOS, xylose, acetic acid, furfural and the residual xylan in pretreated biomass at 180°C.

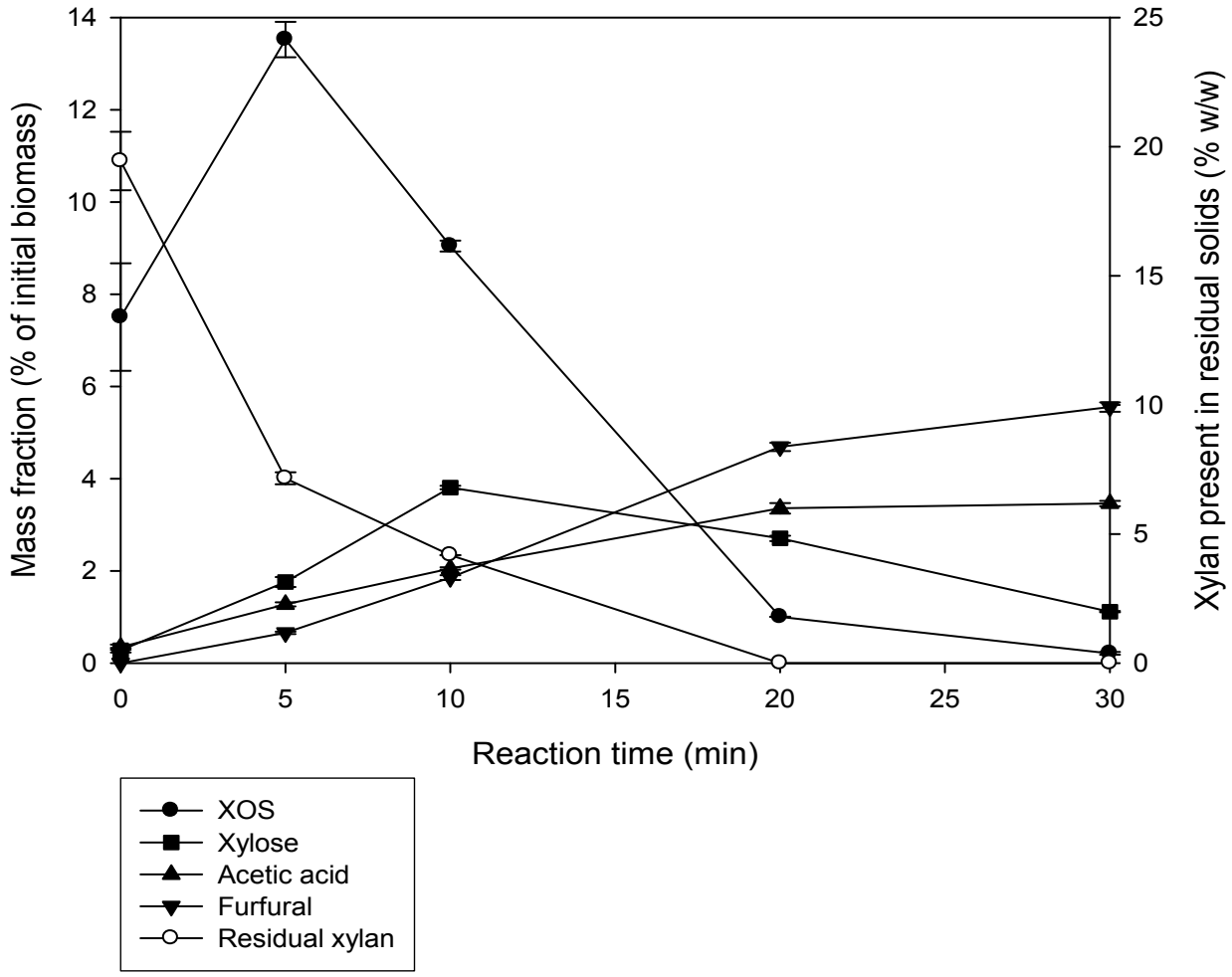

Fig. 3.5. Time course of MxG conversion into XOS, xylose, acetic acid, furfural and the residual xylan in pretreated biomass at 200°C.

Table 3.2. Composition of the liquid phase during autohydrolysis.

Condition (min)	XOS[a]	Xylose	Arabinose	Glucose	Acetic acid	Furfural
	(% of initial dry solid)					
160°C						
0	1.1 ± *	ND[b]	ND[b]	0.2 ± 0.1	ND[b]	ND[b]
10	2.6 ± 0.4	0.1 ± *	0.4 ± *	0.2 ± *	0.2 ± *	ND[b]
20	5.3 ± 0.1	0.2 ± *	0.6 ± *	0.2 ± *	0.4 ± *	ND[b]
30	7.0 ± 0.4	0.3 ± *	0.7 ± *	0.3 ± *	0.5 ± *	ND[b]
40	8.3 ± 0.4	0.5 ± *	0.7 ± *	0.5 ± 0.3	0.6 ± *	ND[b]
50	10.2 ± 0.9	0.7 ± 0.2	0.8 ± *	0.3 ± 0.1	0.8 ± 0.1	0.2 ± 0.1
55	11.1 ± 0.5	0.9 ± 0.1	0.8 ± *	0.3 ± *	1.0 ± 0.1	0.3 ± 0.1
60	11.8 ± 0.4	1.2 ± 0.1	0.8 ± *	0.3 ± *	1.1 ± *	0.5 ± *
65	11.7 ± 0.1	1.4 ± 0.1	0.7 ± *	0.3 ± *	1.2 ± 0.1	0.5 ± 0.1
70	11.6 ± 0.2	1.2 ± *	0.8 ± *	0.3 ± *	1.1 ± *	0.4 ± *
180°C						
0	2.4 ± 0.1	0.1 ± *	0.2 ± 0.1	0.2 ± *	ND[b]	ND[b]
10	10.1 ± 0.5	0.5 ± 0.1	0.7 ± *	0.7 ± *	0.6 ± *	ND[b]
15	12.6 ± 0.2	1.1 ± 0	0.7 ± *	0.7 ± *	1.0 ± *	0.4 ± *
20	13.0 ± 0.2	1.5 ± 0.3	0.6 ± *	0.6 ± *	1.2 ± 0.1	0.6 ± 0.2
30	10.6 ± 0.1	3.0 ± 0.4	0.4 ± 0.1	0.3 ± *	1.8 ± 0.1	1.4 ± 0.2
200°C						
0	7.5 ± 1.2	0.3 ± 0.1	0.5 ± *	0.6 ± *	0.3 ± 0.1	ND[b]
5	13.5 ± 0.4	1.8 ± 0.1	0.5 ± *	0.7 ± *	1.3 ± *	0.7 ± *
10	9.0 ± 0.1	3.8 ± *	0.4 ± *	0.3 ± *	2.1 ± *	1.9 ± 0.1
20	1.0 ± *	2.7 ± 0.1	0.3 ± *	0.3 ± *	3.4 ± 0.1	4.7 ± 0.1
30	0.2 ± *	1.1 ± *	0.1 ± *	0.3 ± *	3.5 ± 0.1	5.6 ± 0.1

Mean ± standard deviation from duplicates.
[a]XOS, expressed as xylose equivalent.
[b]ND = Not detected.
*Standard deviation was less than 0.05.

Table 3.3. Oligomer composition during autohydrolysis.

Condition (min)	XOS[a]	Arabinose	Glucose	Acetic acid
	(% of initial dry solid)			
160°C				
0	1.1 ± *	0.2 ± *	0.9 ± 0.2	ND[a]
10	2.6 ± 0.4	0.3 ± *	1.8 ± *	0.3 ± *
20	5.3 ± 0.1	0.3 ± *	2.0 ± 0.1	0.5 ± *
30	7.0 ± 0.4	0.3 ± *	2.0 ± 0.1	0.7 ± 0.1
40	8.3 ± 0.4	0.3 ± *	1.8 ± 0.3	0.8 ± 0.1
50	10.2 ± 0.9	0.3 ± *	2.0 ± 0.1	0.9 ± *
55	11.1 ± 0.5	0.3 ± *	2.1 ± *	1.0 ± 0.1
60	11.8 ± 0.4	0.3 ± 0.1	2.0 ± 0.1	1.0 ± *
65	11.7 ± 0.1	0.3 ± *	2.0 ± 0.1	1.0 ± *
70	11.6 ± 0.2	0.3 ± *	2.0 ± *	1.0 ± *
180°C				
0	2.4 ± 0.1	0.3 ± 0.1	1.7 ± *	0.4 ± *
10	10.1 ± 0.5	0.4 ± *	1.6 ± *	1.0 ± 0.1
15	12.6 ± 0.2	0.4 ± *	1.6 ± *	1.2 ± *
20	13 ± 0.2	0.3 ± 0.1	1.6 ± *	1.2 ± *
30	10.6 ± 0.1	0.3 ± 0.1	1.8 ± 0.1	1.0 ± *
200°C				
0	7.5 ± 1.2	0.4 ± *	1.6 ± *	0.8 ± 0.1
5	13.5 ± 0.4	0.3 ± *	1.6 ± *	1.3 ± *
10	9.0 ± 0.1	0.2 ± *	1.9 ± *	1.0 ± *
20	1.0 ± *	0.0 ± *	1.6 ± *	0.1 ± 0.1
30	0.2 ± *	0.0 ± *	1.3 ± *	0.1 ± *

Mean ± standard deviation from duplicates.
[a]ND = Not detected.
*Standard deviation was less than 0.05.

Xylose was the major component among all oligomers and was 80% of total oligomer mass (Table 3.3). Oligomers also comprised of 0.2 to 0.4% arabinose and 0.9 to 2.0% glucose. Besides cellulose, short glucan chain also appears in the backbone and side chain of hemicellulose (Girio et al., 2010). The content of acetic acid in oligomers ranged from 0.3 to 1.3% (Table 3.3).

Washed pretreated solid compositions are presented in Table 3.4. Solids decreased throughout the reaction as biomass was hydrolyzed and dissolved. Though the samples were washed three times using distilled water before compositional analysis, total extractives increased for longer pretreatment conditions. In general, pretreatment increased glucan and lignin concentrations. For extractive free solids, the glucan content increased to 60.0, 67.1 and 71.4% (% w/w of extracted free solid) for the three temperature treatments, respectively. The xylan content decreased; xylan concentrations were 12.9% (w/w) at 160°C, 6.8% (w/w) at 180°C and not detectable at 200°C at the end of each autohydrolysis. Acid soluble lignin content decreased and ash content increased as the reaction progressed. The acid insoluble lignin content was maintained at 18 to 22% in extractive free solids.

Carrasco and Roy (1992) reported that plant cell walls contain fast reacting and slow reacting xylans. Sørensen et al. (2008) reported that easily extractable hemicellulose was 60 to 80%. Malony and Chapman (1985) suggested the initial 60 to 70% of xylan degradation followed first order reaction kinetics. Narbarlatz et al. (2004) theorized the released arabinose and acetyl groups originated from hydrolysis of the fast reacting xylan fraction. Compared with the slow reacting xylan fraction, the fast reacting xylan was hypothesized to have higher arabinose and acetic acid contents. Xylan was extracted from 60.5 to 69.2%, which is comparable to XOS production from previous reports: 65.6% from corncobs (Garrote et al., 2007), 58.8% from rice husk (Garrote et al., 2007) and 47 to 61% from brewery's spent grain (Carvalheiro et al., 2004).

There have been three recent studies on XOS production and hydrothermal treatment of MxG. El Hage et al. (2010) recovered 40% xylose of the initial xylan during pretreatment of 25 h at 130°C, 16 h at 140°C and 8 h at 150°C in a 0.6 L stainless Parr reactor. However, the lower reaction temperature, compared to temperatures used in this study, resulted in longer reaction time. Long reaction times are undesirable for scaling up a process.

Table 3.4. Composition of pretreated solids.

Condition (min)	Residual Solids (w/w %)	Composition						
		Extractives[a] (w/w %)	Extractives free solids (w/w % of solids)					
			Glucan	Xylan	Insoluble lignin	Soluble lignin	Ash	
160°C								
0	92.3 ± 0.1[b]	7.2 ± 0.2	42.6 ± 2.5	24.0 ± 1.5	18.4 ± 0.8	1.1 ± *	1.5 ± 0.1	
10	89.0 ± 0.2	8.3 ± 0.1	44.2 ± 2.0	23.2 ± 1.4	19.0 ± 0.2	1.0 ± *	1.0 ± 0.4	
20	85.2 ± *	10.2 ± 0.3	47.7 ± 0.6	21.8 ± 0.2	19.2 ± 0.4	1.0 ± *	1.4 ± 0.1	
30	82.2 ± 0.1	11.0 ± 0.4	50.0 ± 1.1	20.1 ± *	19.3 ± 0.3	0.9 ± *	1.5 ± 0.2	
40	80.6 ± 1.2	12.0 ± 0.8	52.2 ± 0.1	18.9 ± 0.9	19.5 ± 0.6	0.8 ± *	1.8 ± *	
50	77.5 ± 0.5	13.9 ± 0.7	54.2 ± 3.0	15.9 ± 1.0	19.7 ± 0.1	0.7 ± *	1.6 ± *	
55	75.5 ± 0.6	15.4 ± 0.6	55.2 ± 1.4	14.0 ± 1.1	19.5 ± 0.6	0.7 ± *	2.0 ± 0.3	
60	74.5 ± 1.1	16.3 ± 0.3	57.2 ± 2.3	12.6 ± 0.4	19.8 ± 0.6	0.6 ± *	2.0 ± 0.2	
65	75.1 ± 0.4	16.2 ± 0.8	60. ± 1.3	12.2 ± 0.5	21.7 ± 0.4	0.7 ± *	2.2 ± 0.1	
70	75.8 ± *	15.6 ± 0.3	56.8 ± 1.2	12.9 ± 0.1	21.9 ± *	0.7 ± *	2.8 ± 1.0	
180°C								
0	87.2 ± 0.3	9.5 ± 0.2	46.3 ± 0.1	24.0 ± 0.1	20.9 ± 0.4	1.0 ± *	1.5 ± *	
10	77.6 ± 1.3	16.0 ± 0.1	54.9 ± 0.6	16.5 ± 0.9	21.3 ± 0.6	0.8 ± *	1.9 ± *	
15	74.8 ± 0.1	19.1 ± 0.3	61.3 ± 0.2	11.4 ± 0.4	20.8 ± 0.4	0.6 ± *	1.7 ± *	
20	73.9 ± 0.5	20.4 ± *	62.2 ± 0.9	9.9 ± 1.0	20.6 ± 0.1	0.6 ± *	1.9 ± 0.1	
30	71.7 ± 0.9	23.2 ± 0.5	67.1 ± 0.8	6.8 ± 0.5	20.4 ± 0.1	0.6 ± *	1.8 ± 0.4	
200°C								
0	85.1 ± 0.6	14.2 ± 2.1	51.0 ± 2.1	19.4 ± 1.1	19.1 ± 0.8	1.0 ± *	1.8 ± 0.2	
5	74.6 ± 0.5	23.6 ± 1.0	66.6 ± 1.5	7.2 ± 0.2	18.2 ± 0.5	0.6 ± *	2.2 ± *	
10	70.8 ± 0.1	25.2 ± 0.1	70.5 ± 0.8	4.2 ± *	18.1 ± 0.9	0.5 ± *	2.5 ± 0.1	
20	68.0 ± 0.3	24.0 ± *	71.4 ± 1.0	0.0 ± *	19.3 ± 0.4	0.4 ± *	2.6 ± 0.1	
30	67.7 ± 0.2	23.4 ± 0.2	69.6 ± 0.1	0.0 ± *	20.4 ± 0.2	0.4 ± *	2.9 ± *	

Mean ± standard deviation values from duplicates.
[a]Extractives include both water and ethanol extracted material.
[b]Compositional analyses were performed in duplicates and expressed as percentage ± standard deviation of extractive free solids.
*Standard deviation was less than 0.05.

Timilsena et al. (2013) used a similar reactor for autohydrolysis and extracted 55.1% of intial xylan at 150°C, 8 h. Ligero et al. (2011) studied autohydrolysis of MxG for XOS production in a stainless steel reactor heated by oil bath; 160°C and 60 min was the optimum condition. Their conclusion was based on the ratio of soluble xylan weight to total soluble weight, furfural and HMF formation and decomposition rate of α-cellulose and Klason lignin using different temperatures. They also reported the recovery on XOS was 65% of initial xylan; xylose was the dominant monosaccharide in liquid phase; arabinose was released rapidly and quickly degraded.

In this study, 160°C for 60 min was confirmed as an effective condition for producing XOS from MxG using autohydrolysis. Furthermore, 180°C, 20 min and 200°C, 5 min were found efficient for producing XOS. The maximum XOS yield was observed at 200°C (13.5%), followed by 180°C (13.0%) and 160°C (11.8%). Residual xylan was 7.2% at 200°C, 5 min; 9.9% at 180°C, 20 min and 12.6% at 160°C, 60 min in pretreated solids. Compared with Ligero et al (2011), we increased the solids loading from liquid:solid ratio of 20:9 and found the increase did not reduce the final XOS yields. Higher temperatures gave higher extraction of xylan. Otieno and Ahring (2012) used 100, 125 and 145°C for autoclaving acid incubated *Miscanthus sinesis* and reported higher temperature could achieve favorable XOS production and composition. Among three reaction conditions in this study, acetic acid, furfural and formic acid concentrations were similar. Neither HMF nor levulinic acid was detected. These products were formed from degradation of hexoses.

3.4 Conclusions

Effective reaction conditions for producing XOS from MxG were investigated. XOS could be produced from autohydrolysis at 160, 180 and 200°C for 60, 20 and 5 min, respectively. XOS yields up to 13.5% (w/w) of initial dry biomass and a maximum conversion of 69% (w/w) of initial xylan were obtained.

Chapter 4. Changes in mean molecular weight and distribution of degree of polymerization (DP) of xylooligosaccharides (XOS) during autohydrolysis*

4.1 Introduction

Efficient reaction conditions of producing XOS by autohydrolysis were reported in Chapter 3. Three temperature conditions at 160, 180 and 200°C converted 60.5, 66.6 and 69.2% (w/w) of initial xylan into XOS. According to Kabel et al (2002), the prebiotic effects of XOS were affected by molecular weight (MW), degree of polymerization (DP) and the substituted groups of the XOS. Since XOS are produced primarily as prebiotics, these properties affect the commercial value of the XOS from *Miscanthus*. MW and DP of soluble products during autohydrolysis were analyzed by gel permeation chromatography (GPC) and high performance anion exchange chromatography with pulsed amperometric detection system (HPAEC-PAD). The objectives were to monitor the change in molecular weight and DP in solubles and provide more information on XOS products.

4.2 Materials and Methods

4.2.1 Gel permeation chromatography (GPC)

GPC analysis was performed by a TSKgel G3000SWxl column (Tosoh Bioscience, King of Prussia, PA) coupled with refractive index detector. Samples were eluted with 50 mM KNO_3 solution at 25°C with a flow rate of 0.8 mL/ min. Results were integrated by ChemoQuest (Thermo Fisher Scientific, Philadelphia, PA) and calibrated by dextran.

4.2.2 High performance anion exchange chromatography with pulsed amperometric detection system (HPAEC-PAD)

The liquid phase from pretreatment was analyzed for DP of XOS by high performance anion exchange chromatography with pulsed amperometric detection system, HPAEC-PAD

* Published in Bioresource Technology 155 (2014) 359-365.

(Dionex ICS 3000, Sunnyvale, CA). Twenty five µl of each sample (diluted 1:500 with milliQ water) were analyzed by HPAEC-PAD utilizing a Dionex PA-100 column (Dionex) at 1 mL/min running 100% 100 mM NaOH initially with a linear gradient program to 15% 100 mM NaOH containing 1 M sodium acetate over 35 min followed by washing and 15 min of reequilibration in 100 mM NaOH.

4.3 Results and Discussion

4.3.1 Molecular weight migration of the solubles

MW distribution of all soluble parts, including sugar oligomers, sugar monomers, lignin degraded products and all other heat soluble material were revealed (Figs. 4.1, 4.2 and 4.3). In the beginning of the reaction, MW distributions were more wide ranged. At 160°C, with the reaction in progress, the major peak which was located at 10^5 to 10^6 Da started to shift to the left and formed two overlapped peaks at the range of 100 to 2000 Da (Fig.4.1). Similar phenomenon was observed at 180°C (Fig. 4.2) and at 200°C (Fig. 4.3).

4.3.2 The degree of polymerization migration of the solubles

To ascertain detailed information on the length of oligomer chains, HPAEC-PAD was used for oligosacchride separations and quantifications. Though XOS from xylan have arabinose side chains, we assume they exhibit same property as pure xylose oligomers in HPAEC-PAD. Changes in moles of arabinose and each DP of oligosaccharides (X1-X14) during autohydrolysis were recorded. Arabinose peak was observed earlier than other XOS peaks. At 160°C, the profile reached maximum at 60 min (Fig. 4.4). Similar conditions were observed at 180 and 200°C. The highest XOS yield was observed at 180°C, 20 min and 200°C, 5 min (Figs. 4.5 and 4.6). In contrast, when treated at 180°C, 30 min or 200°C, 10 min, the moles of higher DP molecules were reduced but the moles of X2 (xylobiose) and X3 (xylotriose) increased, which implied prolonged reaction times would recover more X2 and X3 products.

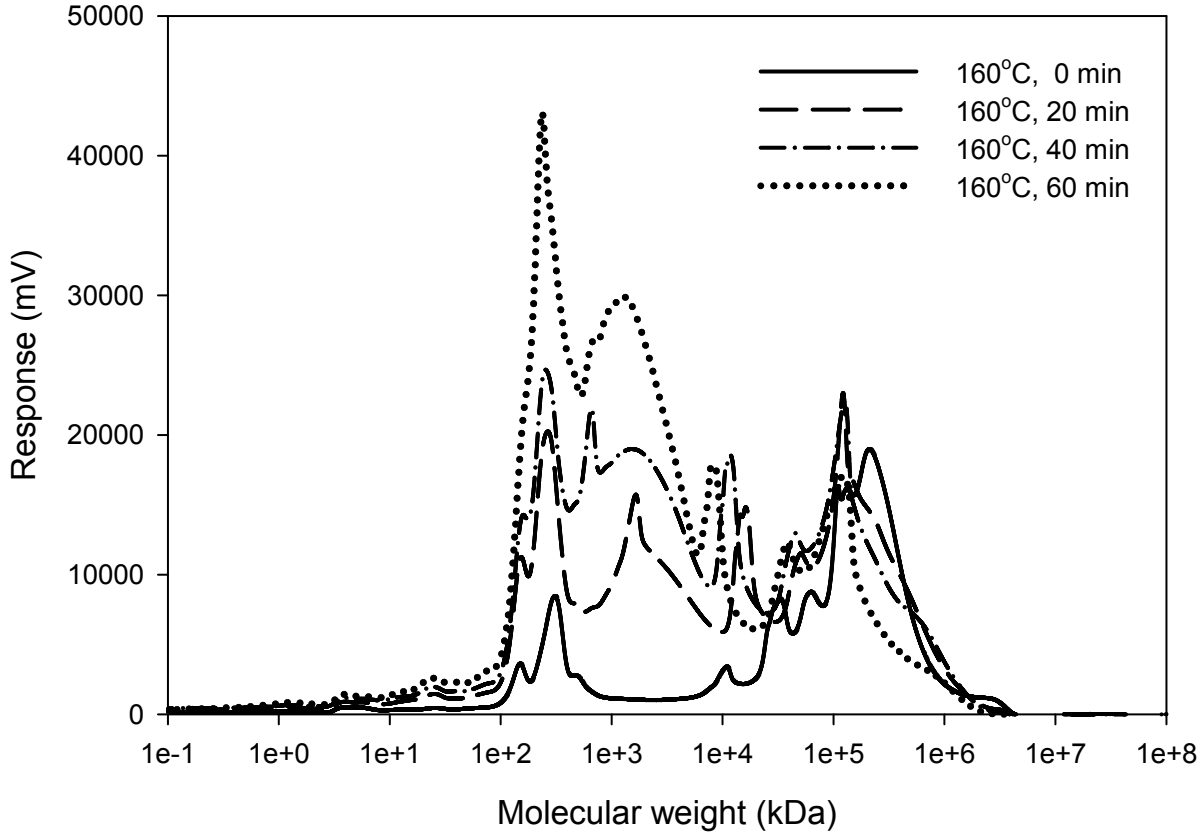

Fig. 4.1. Change in the molar mass distribution of XOS at 160°C. GPC was calibrated by dextran with MW range from 10,200 to 485,000 Da.

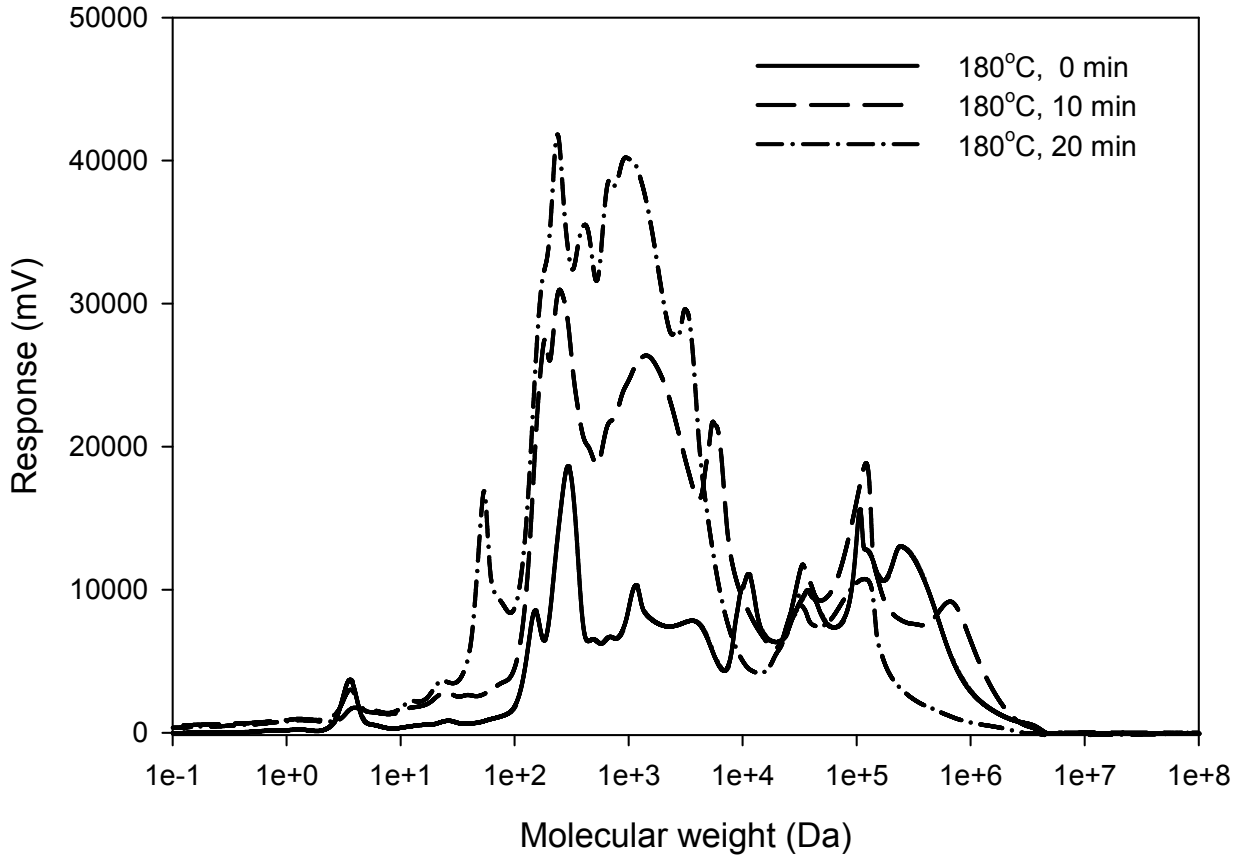

Fig. 4.2. Change in the molar mass distribution of XOS at 180 °C. GPC was calibrated by dextran with MW range from 10,200 to 485,000 Da.

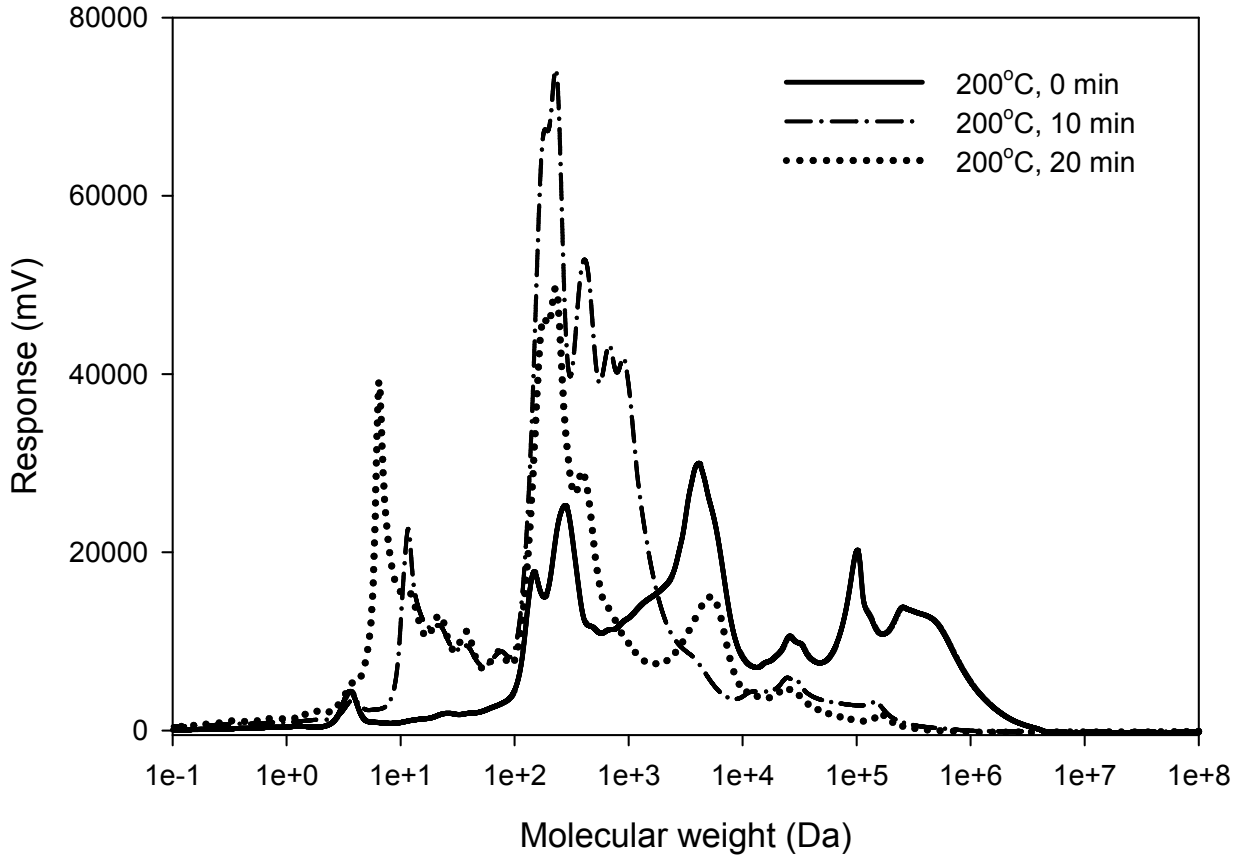

Fig. 4.3. Change in the molar mass distribution of XOS at 200 °C. GPC was calibrated by dextran with MW range from 10,200 to 485,000 Da.

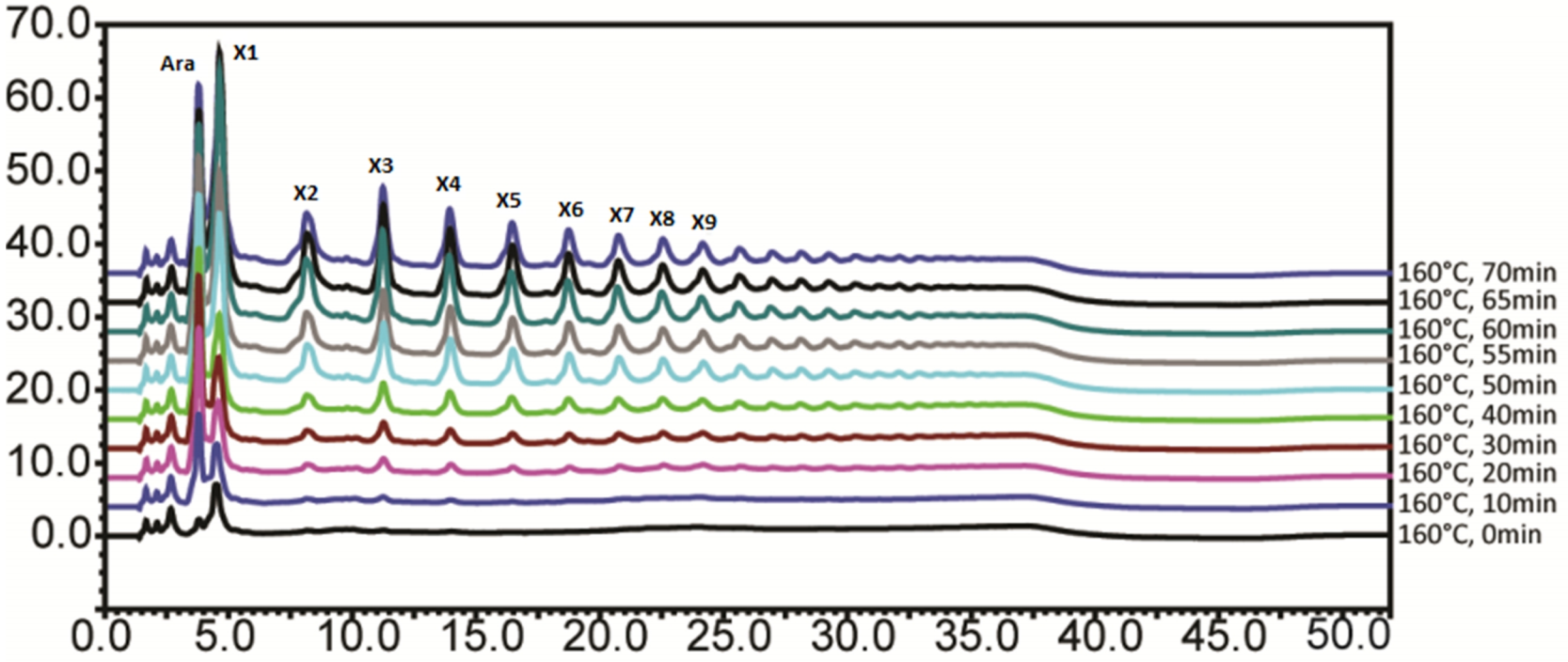

Fig. 4.4. XOS production at each degree of polymerization (DP) at 160°C.

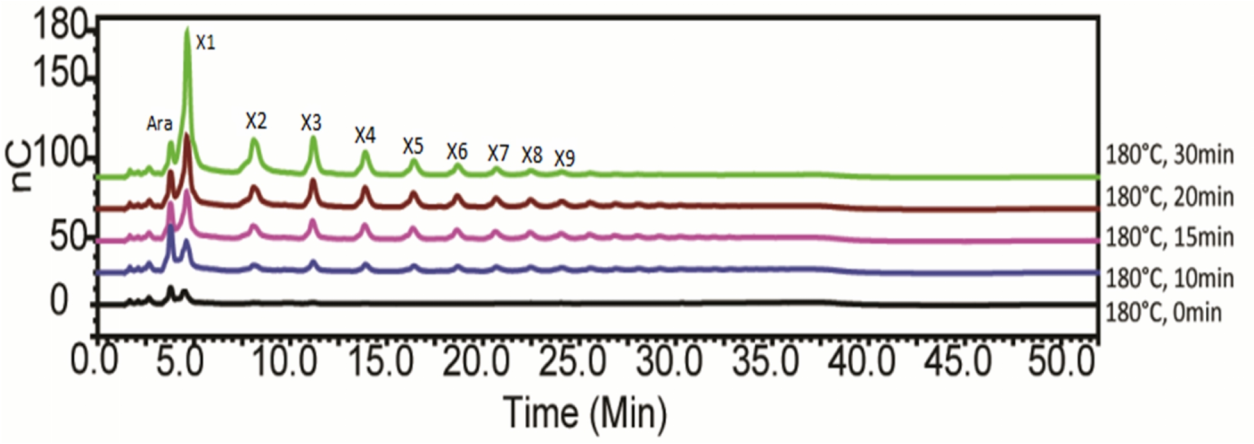

Fig. 4.5. XOS production at each degree of polymerization (DP) at 180°C.

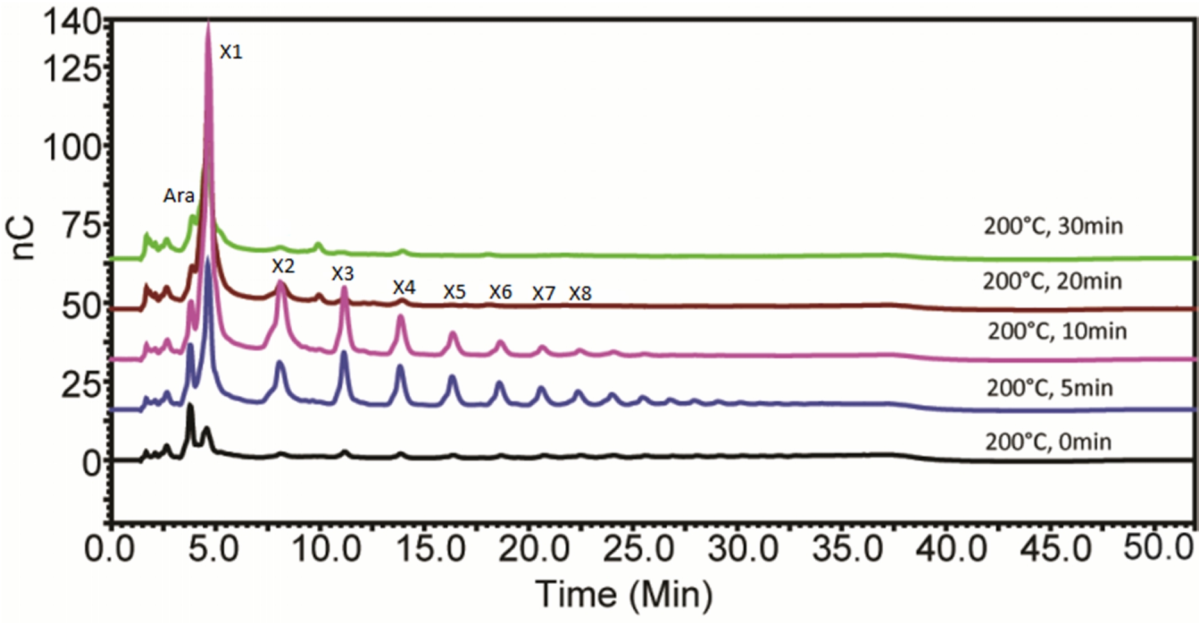

Fig. 4.6. XOS production at each degree of polymerization (DP) at 200°C.

Published reports are few on the evolution of XOS distributions, especially DP, during autohydrolysis of MxG. Cavalheiro et al. (2004) reported that at 170°C and 20 min most of the XOS from brewery's spent grain had DP larger than 9. Narbarlatz et al. (2004) used 179°C and 23 min for treating six agricultural coproducts; 2/3 of XOS had an average molecular mass of 1000 g/mol which is equal to DP 5 or 6. Otieno and Ahring (2012) used sulfuric acid incubation followed by autoclaving on bagasse and recovered 50% of XOS in xylobiose (X2) form.

4.3.3 Comparison of the oligomer composition from three optima conditions

The XOS produced at three conditions had similar profiles on both GPC and HPAEC-PAD, which illustrated there were no differences in the product whether we chose 160, 180 or 200°C (Figs. 4.7 and 4.8).

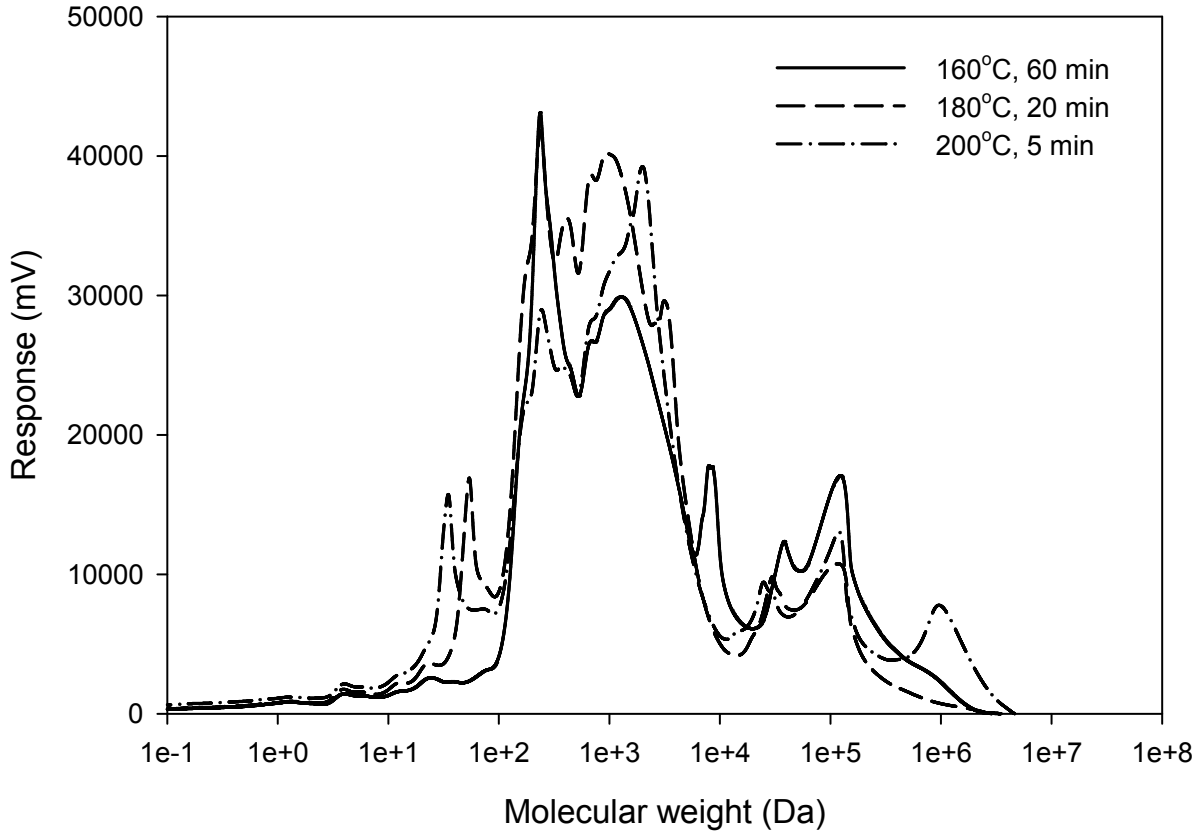

Fig. 4.7. Comparison of the molecular weight distribution at each XOS peak time point.

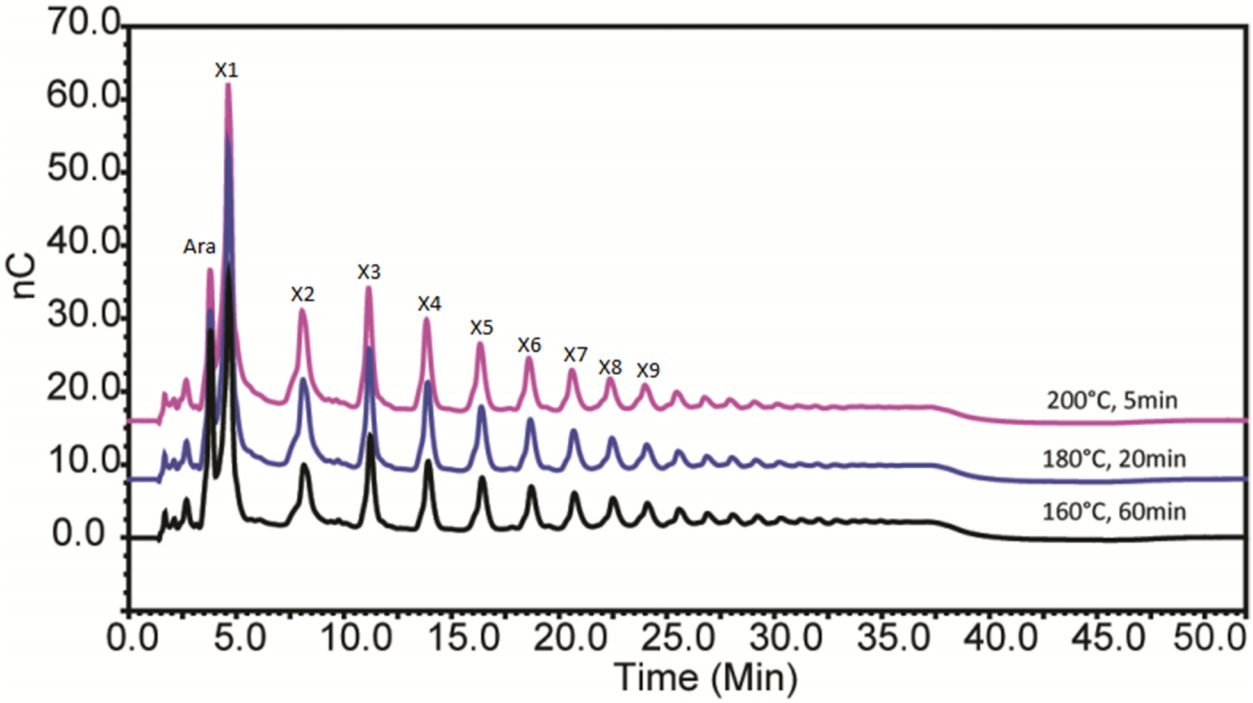

Fig. 4.8. Comparison of DP distribution of XOS at each optimum production time point.

4.4 Conclusions

Molecular weight and DP of the autohydrolyzed product were analyzed by GPC and HPAEC-PAD. Based on GPC results, the soluble material was degraded continuously during autohydrolysis and reduced to a MW of 100 to 2000 Da. The HPAEC-PAD results further revealed the XOS production in each DP. The 160°C, 60 min, 180°C, 20 min and 200°C, 5 min were efficient conditions to produce XOS from MxG. Longer reaction times resulted in lower total XOS yield but the amount of xylobiose and xylotriose may increase. The three production conditions produced similar XOS compositions.

Chapter 5. Purification of XOS from autohydrolyzed MxG using activated carbon adsorption*

5.1 Introduction

XOS were recovered from autohydrolyzed MxG crude solution by using carbon adsorption followed by ethanol/water elution. The activated carbon formed a XOS carbon affinity force to adsorb XOS molecules on its surface. XOS with higher degree of polymerization (DP) had higher affinity with the carbon molecule. The ethanol/water solutions can disrupt the XOS carbon complex and release XOS from the carbon active site. The objectives were to investigate the amount of activated carbon needed for purification, the efficiency of the ethanol/water elution and the composition of the eluted fractions.

5.2 Materials and Methods

The liquid phase from autohydrolysis, which contained XOS, was centrifuged at 2600 x *g* for 10 min. Fifty mL of the crude XOS liquid was placed into a 200 mL Erlenmeyer flask. Activated carbon powder (Darco G60, Sigma-Aldrich, St. Louis, MO) was added to 1, 5, 10 or 20% (w/v) of the liquid volume (1.4, 0.28, 0.14 or 0.07 g XOS/g carbon, respectively). Flasks were placed in a shaker (Max Q4000, Merss Corporation, Indianapolis, IN) set at 100 rpm for 60 min. The mixture was centrifuged at 2600 x *g* for 10 min to remove the supernatant. An aliquot of the supernatant was sampled for residual XOS quantification. XOS enriched activated carbon cake was eluted sequentially using 50 mL ethanol solutions at concentrations of 5, 30, 50, 70 and 95% (v/v). Washed ethanol solutions were oven dried at 49°C to remove all ethanol and adjusted to 10 mL by adding water. Recovered XOS fractions were analyzed for MW distribution, DP distribution and yield based on initial crude XOS liquid using the GPC and HPAEC-PAD method (Chapter 4).

* Published in Bioresource Technology 155 (2014) 359-365.

5.3 Results and Discussion

Refining of XOS from the autohydrolyzed liquid phase was tested by adding 1, 5, 10 or 20% (w/v) activated carbon powder for adsorption (Table 5.1). By analyzing the XOS content in liquid phase after adsorption, XOS adsorption ratios on carbon were 5.8, 46.8, 98.3 and 100%, respectively, which indicated the activated carbon ratios of 1 and 5% (w/v) were not enough for XOS recovery. Based on XOS concentration in liquid phase, activated carbon powder had the capacity of adsorbing 140 mg XOS/g carbon powder. Yang et al. (2007) used an adsorption column packed with activated carbon powder to recover XOS from xylanase hydrolyzate and observed the capacity of the column was 35.1 mg XOS/ g carbon powder. With the elution using ethanol/water solution, the highest XOS recoveries were observed using 30 and 50% ethanol solution (Table 5.1). Not all XOS could be eluted by ethanol; the best XOS recovery was at 47.9% (w/w) of initial XOS by using 10% (w/v) carbon, followed by 35.7% (w/w) of initial XOS by using 20% (w/v) carbon (Table 5.1).

To analyze the MW distribution of oligomers in each recovered ethanol/water fraction, Samples from 10 and 20% carbon adsorption sets were analyzed by GPC. As shown in Figs. 5.1 and 5.2, five ethanol/water fractions were observed to have different compositions based on their MW distribution profiles. Higher ethanol elution recovered higher MW products (Figs. 5.1 and Fig. 5.2). To acquire more detailed information on the oligomers released from adsorption, fractionated samples from 10 and 20% carbon treatments were analyzed by Dionex chromatography (Figs. 5.3 and 5.4; Table 5.2). For 10% carbon treatment, the 5% ethanol/water fraction was composed primarily of xylobiose (X2) and xylotriose (X3). The xylose (X1) had low recovery in 5% fraction because most of the monomer was washed out by distilled water. The 30% ethanol/water fraction was composed primarily of xylobiose (X2), xylotriose (X3), xylotetarose (X4), xylopentaose (X5) and xylohexaose (X6) (Fig. 5.3). The 50% ethanol/water fraction was composed primarily of xylotriose (X3) to xylohexaose (X6) with more xylohepatose (X7), xylooctaose (X8) and xyloneptaose (X9) recovery (Fig. 5.3). An ethanol/water fraction more than 50% did not result in efficient recovery of XOS (Fig. 5.3). In 10% carbon treatment, the highest recovery of initial oligomers was X3 (86.9%) and X2 (70.5%) followed by X4 to X9 (Table 5.2). For 20% carbon treatment, overall recovery was lower than 10% carbon treatment (Table 5.2) which indicated recovery efficiency of XOS was affected by total carbon addition.

Elution of oligomers was delayed with 20% carbon treatment (Figs. 5.3 and 5.4). Compared with 10% carbon treatment, the 5% ethanol/water fraction had more X1 (Fig. 5.4); 30% ethanol/water fraction had more X2 and less X4, X5 and X6 (Fig. 5.4); The 50% ethanol fraction had more X4 and X5 but less X6, X7, X8 and X9 (Fig. 5.4). In 20% carbon treatment, the highest recovery of initial oligomers was for X2 (91.8%) and X3 (80.7%) followed by X4 to X9 (Table 5.2). Excess carbon provided more affinity for XOS and therefore delayed its elution. Our results corresponded with previous reports that higher DP oligomers were eluted out with higher ethanol solution (Zhu et al., 2006).

Carbon adsorption is a popular method for recovering sugar oligomers (Otieno and Ahring, 2012). Recent reports on use of activated carbon for recovering oligosaccharides from honey (Morales et al., 2006) and purification of fructooligosaacharides (Kuhn and Filho, 2010) have shown promising results. Zhu et al. (2006) used activated carbon for recovering xylooligosaccharides from corn stover and corncobs, followed by ethanol elution; most of the XOS adsorbed on carbon could be recovered by 15% ethanol. The best recovery rate was observed by adding 10% carbon powder which corresponded with the results in this study. Yang et al. (2007) used a packed charcoal column to recover the XOS from xylanase hydrolyzate, and achieved 95% recovery with purity of 71.4%. Compared to this study, the difference in the recovery for Yang et al. (2007) originated from the use of pure alkaline extracted xylan for XOS production and xylobiose (X2) was the major product for carbon recovery after enzyme reaction. The XOS mixture from autohydrolysis contained many byproducts, such as degraded lignin and oligosaccharides, with wide range of DP that increased the difficulty in purification. The used activated carbon may not be reused in XOS recovery directly because not all adsorbed material is washed out during elution. However, reactivation and recycle of activated carbon is available in industry through heating used carbon above 1,700°F (926.6°C) to volatile or oxidize adsorbed material into carbon char. The heated activated carbon could regenerate the adsorptive ability.

Table 5.1. Recovery of XOS using activated carbon and aqueous ethanol extraction.

Carbon: XOS liquid (w/v %)		1%	5%	10%	20%
XOS adsorbed on carbon[a]		5.8 ± 2.6	46.8 ± 2.9	98.3 ± 1.0	100 ± *
Elution Yield (% of initial XOS)	5% EtOH	1.1 ± 0.5	4.6 ± 0.2	4.8 ± 1.3	1.4 ± 0.6
	30% EtOH	1.7 ± 0.1	12.3 ± 0.2	22.2 ± 1.4	14.7 ± 0.1
	50% EtOH	0.8 ± 0.1	4.9 ± 0.2	13.2 ± 0.2	12.1 ± 0.7
	70% EtOH	0.3 ± 0.1	2.4 ± 0.4	7.1 ± 0.6	6.6 ± 0.2
	95% EtOH	0.1 ± 0.2	0.5 ± 0.1	0.7 ± 0.1	0.9 ± 0.1
Total yield[b] (% of initial XOS)		4.0	24.6	47.9	35.7
Recovery from elution[c] (% of adsorbed XOS)		69.0	52.6	48.7	35.7

[a]XOS adsorbed on carbon = $[1 - (XOS\ left\ in\ liquid)/(initial\ XOS)] * 100\%$

[b]Total yield = $[(Total\ XOS\ yield\ from\ EtOH\ elution)/(initial\ XOS)] * 100\%$

[c]Recovery from elution = $[(Total\ XOS\ yield\ from\ \ EtOH\ elution)/(XOS\ adsorbed\ on\ carbon)] * 100\%$
*Standard deviation was less than 0.05.

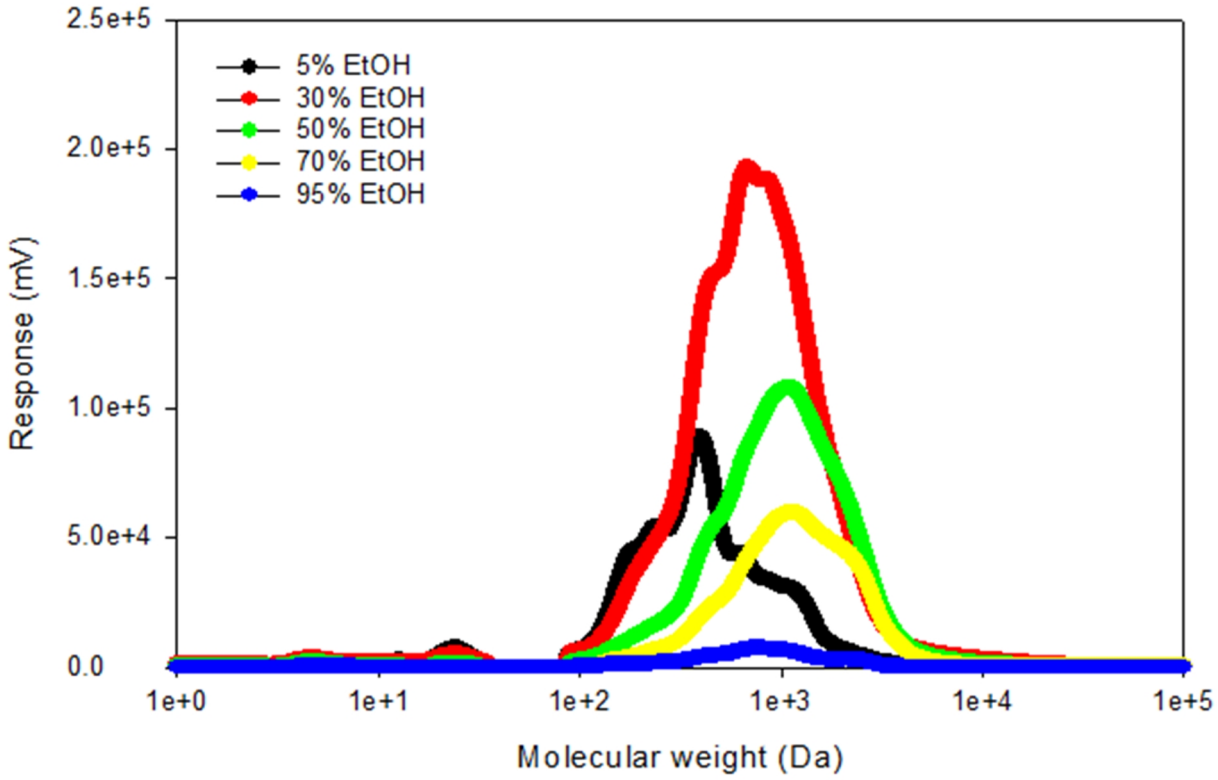

Fig. 5.1. Molecular weight distribution from 10% carbon adsorption.

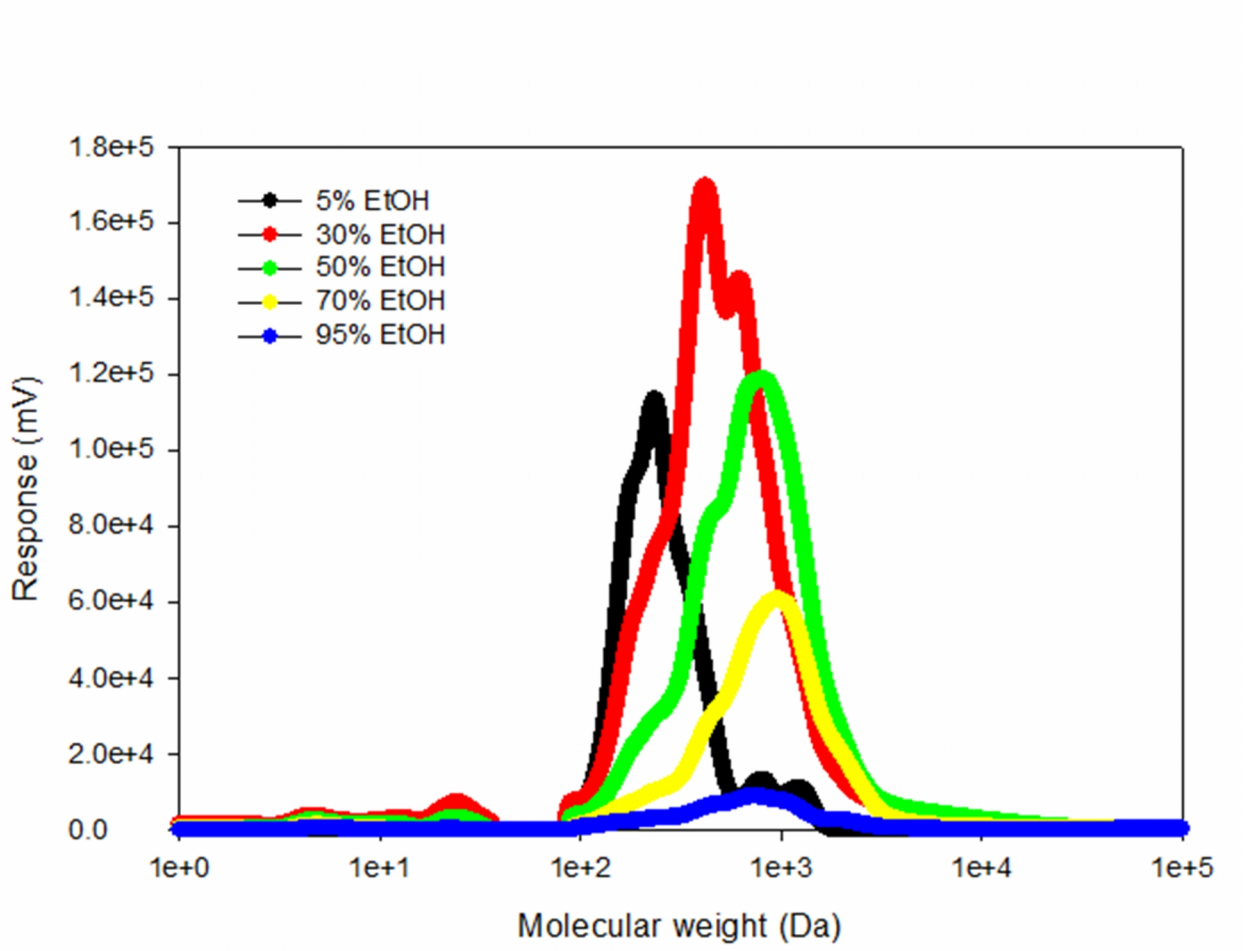

Fig. 5.2. Molecular weight distribution from 20% carbon adsorption.

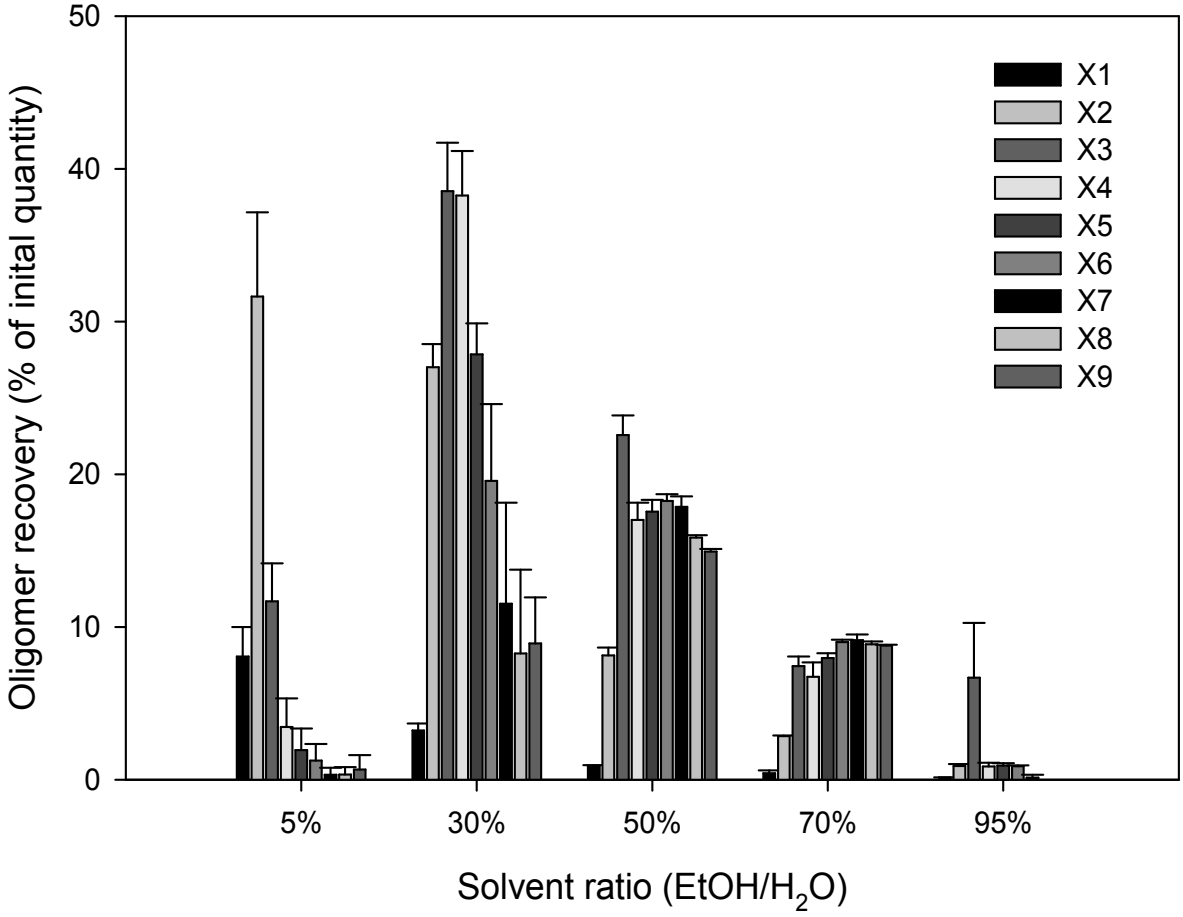

Fig. 5.3. Recovery of XOS in each DP using 10% (w/v) activated carbon adsorption. (Initial quantity is the amount of mono DP oligomer existed in autohydrolyzed liquid.)

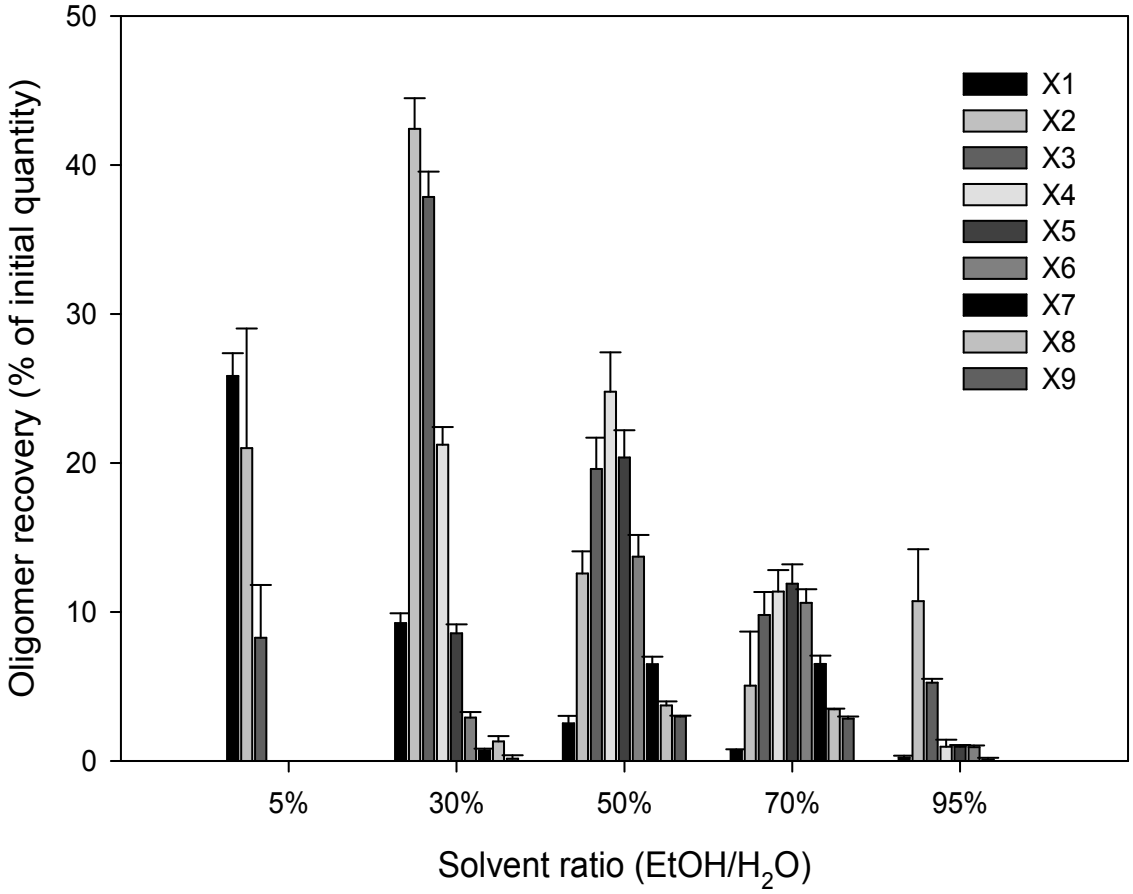

Fig. 5.4. Recovery of XOS in each DP using 20% (w/v) activated carbon adsorption. (Initial quantity is the amount of mono DP oligomer existed in autohydrolyzed liquid.)

Table 5.2. DP analyses of final recovered XOS fractions following activated carbon adsorption and aqueous ethanol elution.

10% Carbon EtOH/H_2O	X1	X2	X3	X4	X5	X6	X7	X8	X9
	(% recovery of each DP from crude XOS solution)								
5%	8.1 ± 1.9	31.6 ± 5.5	11.7 ± 2.5	3.5 ± 1.9	1.9 ± 1.4	1.3 ± 1.1	0.3 ± 0.5	0.3 ± 0.5	0.7 ± 0.9
30%	3.2 ± 0.5	27.0 ± 1.5	38.5 ± 3.2	38.2 ± 2.9	27.8 ± 2.0	19.6 ± 5.0	11.5 ± 6.6	8.3 ± 5.5	8.9 ± 3.0
50%	0.9 ± *	8.1 ± 0.5	22.6 ± 1.3	17.0 ± 1.1	17.5 ± 0.8	18.2 ± 0.4	17.9 ± 0.7	15.8 ± 0.2	14.9 ± 0.2
70%	0.4 ± 0.2	2.9 ± *	7.4 ± 0.6	6.7 ± 0.9	8.0 ± 0.3	9.0 ± 0.2	9.1 ± 0.4	8.9 ± 0.2	8.8 ± 0.1
95%	0.1 ± *	0.9 ± 0.1	6.7 ± 3.6	0.9 ± 0.3	0.9 ± 0.2	0.9 ± 0.1	0.1 ± 0.2	ND[a]	ND[a]
Total recovery	12.8	70.5	86.9	66.3	56.2	48.9	39.0	33.3	33.3
20% Carbon EtOH/H_2O	(% recovery of each DP from crude XOS solution)								
5%	25.8 ± 1.5	21.0 ± 8.0	8.3 ± 3.5	ND[a]	ND[a]	ND[a]	ND[a]	ND[a]	ND[a]
30%	9.2 ± 0.7	42.4 ± 2.1	37.8 ± 1.7	21.2 ± 1.2	8.6 ± 0.6	2.9 ± 0.4	0.7 ± 0.1	1.3 ± 0.4	0.2 ± 0.2
50%	2.5 ± 0.5	12.6 ± 1.5	19.6 ± 2.1	24.8 ± 2.6	20.4 ± 1.8	13.7 ± 1.5	6.5 ± 0.5	3.7 ± 0.3	3.0 ± 0.1
70%	0.7 ± 0.1	5.0 ± 3.6	9.8 ± 1.5	11.4 ± 1.4	11.9 ± 1.3	10.6 ± 0.9	6.5 ± 0.6	3.5 ± *	2.8 ± 0.1
95%	0.2 ± 0.1	10.7 ± 3.5	5.2 ± 0.3	0.9 ± 0.5	1.0 ± 0.1	0.9 ± 0.1	0.1 ± 0.1	ND[a]	ND[a]
Total recovery	38.5	91.8	80.7	58.3	41.8	28.1	13.8	8.5	6.0

Mean ± standard deviation; X1= xylose, X2= xylobiose; X3= xylotriose, X4= xylotetarose, X5= xylopentose; X6= xylohexaose; X7= xylohepatose; X8= xylooctaose; X9= xyloneptaose.
*Standard deviation was less than 0.05.
[a]ND = Not detected.

5.4 Conclusions

Activated carbon was used for XOS recovery from autohydrolyzed liquid. By adding the activated carbon powder at 1, 5, 10 or 20%, XOS was adsorbed at the ratio of 5.8, 46.8, 98.3, or 100%. The 1 and 5% carbon additions were not sufficient to capture all XOS; the capacity of carbon adsorbing was 0.14 g XOS/g carbon powder. Ethanol/water solutions were used to release XOS from carbon. Most of the XOS were recovered in 30 and 50% ethanol/water elution. The highest recovery 47.9% (w/w) of total XOS from initial XOS was observed by adding 10% (w/v) activated carbon. Solubles with higher MW came out in higher ethanol fraction. DP of oligomers in each ethanol fractions were analyzed further by Dionex chromatography. Lower ethanol fraction recovered lower DP oligomers. Highest recover of 91.8% xylobiose (X2) and 86.9% xylotriose were observed. The amount of carbon added increased the elution time of XOS.

Chapter 6. Separation of xylose oligomers using centrifugal partition chromatography (CPC)*

6.1 Introduction

In Chapter 5, recovery of XOS was performed by activated carbon adsorption and with ethanol/water elution. The investigation on XOS mixture recovery was useful from the view point of industrial scale production of prebiotics. However, there is a demand for recovering homogeneous mass xylose oligomers for research and pharmaceutical purposes (Lau et al., 2011). Moreover, the technique for producing the single weight XOS molecules is not technically mature, which results in high prices for these products. The objective was to separate homogeneous mass xylose oligomer from autohydrolyzed MxG crude solution by centrifugal partition chromatography (CPC). The crude solution has many undesirable components such as extractives, inhibitors and lignin degraded products. CPC has potential to provide a faster and scalable method to purify homogenous mass xylose oligomers. Previous purification reports (Lau et al., 2011; Lau et al., 2013) were based on pure xylan hydrolyzate; we are the first to use whole biomass hydrolyzate for xylose oligomer separation.

6.2 Materials and Methods

6.2.1 MxG hydrolyzate preparation

Autohydrolysis was performed in a tubular reactor inserted in a fluidized bed sand bath for fast heating (Khullar et al., 2013). The 316 stainless steel tubing (SS-T12-S-065-20, Swagelok, Chicago Fluid System Technologies, Chicago, IL) reactors had an outside diameter of 19.1 mm, a wall thickness of 1.7 mm, and a length of 104.8 mm. Reactors were capped with 19.1 mm, 316 stainless steel Swagelok caps (SS-1210-C, Swagelok) on both ends. The loaded reactors were immersed in a fluidized sand bath (IFB-51 Industrial Fluidized Bath, Techne Inc., Burlington, NJ) preheated to 180°C and cooled in flowing room temperature tap water. Autohydrolysis was performed at water to solid ratio of 9:1, at 180°C for 20 min. In each tubular reactor, 5 g of MxG was mixed with 45 g of water. The pretreated solids and liquids were

* The research was collaborated with Dr. Danielle Julie Carrier and Ms. Kalavathy Rajan from the Department of Biological and Agricultural Engineering, University of Arkansas.

separated by centrifugation (2600 × g, 5 min) in an Eppendorf 5804R centrifuge. This procedure was repeated in six reactors for four batches and corresponding hydrolyzates were combined. The resulting volume, determined to be 420 mL, was filtered through a 0.45 μm filter membrane (Millipore, Bedford, MA) and dried in a 49°C oven, removing approximately 415 mL of water. The resulting crude dried mixture was referred to as "XOS concentrate" throughout the work.

6.2.2 Sugar and oligomer characterization

Xylose, glucose, arabinose, galactose and xylose oligomers (from DP2 to DP6) content in the XOS concentrate was determined using a Waters Alliance HPLC system (Model 2695, Waters Corporation, Milford, MA) equipped with SP0810 (Shodex, Kawasaki, Japan) or Bio-Rad Aminex-HPX 42A (Bio-Rad, Hercules, CA) columns for monomer and oligomer quantification, respectively. HPLC was equipped with SP-G precolumn for monomer and Micro-Guard Deashing precolumn for oligomer determinations. Purified and 0.22 μm filtered water was used as eluent. Column temperature was 85°C. Eluent flow rate was 0.2 mL/min, and monomers or oligomers were detected with a refractive index detector (Model 2414, Waters Corporation, Milford, MA), which was maintained at 50°C. Concentrations of xylose, glucose, arabinose, galactose and xylose oligomers (DP2 to DP6) were determined using in house calibration curves generated from commercial standards.

Total dissolved solids and sugar contents of the concentrate were determined following NREL LAP-001 (Sluiter et al., 2008a) and NREL-LAP-014 (Sluiter et al., 2008b) protocols, respectively. Accordingly, the total yield of xylose oligomers in the XOS concentrate was determined as follows:

$$\text{Yield (\%)} = (W_h - W_i) \times 0.88 \times 100 \qquad (1)$$

Where W_h was the mass fraction of xylose in the concentrate after dilute acid hydrolysis, W_i was the initial mass fraction of xylose in the concentrate and 0.88 is the anhydrous correction factor for xylose (Sluiter et al., 2008c). The total phenolic content of the concentrate was determined using the Folin & Ciocalteau's (F-C) method, based on a previously published protocol (Ainsworth and Gillespie, 2007).

6.2.3 Xylose oligomer separation by CPC

A bench scale SCPC-250 system from Armen Instruments (Dallas, TX) equipped with CherryOne Beta (C1) countercurrent chromatography control system (Chicago, IL) was used for fractionating and purifying the XOS concentrate. Samples were processed by ultrapure nitrogen at 43 psig and with an evaporative light scattering detector (ELSD) (SofTA Corp, Westminster, CO). Butanol:methanol:water solvent system in 4:1:4 (v/v/v) was used for the CPC separation (Lau et al., 2013). Solvents for the biphasic system were prepared by shake flask method, where 889 mL each of butanol and water were mixed with 222 mL of methanol in a 2 L separation funnel and agitated thoroughly. The upper butanol rich organic phase and the lower aqueous phase were collected separately after 4 h and used as the mobile and stationary phases, respectively, when the CPC was operated in the ascending mode. One g of dried XOS concentrate was dissolved in 20 mL of butanol rich phase and 8 mL of the aqueous rich phase. The mixture was vortexed and filtered through a 1µm PTFE syringe filter (Thermo Scientific National, Rockwood, TN) and injected into the CPC system.

Stationary and mobile phases were loaded in the ascending mode at 500 rpm. Equilibrium was reached at retention volumes of 114 and 136 mL, respectively. The CPC run time was 344 min, at 2300 RPM and at a flow rate of 8.14 mL/min. The UV detector in the controller was equipped with a preparatory flow cell that was set at 254 nm for real time monitoring. Fraction collection was started after 60 min and fractions of approximately 8.1 mL each, were collected every min. To accomplish this task, two fraction collectors were connected in series: Foxy R1 (Teledyne Isco, Lincoln, NE) and Waters Fraction Collector III (Waters Corporation, Milford, MA). After 240 min of run time, the CPC was operated in the descending mode allowing for unseparated compounds to exit the column and be collected. All 284 CPC fractions were dried in a Savant SpeedVac Concentrator SPD 1010 (Thermo Scientific, Ashville, NC), at 7 Torr for 6 h and reconstituted in 0.5 mL of water. The reconstituted fractions were filtered through a 0.22 µm nylon syringe filter (Thermo Scientific National, Rockwood, TN) and analyzed using HPLC to determine the concentrations of xylose monomer and oligomers (DP2 to DP6).

The CPC fractionation of MxG xylose oligomers was repeated twice. Fractions were consolidated based on the concentration of each xylose oligomer. The purity of consolidated samples was calculated as:

$$\% \text{ Purity} = \frac{Weight\ of\ xylose\ oligomer}{Total\ weight\ of\ each\ fraction} \times 100 \quad (2)$$

6.2.4 ESI-MS identification of xylose oligomers

Samples were dried in SpeedVac and mixed with 0.1 % formic acid solution in methanol, at 20:1 ratio and directly injected into the mass spectrometer with a syringe pump. Gas phase ions created using electrospray ionization (ESI) were analyzed with a quadrupole/time of flight (Q-TOF) mass analyzer (Bruker ultrOTOF-Q, Bruker Daltonics Inc., Billerica, MA). The solvent (methanol) flow rate was 3 μL/min and N2 gas at 1 bar was used for nebulization. The source temperature was 180°C. Other instrument parameters were adjusted to optimize signal in the mass to charge ratio (m/z) range of 100 to 800 and the mass spectra were obtained in positive ion mode.

6.3 Results and Discussion

6.3.1 Xylose oligomers production

Autohydrolysis of MxG at 180°C resulted in xylan being hydrolyzed into xylose monomer and oligomers. Acetyl groups present on hemicellulose chains were cleaved during heating and provided an acid source, leading to decreased pH and increased xylan cleavage. Incubation at 180°C for 20 min led to conversion of 63.4% (w/w) of xylan into xylose and xylose oligomers. The hydrolyzates were pooled and concentrated and the total dissolved solids content of the XOS concentrate was determined to be 71.2% (w/w). In previous works, MxG autohydrolysis in a 0.6 L stainless Parr reactor, at temperatures ranging from 130 to 150°C was reported to yield 40% (w/w) of initial xylan content (El Hage et al., 2010). In a stainless tube reactor heated at 160°C for 60 min, 65% (w/w) of xylan was recovered as xylose and xylose oligomers (Ligero et al., 2011). Autohydrolysis conditions reported in the current work, provided comparable yields for the production of crude xylose oligomers concentrate.

The carbohydrate composition of the XOS concentrate, adjusted for moisture content, was determined to be 39.8% xylose, 4.4% glucose, 5.1% arabinose and 2.7% galactose. The total

xylose oligomer content, determined as per equation (1), was 30.1%. Distribution of xylose oligomers (DP2 to DP6) in the concentrate varied from 0.6 to 15.9% dry weight, as shown in Table 6.1 and it was determined that DP2 to DP6 constituted 95.5% of the total xylose oligomers. The total phenolic content of the concentrate was 4.1% gallic acid equivalent. Presence of phenolic compounds indicated that a certain degree of lignin degradation had occurred during the autohydrolysis reaction. It was calculated that to produce 1 g of the XOS concentrate, autohydrolysis of 3.7 g of MxG biomass was required. Conversely, 1 g of the concentrate used for CPC fractionation contained, 159.2 mg of DP2, 59.0 mg of DP3, 56.0 mg of DP4, 8.1 mg of DP5 and 5.6 mg of DP6.

Table 6.1. Composition of xylose oligomers in in the autohydrolyzed XOS concentrate.

Oligomer	% Dry wt.[a]
Xylobiose (DP2)	15.9 ± 1.5
Xylotriose (DP3)	5.9 ± 0.8
Xylotetraose (DP4)	5.6 ± 0.7
Xylopentaose (DP5)	0.8 ± 0.2
Xylohexaose (DP6)	0.6 ± 0.2
Total	28.8 ± 0.5

[a] Mean and standard deviation, *n*=3.

6.3.2 Xylose oligomers separation and purification by CPC

The xylose oligomers present in the concentrate were separated using centrifugal partition chromatography (CPC), generating 284 fractions. The ELSD chromatogram corresponding to a typical CPC separation is presented in Fig. 6.1; fractions corresponding to the highlighted area under the curve were consolidated. The HPLC-RID chromatograms of the original concentrate and the CPC consolidated fractions are presented in Fig. 6.2. The mean yields of xylose oligomers, calculated on a dry weight basis of the concentrate, as well as the corresponding purities are presented in Table 6.2. Recovery of DP2 to DP6 oligomers varied from 61.9 to 90.2%, while purity fluctuated from 31.5 to 63.2%. The recovery of CPC

fractionated xylose oligomers was the highest for DP2 at 90.2%, based on the original composition of XOS concentrate (Table 6.2). The consolidated DP2 and DP3 fractions had comparatively higher purities of 61.9 and 63.2%, respectively. The purities of CPC fractionated and consolidated MxG xylose oligomers were calculated based on their total mass fractions (Eqn. 2). In earlier reports, purities of xylose oligomers produced from purified xylan were higher, but were calculated based on area under the (chromatogram) curve, relative to other DPs and not on a mass basis (Qing et al., 2010; Lau et al., 2013)

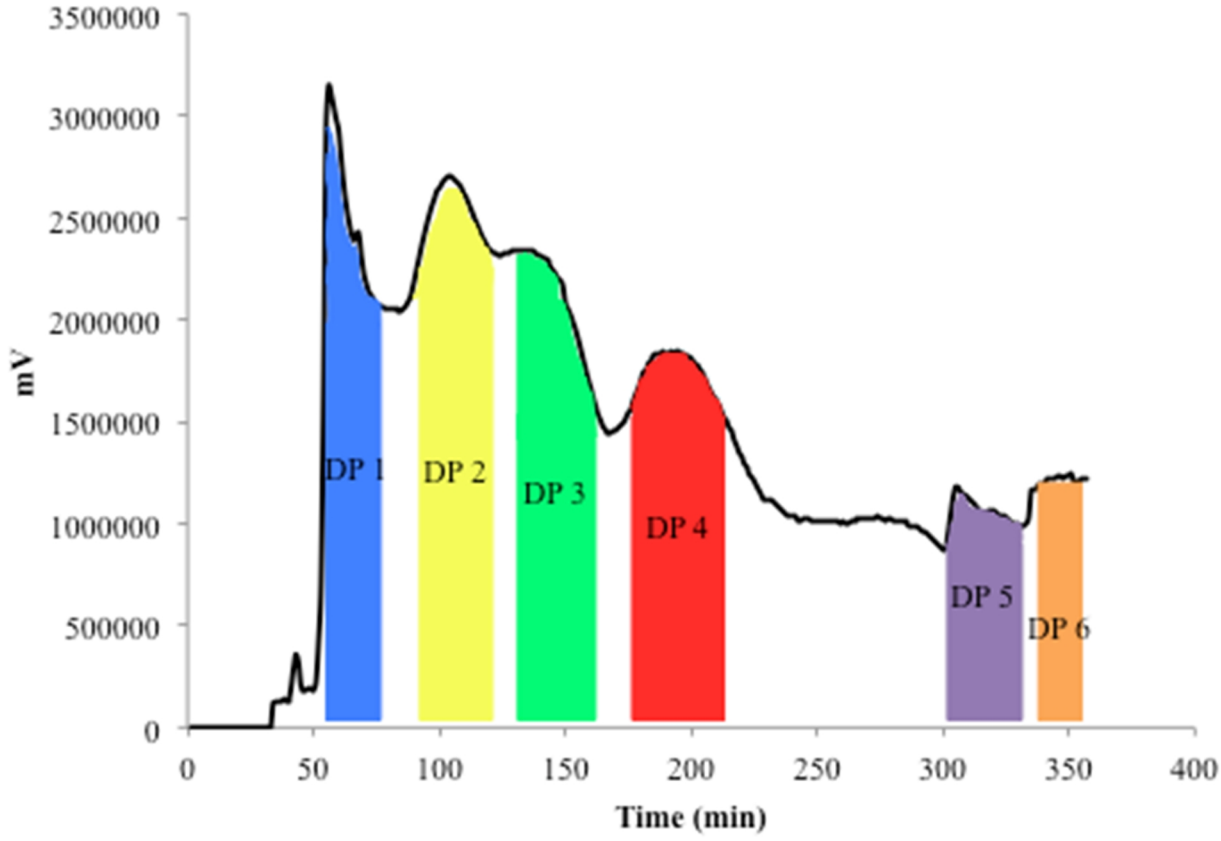

Fig. 6.1. ELSD chromatogram of centrifugal partition chromatography for separation of xylose oligomers from autohydrolyzed XOS concentrate.

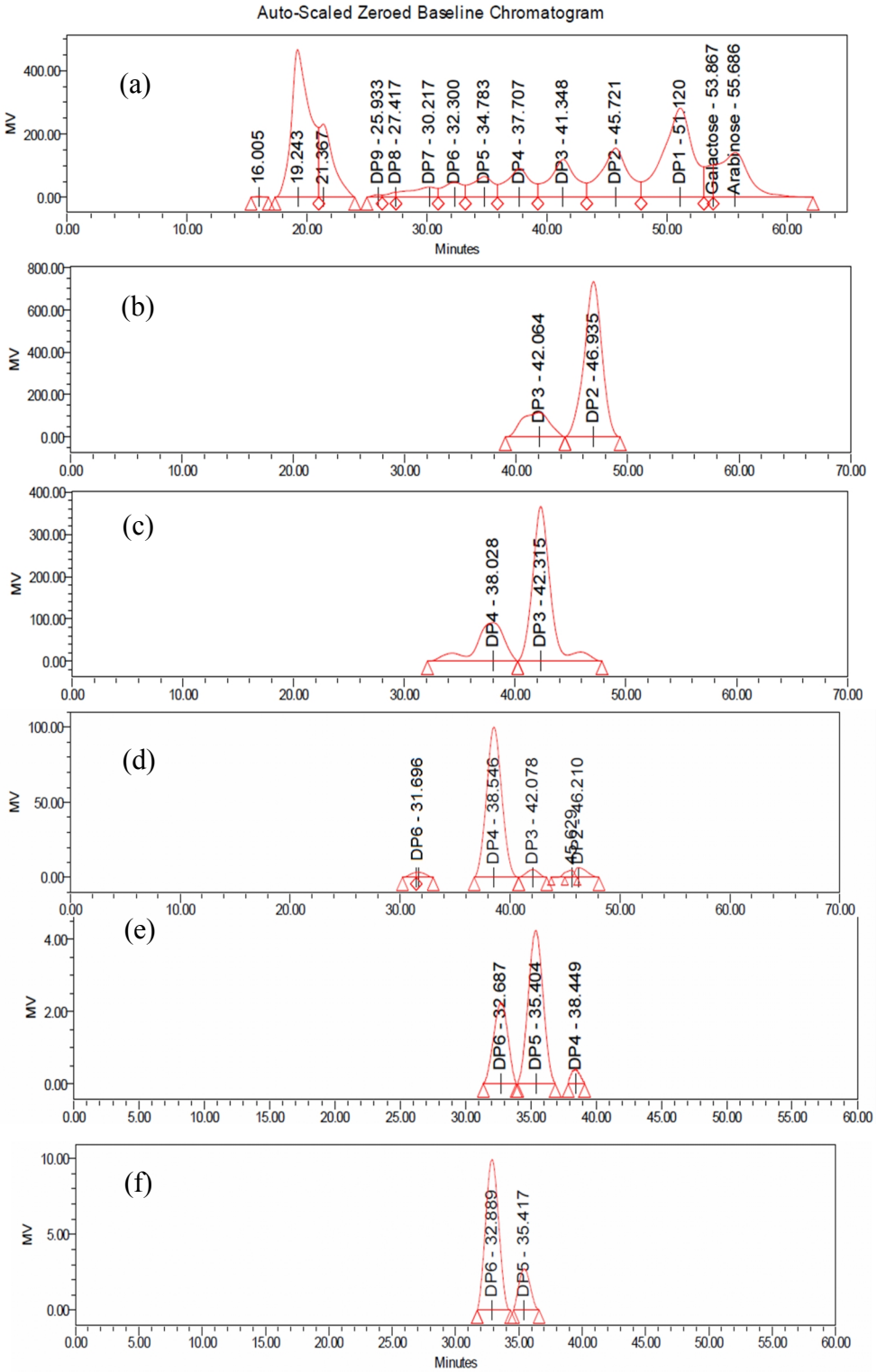

Fig. 6.2. HPLC-RID chromatogram of (a) original XOS concentrate and the consolidated xylose oligomers, (b) DP2 fraction, (c) DP3 fraction, (d) DP4 fraction, (e) DP5 fraction and (f) DP6 fraction.

Table 6.2. Yield of MxG xylose oligomers during centrifugal partition chromatography separation.

Fractionated compounds	Yield of each compound [a] (mg/g)	Recovery [b] (%)	Purity [c] (%)
DP2-Xylobiose	143.5 ± 6.0	90.2	61.9 ± 1.9
DP3-Xylotriose	38.1 ± 5.0	64.5	63.2 ± 2.3
DP4-Xylotetraose	39.8 ± 1.0	71.2	44.5 ± 1.9
DP5-Xylopentaose	4.9 ± 0.1	61.9	31.5 ± 1.0
DP6-Xylohexaose	3.9 ± 0.3	68.9	51.3 ± 1.0

[a] Mean and standard deviation, *n*=2.
[b] % Recovery was calculated based the theoretical maximum yield.
[c] % Purity was calculated based on the total weight of each fraction.

6.3.3 ESI–MS verification of CPC separated fractions

Qualitative analysis of the CPC fractionated DP2 and DP3, performed using ESI–MS, was useful to verify their identity. As shown in Fig. 6.3a, the major signals in consolidated DP2 fractions were m/z 305.1 [M+Na]+ and 321.1 [M+K]+ which corresponded to individual pentobiose molecule bound with sodium and potassium ions. Similarly, the major signals in consolidated DP3 fractions were m/z 437.1 [M+Na]+ and 453.1 [M+K]+ (Fig. 6.3b) which corresponded to individual pentotriose molecule bound with sodium and potassium ions. The ESI-MS spectrums validated that the DP2 and DP3 were isolated and were the main component in each fraction.

(a)

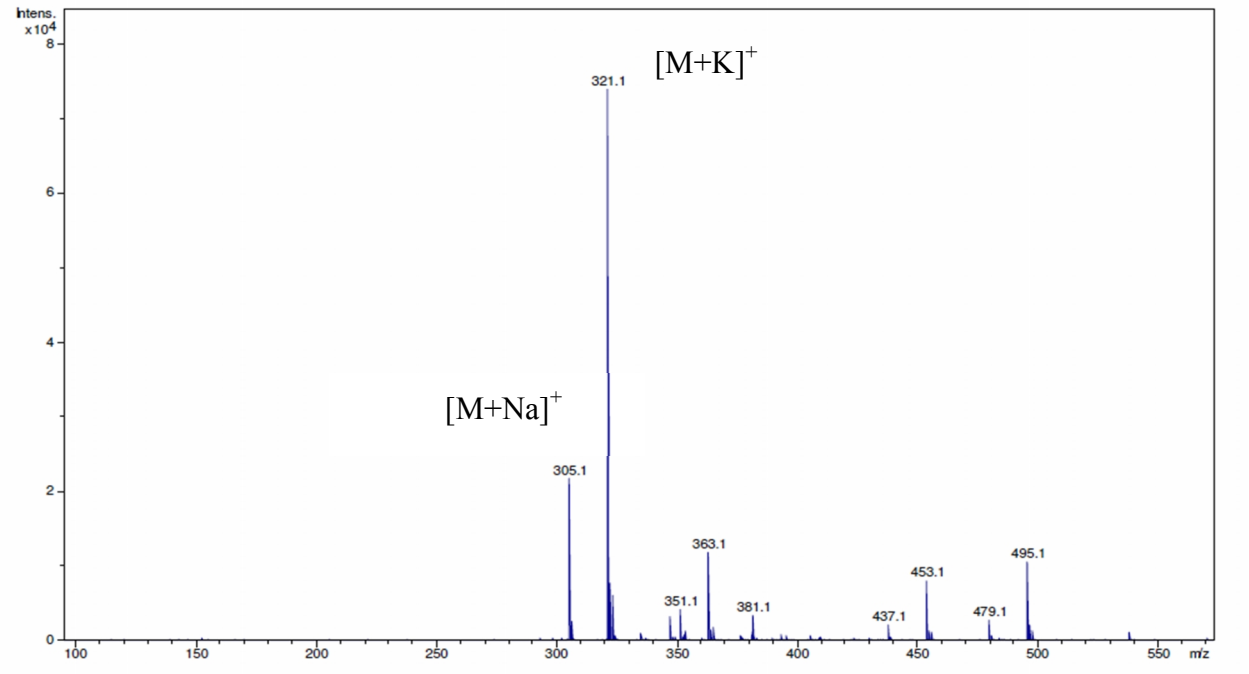

(b)

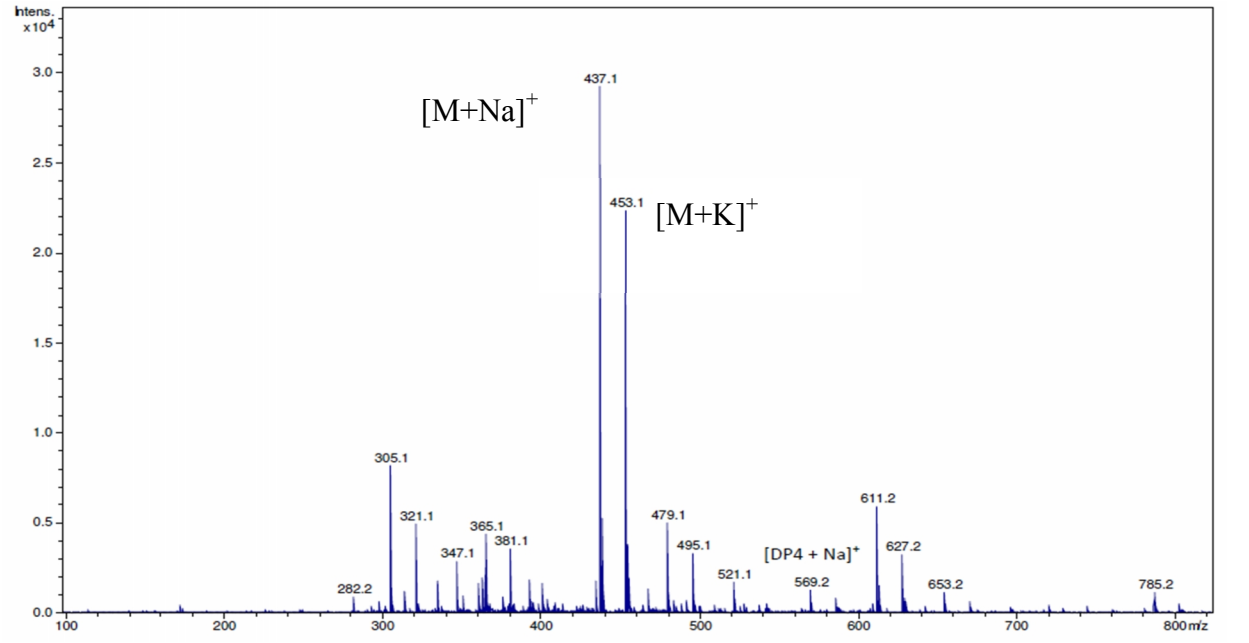

Fig. 6.3. ESI mass spectrum of consolidated xylose DP2 and DP3 purified from crude XOS concentrate by CPC. (a) DP2 fraction, (b) DP3 fraction.

Low MW xylose oligomers of sizes DP2 to DP5, at 70% purity, were reportedly fermented *in vitro* as well as *in vivo*, by prebiotic organisms belonging to the *Bifidobacterium* spp. (Hopkins et al., 1998). In one particular study, 90% of DP3 and 84% of DP2 were utilized preferentially by *Bifidobacterium adolescentis* (Gullón et al., 2008). Similarly certain strains of *Lactobacillus* spp. were reported to utilize preferentially xylose DP2 to DP4 when compared to other oligosaccharides, during mixed acid fermentations (Kontula et al., 1998). There are several enzymatic and chemical hydrolysis methods reported for the production of xylose oligomers from lignocellulosic biomass. However, few reports are addressing fractionation practices. Cara et al. (2012), described the production and separation of glucose and xylose oligomers by gel filtration chromatography, but did not separate xylose oligomers into individual DP components. Jayapal et al. (2013), extracted hemicellulose from sugarcane bagasse and produced xylose oligomers using xylanases. They detected their product with reducing sugar and thin layer chromatography assays, with no report on fractionation.

Lau et al. (2011) used centrifugal partition chromatography (CPC) in separation and purification of xylose oligomers from acid hydrolyzed birchwood xylan. Fractions were obtained from xylose DP2 to DP5. With the adoption of a 4:1:4 volumetric ratio of butanol:methanol:water system, Lau et al. (2013) recovered 12.5 mg/g xylan of 81.2% pure xylobiose, 9.6 mg/g xylan of 71.0% pure xylotriose, 14.2 mg/g xylan of 62.4% pure xylotetraose and 21 mg/g xylan of 51.9% pure xylopentaose from autohydrolyzed birchwood xylan. Fractionating crude MxG hydrolyzate, containing other carbohydrates and lignin derivate, increased the complexity of separation and therefore reduced the purity of CPC fractions.

6.4 Conclusions

Xylose oligomers were purified from 1 g autohydrolyzed XOS concentrate by CPC with a solvent system composed of 4:1:4 (v/v/v) butanol:methanol:water. Using CPC techniques, 230 mg (80%) DP2 to DP6 oligomers were fractionated from 1 g XOS concentrate. Recoveries of individual xylose oligomers were 90.2% DP2, 64.5% DP3, 71.2% DP4, 61.9% DP5 and 68.9% DP6. Purities of DP2 to DP6 fractions were 61.9, 63.2, 44.5, 31.5 and 51.3%, respectively. Presence of DP2 and DP3 in the CPC purified fractions was validated by mass spectrometry analysis.

Chapter 7. Production of high purity xylooligosaccharides from autohydrolyzed *Miscanthus x giganteus*

7.1 Introduction

Autohydrolysis of cellulosic materials has been demonstrated to be an effective method for production of XOS for numerous sources of biomass using optimized reaction conditions. Acetic acid released from the hemicelluloses creates an acidic environment that cleaves xylan into XOS. Autohydrolysis can convert 60 to 70% of initial xylan and is compatible with cellulose pretreatment for subsequent biochemical conversion to glucose. Nevertheless, most commercial plants still adopt a chemical enzymatic method for XOS production. The chemical enzymatic method is an alternative method for XOS production, which includes extracting semi purified xylan with caustics followed by partial enzymatic hydrolysis of the xylan using xylanase. Even though the chemical enzymatic method involves more steps and extensive use of akali in preparing semi purified xylan, purification of XOS is simpler than from autohydrolysis hydrolysates. This is most likely the reason autohydrolysis method is not favored commercially.

Purification of XOS from biomass autohydrolyzate is difficult because the hydrolyzate is a complex solution (Vázquez et al., 2006). There is a variety of compounds derived from extractives, acid soluble lignin, carbohydrates, protein and lipids that are present along with XOS in the hydrolyzate. The pigments, furfural, phenolics, free fatty acid and amine related derivatives are typically being removed through combination of solvent extraction, membrane filtration and chromatography. Food grade XOS typically has a purity of 75 to 95% (Aachary and Prapulla, 2011).

The complexity of current purification methods for recovery of XOS form biomass hydrolysates makes them costly. The objective of this chapter was to investigate the purification procedure for high purity XOS production from autohydrolyzed MxG. Following Chapter 5, ethanol fractions from activated carbon adsorption and ethanol/water elution increased the XOS purity from 39.8 to 69.5% (w/w). The collected ethanol fractions were further treated with ion exchange resins to remove any heavy metal ions, negatively charged organic compounds and

pigments. The recovered material is finally filtered, dried, and ground to produce the final product of MxG XOS powder.

7.2 Material and Methods

7.2.1 Raw materials

In 2012, MxG was harvested from the University of Illinois Energy Farm. It was oven dried at 49°C, sliced and ground using a hammer mill (model MHM4, Glen Mills, Clifton, NJ) equipped with a screen (250 μm openings) and stored at 4°C. The moisture content (NREL/TP-510-42621) of ground MxG was 5.0%. Commercial XOS (Wako XOS) sample was purchased from Wako Chemicals USA (Richmond, VA). The Wako XOS were composed mainly of xylobiose (X2) and xylotriose (X3). Purified xylobiose (X2), xylotriose (X3), xylotetraose (X4), xylopentaose (X5) and xylohexaose (X6) were purchased from Megazyme International (Wicklow, Ireland) and used as chromatographic standards. Ion exchange resins Amberlite IR120Na, Amberlite IR96 and Amberlite FPA90Cl were obtained from Dow Chemical (Midland, MI). All chemicals and laboratory reagents, unless stated otherwise, were of analytical quality and were supplied from Fisher Scientific (Springfield, NJ).

7.2.2 Scale up of MxG autohydrolysis, carbon adsorption and ethanol elution

Autohydrolysis was performed in water:solid ratio at 7:1 (12.5% w/w solids) in 500 mL stainless pipe reactors. The reactors were rapidly heated in a fluidized sand bath to 200°C and incubated for 20 min. The autohydrolysis reactions were quenched by immediately immersing the reactors in a water bath. Pretreated solids and liquids were separated by vacuum filtration though glass fibers filters (Whatman GF/D, Fisher Scientific, Springfield, NJ). An aliquot of the pretreated liquid was filtered through a 0.2 μm membrane and analyzed for sugars and organics acids. A second aliquot was end-hydrolysis with 4% sulfuric acid to determine XOS content as described in Chapter 3.

Two liters of the filtered pretreated liquid, a concentrated source of XOS, was placed in a 5 L plastic vessel. Activated carbon powder (Darco G60, Sigma–Aldrich, St. Louis, MO) was

added until 10% (w/v) of the liquid volume. The bucket containing the carbon mixture was placed in a water bath set at 30°C and stirred at 80 rpm for 60 min. Every 15 min, the whole mixture was stirred manually using a spatula. The mixture was vacuum filtered to recover the solids. An aliquot of the filtrate was sampled for residual XOS quantification. The XOS enriched carbon cake was washed by 2 L distilled water and eluted sequentially using 2 L ethanol solution at the concentration of 5, 30, 50, 70 and 95% (v/v). The eluted ethanol fractions were incubated in 80°C water bath for 2 h to evaporate the ethanol and concentrated in a static oven at 49°C to constant weight.

7.2.3 Treatment of XOS solution with ion exchange resins

The oven dried 30, 50 and 70% ethanol fractions were resuspended in DI water and combined into a XOS solution at a concentration of 2.74 g XOS/100 mL (Step 1). The XOS solution was treated in sequence with Amberlite IR120Na (Step 2, a strong cation exchange resin), Amberlite IR96 (Step 3, a weak anion exchange resin) and Amberlite FPA90Cl (Step 4, a strong anion exchange resin) to remove impurities. Each resin was added at the mass ratio of resin/liquor of 1:10. Resins were incubated with XOS solution at ambient temperature for 24 h.

7.2.4 Quantification of colorants removal during purification

Color intensity of the XOS samples was measured with a UV-VIS spectrophotometer (Evolution 60s, Thermal Scientific, Waltham, MA) by measuring absorbance (optical density, OD) between the wavelengths 200 and 500 nm. One milliliter of the XOS sample at each purification stage was added into a 1 cm wide cuvette (ThermoElectron, Madison, WI) for absorbance measurement. The crude XOS solution was diluted 10x to ensure it was within the linear measurement range.

7.2.5 Filtration, drying and commination

The refined XOS solution was filtered through a 0.22 μm vacuum filter unit (EMD Millipore Steriflip, Millipore Corp, Bedford, MA) to obtain a clear and pathogen free solution.

The filtered Step 4 solution was oven dried at 45°C to constant weight and milled by pestle and mortar to form fine powders. The XOS powder was named MxG XOS.

7.2.6 Analytical methods

The composition analysis of MxG harvested at 2012 was conducted by following NREL standard procedure "Determination of extractives in biomass (TP-510-42619)", "Determination of structural carbohydrates and lignin in biomass (TP-510-42618)" and "Determination of ash in biomass (TP-510-42622)". Descriptions of these procedures can be found in Chapter 3.

Monosaccharides (arabinose, galactose, glucose, xylose), acetic acid, and degradation products (furfural, hydroxymethylfurfural (HMF), levulinic acid, formic acid) were quantified by HPLC coupled with a refractive index detector (Model 2414, Waters Corporation, Milford, MA). Sugars were analyzed in a Bio-Rad Aminex HPX-87P column with B-pure purified water as mobile phase flowing at 0.6 ml/min and 85°C. Organic acids and residual ethanol in XOS samples were analyzed in a Bio-Rad Aminex HPX-87H column with 0.005M H_2SO_4 as mobile phase flowing at 0.6 mL/min and 50°C.

Total XOS content in pretreated liquid was quantified by 4% H_2SO_4 (w/w) posthydrolysis at 121°C for 60 min (NREL-LAP-014). An increase in the concentration of sugars following acid hydrolysis was used to calculate XOS yield and composition. The equation used for XOS content calculation is presented in Chapter 6.

Refined XOS solution was analyzed for degree of polymerization (DP) of oligomers by high performance anion exchange chromatography with pulsed amperometric detection system, HPAEC-PAD (Dionex ICS 3000, Sunnyvale, CA). Twenty five mL of each sample (diluted 1:200 with milliQ water) were analyzed by HPAEC-PAD utilizing a Dionex PA-100 column (22 x 30 mm, Dionex). The system was operated at 1 mL/min running 100% 100 mM NaOH (mobile phase A) initially with a linear gradient program to 12% 100 mM NaOH containing 1 M sodium acetate (mobile phase B) over 20 min followed by reequilibration in 100 mM NaOH for 15 min. Standard curves of X1 to X6 were plotted for peak area vs concentration; oligomer amount was calculated by applying sample peak area to standard curves (Rantanen et al., 2007; Bowman et al., 2011).

7.3 Results and Discussion

7.3.1 Effect of newly harvested MxG for XOS production

The 2012 newly harvested MxG was used for autohydrolysis. This MxG had (%w/w, db): 39.4% glucan, 22.3% xylan, 0.7% acid soluble lignin, 17.0% acid insoluble lignin and 8.0% extractives, as measured using the standard NREL procedures (Table 7.1). Compared with the MxG harvested in 2011, the amount of extractives (water and ethanol) was reduced from 11.8 to 8.0%. Nevertheless, the compositions on an extractive free basis were similar for the MxG 2011 and 2012 samples, which indicated the cell wall composition remained consistent for the two harvest years (Table 7.2). The autohydrolysis of 2012 MxG was performed in 25 mL pipe reactors at 180˚C, the results of XOS production matched with the results from 2011 MxG (data not shown).

Table 7.1. Compositions of MxG harvested in 2012 (NREL procedure).

Component	Amount (%w/w, db)
Extractives[a]	8.0 ± 0.25
Glucan[a]	39.4 ± 0.29
Xylan[b]	22.3 ± 0.11
Acid soluble lignin	0.7 ± 0.01
Acid insoluble lignin	17.0 ± 0.03

[a]Ethanol & hot water extractables.
[b]Anhydrous monosaccharides.

Table 7.2. Compositions of MxG harvested in 2011 and 2012 on an extract free basis[a].

Composition (% w/w)	MxG 2011	MxG 2012
Acid soluble lignin	0.76 ± 0.01	0.75 ± 0.01
Acid insoluble lignin	18.50 ± 0.01	18.50 ± 0.03
Glucan	42.80 ± 0.95	42.80 ± 0.32
Xylan	24.07 ± 0.31	24.20 ± 0.12

[a]Extracted with ethanol and water.

According to Thammasouk et al. (1997), the hot water and 95% ethanol extractions applied may elute some glucan and Klason lignin from the biomass besides small molecules. Filbakk et al. (2011) found the drying and storage conditions affected the amount of extractives in wood pellets.Since the harvesting time and storage condition of MxG were different, it was reasonable to find the extractives varied from consecutive years. The similar composition of extractive free MxG and XOS production kinetics indicated the reproducibility of autohydrolysis for MxG from different years.

7.3.2 Scale up of MxG autohydrolysis, carbon/ethanol purification

Pretreated liquid was collected after autohydrolysis at 200°C, 20 min in 500 mL pipe reactors. Initial total xylose concentration was 1.34 g/100 mL with 0.18 g/100 mL xylose (DP1). XOS were recovered by activated carbon adsorption 10% (w/v) and eluted with 5, 30, 50, 70 and 95% (v/v) of ethanol/water solution. As shown in Table 7.3, the recovery from 2 L of pretreated liquid resulted in 1.94 g of 5% fraction, 7.07 g of 30% fraction, 5.35 g of 50% fraction, 2.22 g of 70% fraction and 0.55 g of 95% fraction. XOS content in 30 to 70% ethanol fractions were 55 to 61% of the total weight. Most of xylose (DP1) was eluted into the 5% ethanol fraction, and nearly 2% (w/w) free xylose existed in 30% ethanol fractions.

Due to nonspecific binding property, activated carbon can be used in two different ways. The first method is to add a small amount (0.5 to 1.5%) of activated carbon into XOS solution for color and impurities removal. Because XOS also are captured by activated carbon, the loss is proportional to carbon addition. The second method is to add sufficient carbon to capture all XOS in solution and elute with ethanol.This second method allows fractionation of XOS in different DP based on ethanol concentration. The drawback of this method is the recovery of XOS is lower for higher DP molecules, which may result in added loss of XOS.

7.3.3 Production of high purity XOS from autohydrolyzed MxG

The dried and resuspended 30, 50 and 70% ethanol fractions were combined to form XOS rich solution (Step 1) and treated with ion exchange resins for further purification (Fig. 7.1).

As shown in Fig. 7.2, the combined XOS rich solution had 69.5% (w/w) xylose oligomers and 81.6% (w/w) total substituted oligosaccharides (TSOS). TSOS represented total amount of arabinose, glucose, xylose oligomers and substituented acetyl groupsin XOS rich solution. With the incubation of strong cation exchange resin IR120Na for 24 h (Step 2), the percentages of XOS and TSOS in dried XOS solution increased to 70.4 and 82.5% (w/w), respectively. Through the treatment of weak anion resin IRA96 (Step 3), the ratio of XOS and TSOS increased to 77.6 and 90.5% (w/w), respectively. Further treatment with polishing resin FPA90Cl (Step 4) decreased the XOS and TSOS to 76.6 and 89.3% (w/w), respectively. There was 9.5% (w/w) loss of xylose oligomers during three stages of resin treatment. The final MxG XOS powder was made by vacuum filtration through a 0.22 μm membrane, drying in a 45°C static oven, and milling.

Table 7.3. Weight and purity of recovered XOS fractions.

EtOH/H_2O 10% carbon	Rep 1 (g)	Rep 2 (g)	Average ± std (g)	XOS[a] (% w/w)	Xylose (DP1) (% w/w)
5%	1.98	1.90	1.94 ± 0.06	27.9 ± 0.4	11.4 ± 0.6
30%	7.02	7.11	7.07 ± 0.06	55.1 ± 0.8	2.0 ± 0.1
50%	5.29	5.41	5.35 ± 0.08	61.6 ± 1.3	ND[b]
70%	2.22	2.21	2.22 ± 0.01	58.7 ± 0.5	ND
95%	0.53	0.56	0.55 ± 0.02	38.2 ± 2.1	0.2 ± 0.2

[a]Anhydrous xylose oligomers.
[b]ND = Not detected.

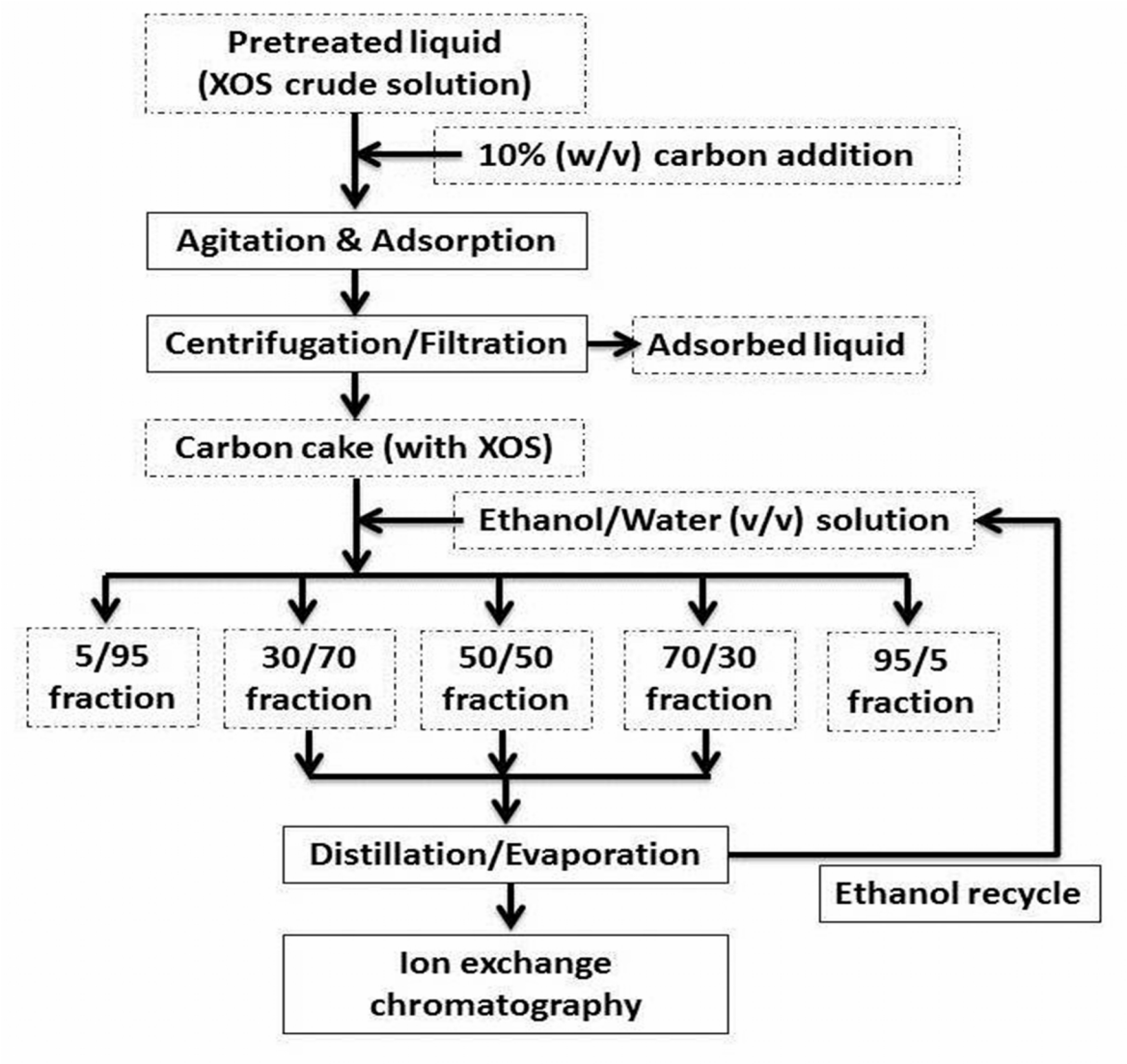

Fig. 7.1. XOS purification scheme.

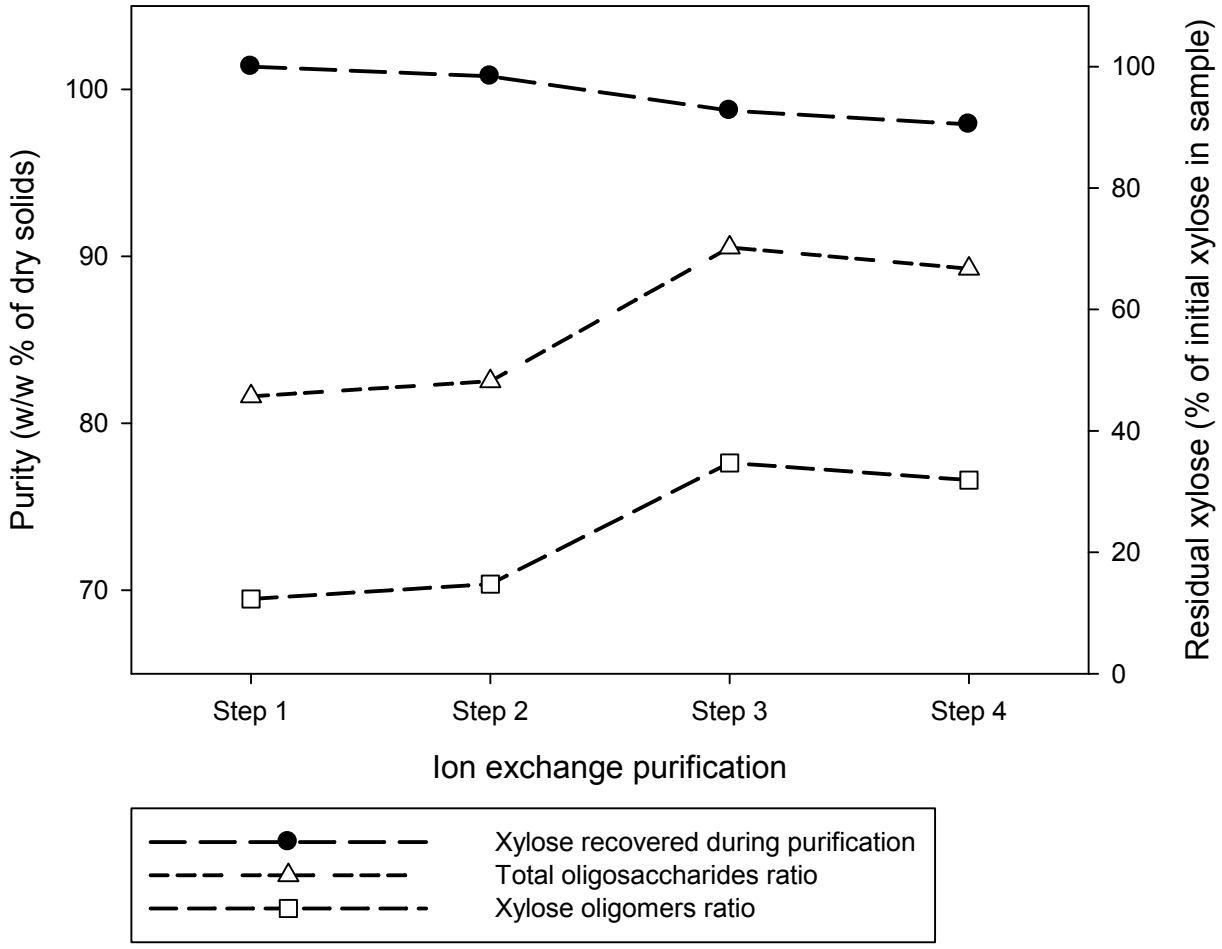

Fig. 7.2. Purity of XOS solutions and residual xylose ratio during purification.

Ion exchange resins have been used widely for industrial sugar and high fructose corn syrup purification and decolorization. Since the resin chemistry has been well developed, there are many options to serve different purification purposes that are suitable for XOS purification. Heavy metals were removed using Amberlite IR120 Na (Step 2, cation resin Fig 7.3 a). This is a gel type strong cation exchange resin with polystyrene matrix and sulfonic ligand. IR120 Na is a general purpose cation exchange resin, which is used for water softening. It exchanges heavy metal ions with sodium ions. Since metal ion exchange was target for Step 2, it was reasonable

and favorable to observe that overall purity (TSOS) only increased from 81.6 to 82.5%. Organic acids were next removed using Amberlite IRA96 (Step 3, Anion Resin, Fig 7.9a). This is a weak anion exchange resin with styrene divinylbezene matrix and tertiary amine ligand. IRA96 is used primarily for acid removal in water purification and has been tested for XOS purification from rice husk and *Eucalyptus globulus* hydrolyzate (Vegas et al., 2006; Vázquez et al., 2007; Gullón et al., 2010). Vázquez et al. (2007) compared the use of IRA96 and IRA400 (a strong anion exchange resin with polystyrene divinylbenzene matrix and quaternary ammonium ligand) in eucalyptus XOS purification, and observed IRA400 and IRA96 produced similar quality of XOS solution but the loss of XOS was less using IRA400. However, when testing these two anion ion exchange resins, we found the performance of IRA96 was better than IRA400 in treating MxG XOS solution (XOS purity 72% vs. 66%); whereas, the loss of XOS was greater in IRA96. Color agents were finally removed using Amberlite FPA90Cl (Step 4). This is a food grade strong anion exchange resin with polystyrene matrix and quaternary ammonium ligand, often is used in sugar and pharmaceutical industry for color removal. FPA90Cl is suitable for trapping high molecular weight organic color bodies. The strong anion exchange resins are noted to adsorb phenolic compounds, which are predicted to be major colorants because they derive from the lignin (Alexandratos, 2009). With the decrease of the oligosaccharide purity by FPA90Cl treatment, some of the XOS may have bound with the lignin fragment and were removed by FPA90Cl as colorants.

While crude XOS solution was dark brown in color, the carbon/ethanol elution lightened the color to yellow and the sequential ion exchange chromatography further reduced the color into pale yellow (Fig. 7.3-(a)). Outer appearance of milled and dried XOS end product was shown in Fig. 7.3-(b). Absorbance of XOS liquid from 200 to 500 nm wavelengths was shown in Fig. 7.4. Amount of impurities and color pigments were monitored at UV 230 nm and UV 280 nm. Treatment with the resins reduced absorbances at 230 and 280 nm reduced from OD 4.44 to 1.84 and from OD 3.67 to 1.51, respectively.

(a)

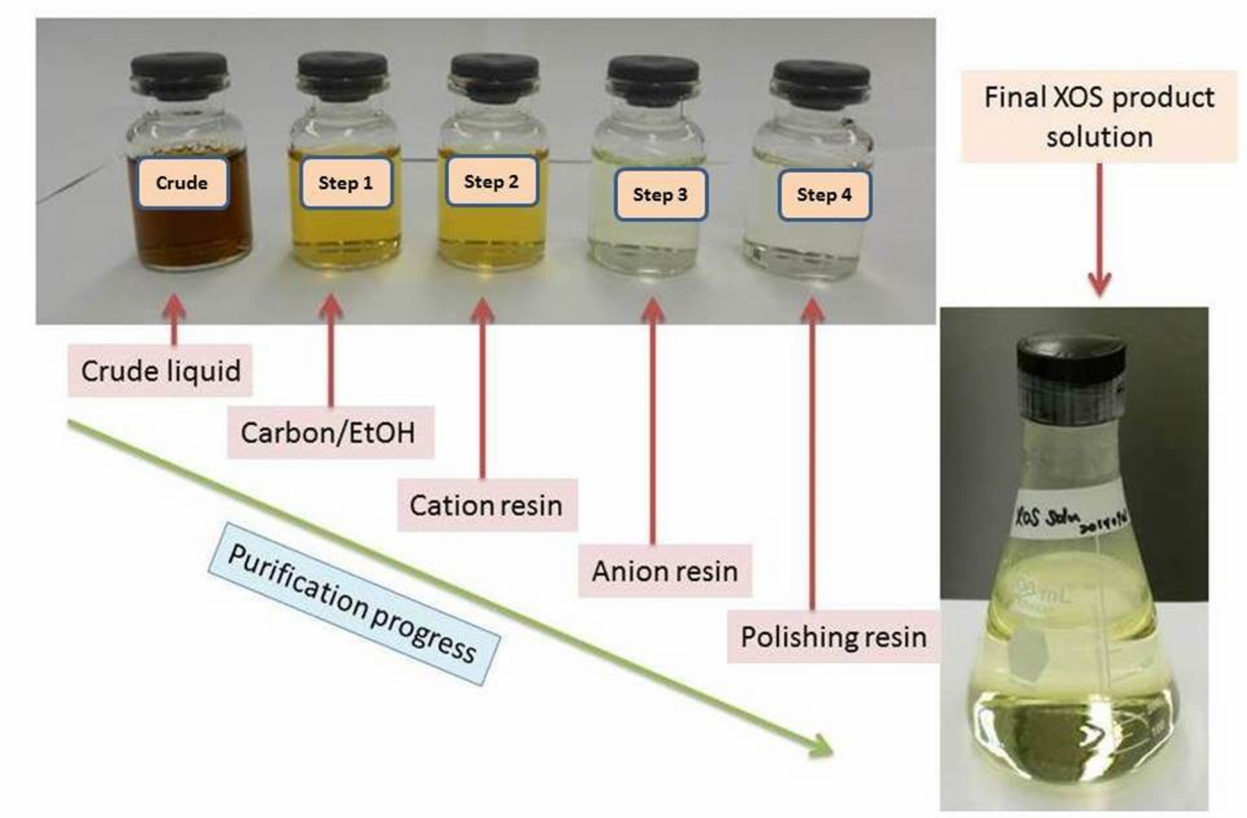

(b)

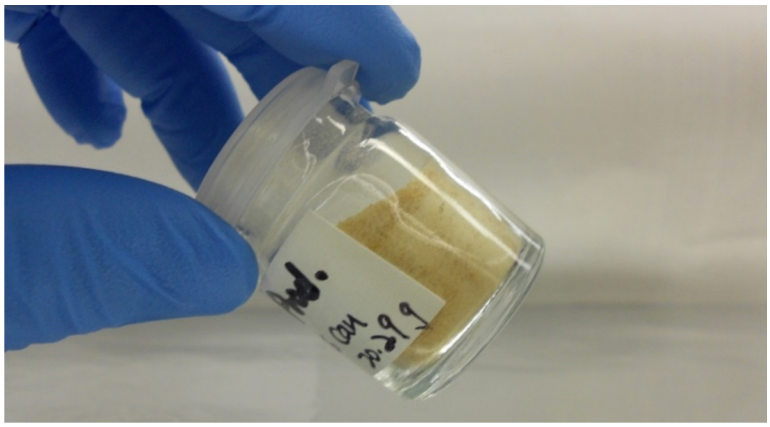

Fig. 7.3. Intermediate and end XOS products. (a) From crude XOS solution to purified solution; (b) XOS end product.

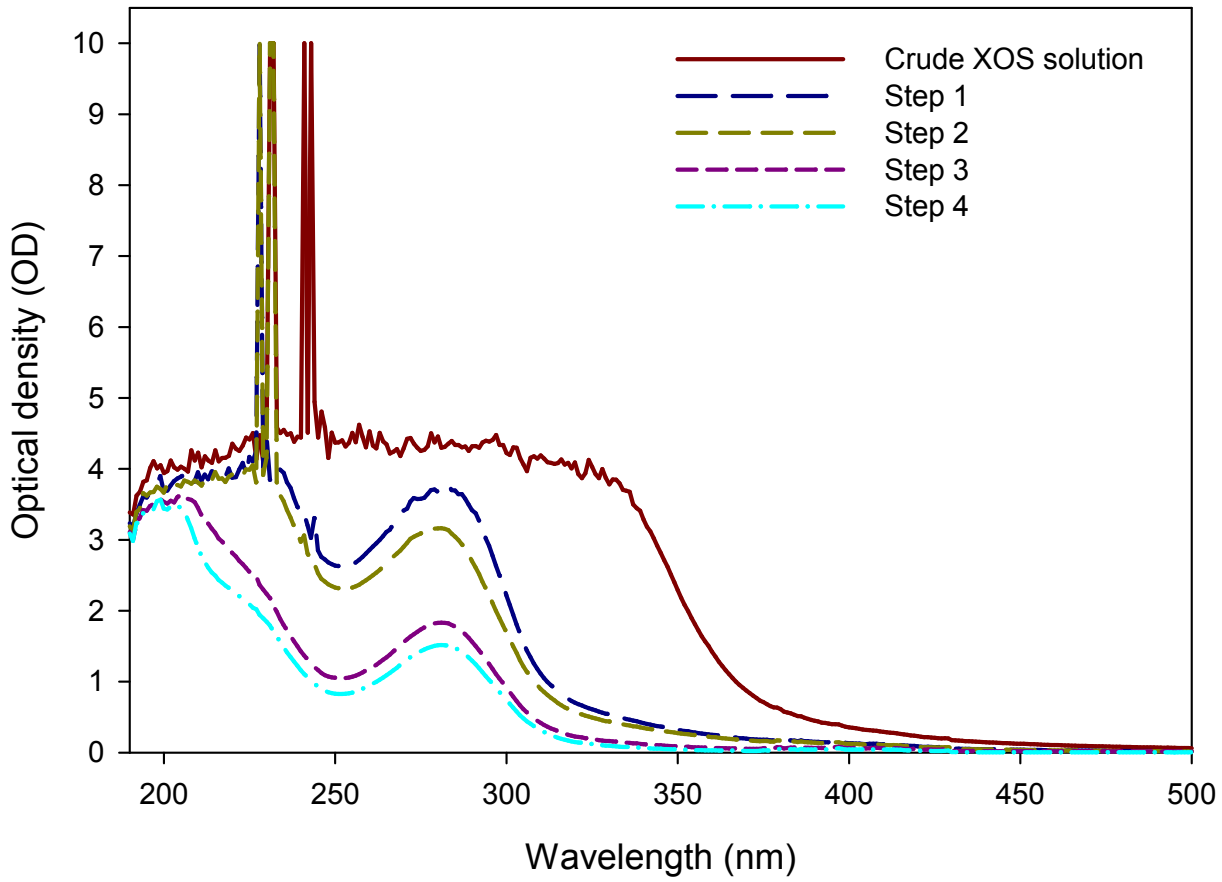

Fig. 7.4. Absorbance of XOS solutions between 200 and 500 nm.

Commercially available XOS had color from light yellow to pure white. Bleach is an option for fast reduction of color; however, it did not improve the purity and may be undesirable for a food product. The oxygen bleach method has been reported to reduce the color in XOS solution (Izumi et al., 2005). We noticed the color of the purified XOS solution turned deeper yellow even under 45°C oven drying. As a carbohydrate, XOS has a strong tendency toward colorization. The absorbance at 230 and 280 nm were used to evaluate purity and quality of XOS (Fujikawa et al., 2009). Fujikawa et al. (2009) stated a XOS purification method that produced XOS solution with absorbance less than OD 1 at 230 and 280 nm at 2% saccharide concentration; and by heating at 121°C for 6 h, the colorless XOS solution became light brown.

Detailed composition of MxG XOS and commercial Wako XOS were performed by acid hydrolysis and analyzed by HPLC (Fig. 7.5; Table 7.3). The sample was hydrolyzed in 4% H_2SO_4 to quantify sugar monomers and organic acids. With Aminex HPX-P column (the sugar column), the chromatogram revealed the major component sugars in MxG XOS were xylose, glucose and arabinose (Fig 7.5-(a)). The chromatogram from Aminex HPX-H column further validated sugar results from HPX-P column and revealed the amount of acetic acid and residual ethanol. Besides 76.6% of xylose oligomers, there were 1.5% arabinose oligomers, 4.4% glucose oligomers and 6.7% bound acetyl group. Purity of MxG XOS end product was 89.3% TSOS if oligomers of xylose, arabinose, glucose and acetyl group were included (Table 7.3). The composition of MxG XOS was compared with a commercially marketed XOS product (Wako). The amount of xylose oligomers (76.6 vs. 77.8%) were similar, but MxG XOS had less arabinose and glucose oligomers (1.5 vs. 9.4%; 4.4 vs. 6.2%) and higher bounded acetyl groups (6.7 vs. 0.0%).. Purities of MxG XOS and Wako XOS were determined to be 89.3 and 93.4%, respectively (Table 7.4).

Table 7.4. Composition of MxG XOS and Wako XOS.

Composition	MxG XOS[a]	Wako XOS
	% (w/w) of sample dry weight	
Xylose oligomer[c]	76.6 ± 1.6	77.8 ± 0.7
Arabinose oligomer[c]	1.5 ± *	9.4 ± 0.1
Glucose oligomer[c]	4.4 ± 0.1	6.2 ± 0.1
Acetyl group in oligomer	6.7 ± *	ND[b]
Total	89.3	93.4

*Standard deviation was less than 0.05.
[a]No free glucose or acetic acid was detected. pH of the MxG XOS sample is 6.3.
[b]ND = Not detected.
[c]Anhydrous monosaccharides.

(a)

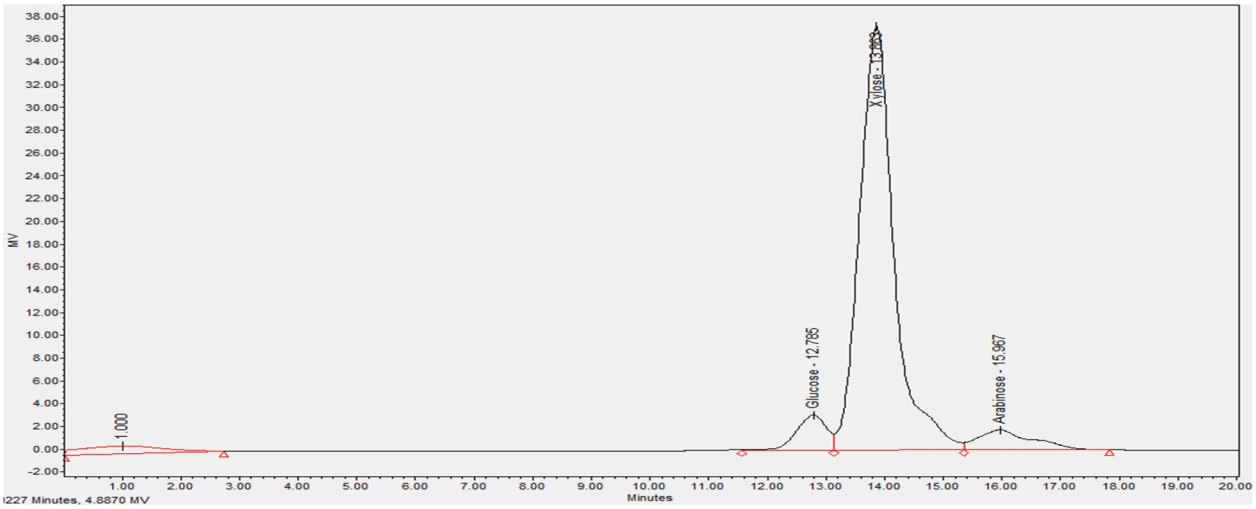

(b)

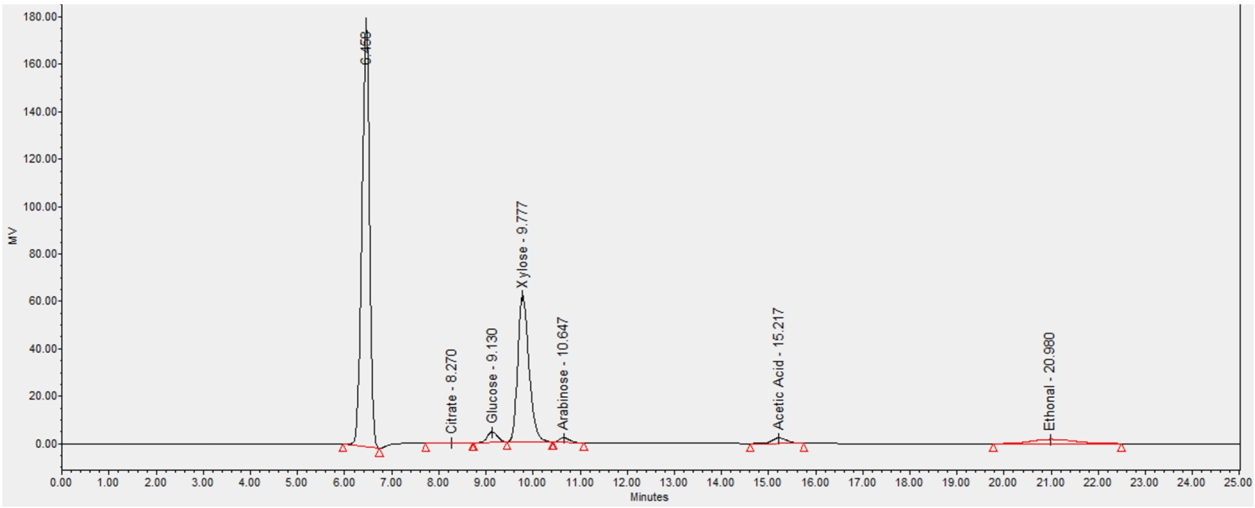

Fig. 7.5. HPLC profile of 4% acid hydrolyzed XOS end product. (a) analyzed by Bio-Rad Aminex HPX-P column; (b) analyzed by Bio-Rad Aminex HPX-H column.

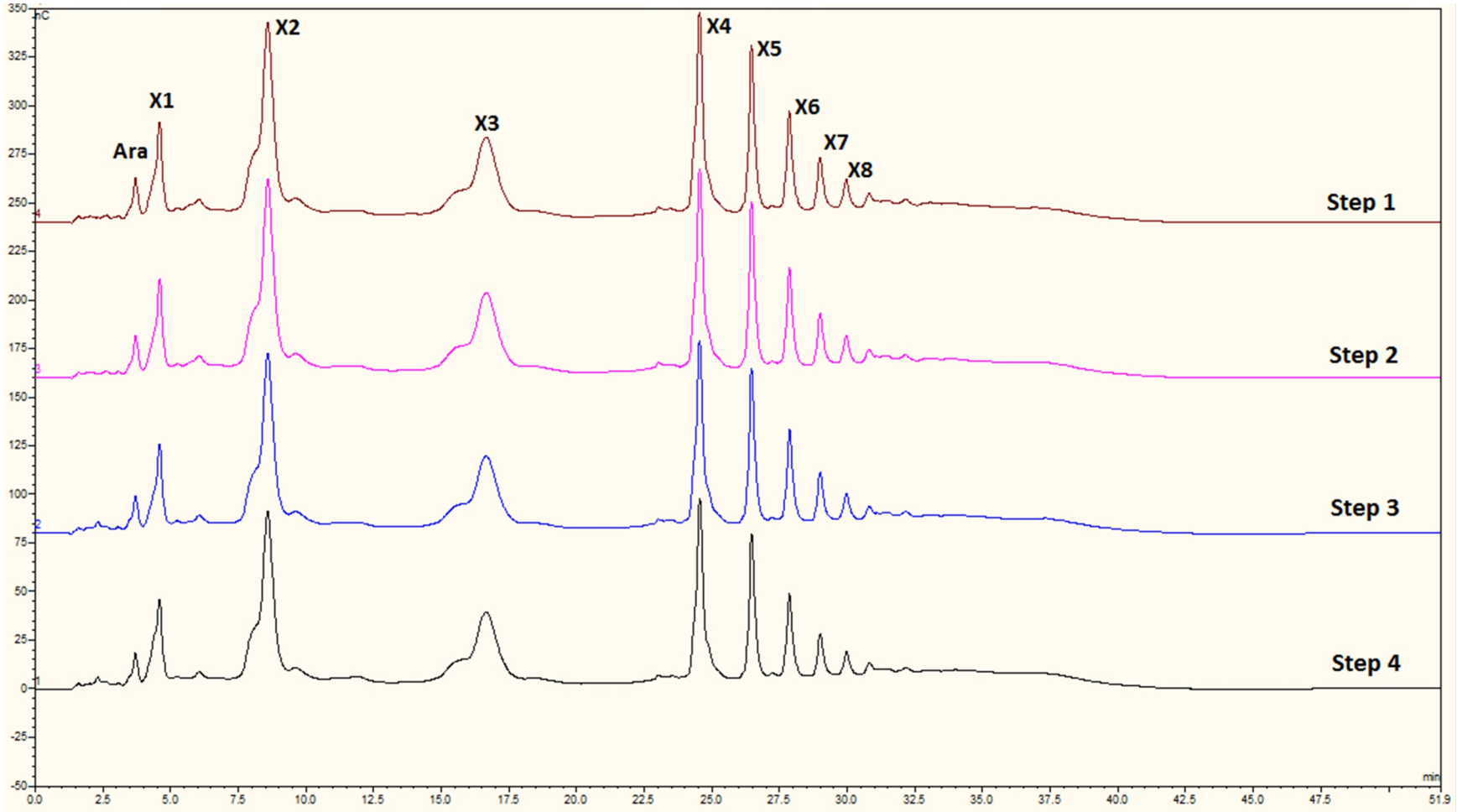

Fig. 7.6. Composition of XOS solutions in each DP during purification.

Composition separated by for MxG XOS and Wako XOS are shown (Fig 7.6) and reported in Table 7.5. As shown in Fig. 7.6, The HPAEC-PAD chromatogram revealed the ion exchange resins treatments (Step 1 to Step 4) did not change the oligomer composition. The MxG XOS product was high in X2 (xylobiose), X3 (xylotriose), X4 (xylotetraose) and X5 (xylopentaose) (Fig. 7.6). Specific amounts of each DP in MxG XOS were 1.7% xylose (X1), 8.9% xylobiose (X2), 11.3% xylotriose (X3), 8.8% xylotetraose (X4), 9.0% xylopentaose (X5) and 5.8% xylohexaose (X6) and accounted for 45.4% MxG XOS dry weight (Table 7.4). The commercial product Wako XOS was high in X2 and X3. There was 18.5% X2, 6.5% X3 and 1.5% X4, 3.2% X6 in Wako XOS.

MxG XOS and the commercial sample had similar amount of xylose, and the commercial sample had higher amounts of arabinose and glucose and a lower amount of acetyl groups. Recovery of XOS by HPAEC-PAD is incomplete because standards for xylan with sidegroups (arabinose or glucose) are not available and therefore could not be detected. Rantanen et al. (2007) reported the difference of DP3 oligomers between xylotriose and a xylobiose bound with an arabinose. The arabinose bounded XOS did not elute in HPAEC-PAD following DP; therefore, these peaks were not easy to determine and the total X1 to X6 contents (Table 7.5) were lower than overall xylan contents (Table 7.4).

Table 7.5. Composition of MxG XOS and Wako XOS in DP.

Composition	MxG XOS[a]	Wako XOS
	% (w/w) of sample dry weight	
Xylose (X1)	1.7 ± 0.4	ND[a]
Xylobiose (X2)	8.9 ± 0.2	18.5 ± 0.8
Xylotriose (X3)	11.3 ± 0.5	6.5 ± 0.5
Xylotetraose (X4)	8.8 ± 0.1	1.5 ± 0.4
Xylopentaose (X5)	9.0 ± 0.3	ND
Xylohexaose (X6)	5.8 ± 0.5	3.2 ± 0.1
Total (X1~X6)	45.4	29.7

[a]ND=Not detected.

The overall purification procedure of MxG XOS was shown in Fig. 7.7. To summarize the whole process: Dried MxG was first milled into a fine powder (comminution). Autohydrolysis was performed in the range of 160 to 200°C to break down xylan. Pretreated solid and liquid were separated by centrifugation or filtration. The pretreated solid could be used in fuel ethanol production –though ethanol fermentation was beyond the scope of this study, while the pretreated liquid was crude XOS solution. Activated carbon was added at 10% (w/v) to adsorb XOS in solution. Carbon slurry was separated by centrifugation or filtration to remove adsorbed liquid. The XOS adsorbed on carbon were eluted by ethanol solutions. Collected ethanol fractions were distilled for ethanol recycle. To remove impurities, the recovered XOS solution was treated with strong cation exchange resin, weak anion exchange resin and polishing resin in sequence. The polished solution was dried and milled to obtain MxG XOS.

Vázquez et al. (2005, 2007) recovered XOS from *Eucalyptus globulus* (Table 7.6) with the combination of vacuum evaporation, solvent precipitation, and solvent extraction to recover TSOS of 70.6 to 82.2% purity (Fig. 7.8). Vegas et al. (2006) used a combination of nanofiltration, solvent extraction and ion exchange chromatography to recover 90.7% TSOS purity. Gullón et al. (2010) improved the method from their previous report (Gullón et al., 2008) and used a combination of diafiltration, concentration, ultrafiltration and ion exchange chromatography to recover 90.7% TSOS purity (Fig. 7.9). We adopted the carbon adsorption to substitute for the energy and capital intensive membrane filtration step; the ethanol can be recovered and resused; the final purity of the MxG XOS was similar to other reported purities.

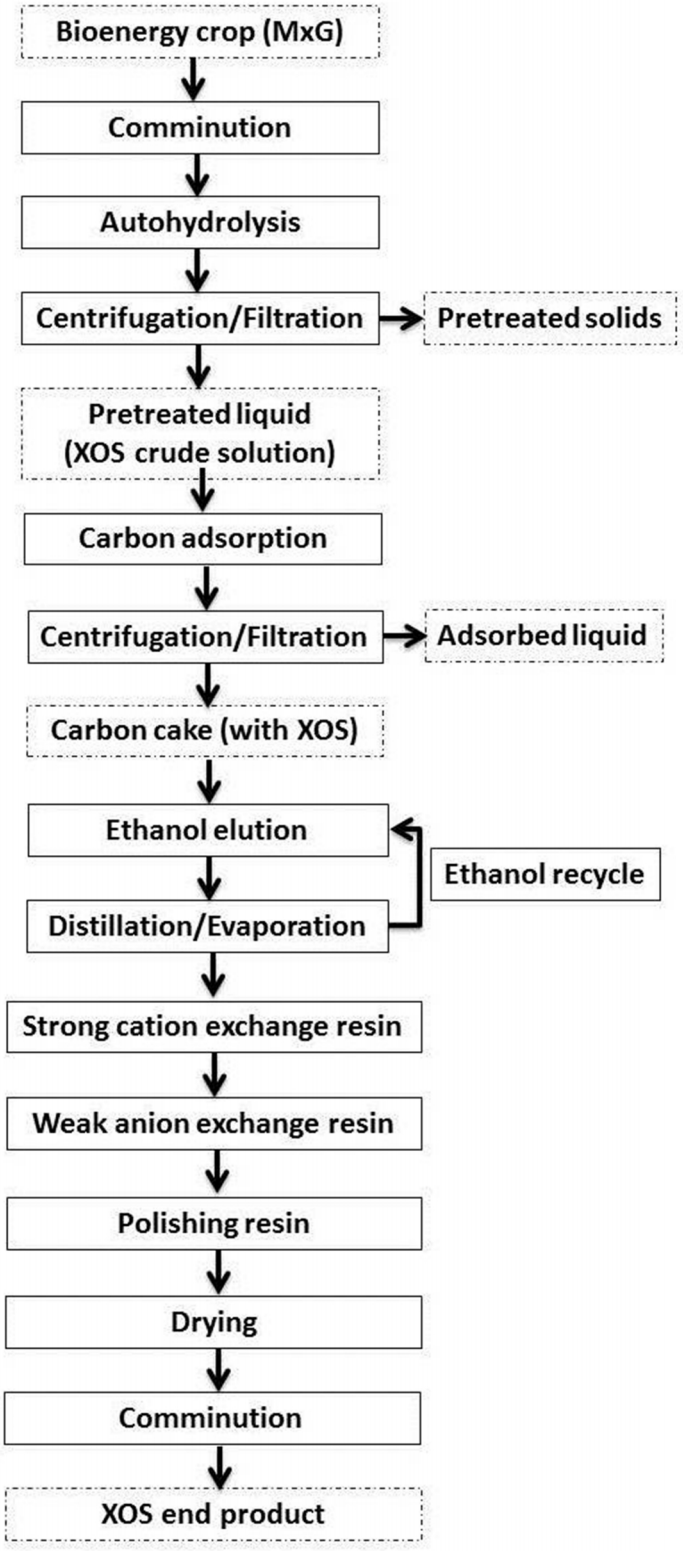

Fig. 7.7. Schematic diagram of XOS produced and purified from bioenergy crop.

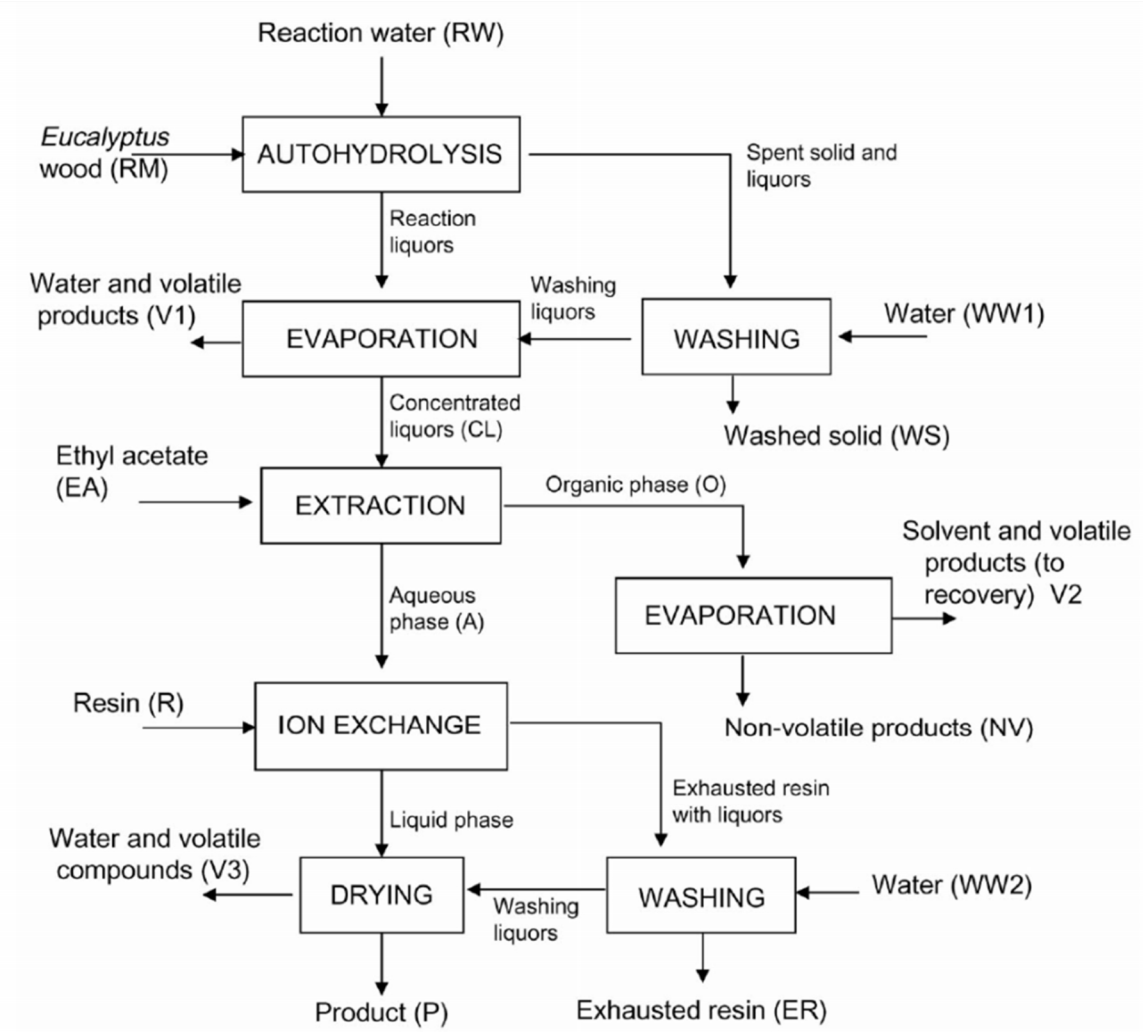

Fig. 7.8. Comparison of XOS purification procedure with published reports (Vázquez et al., 2007).

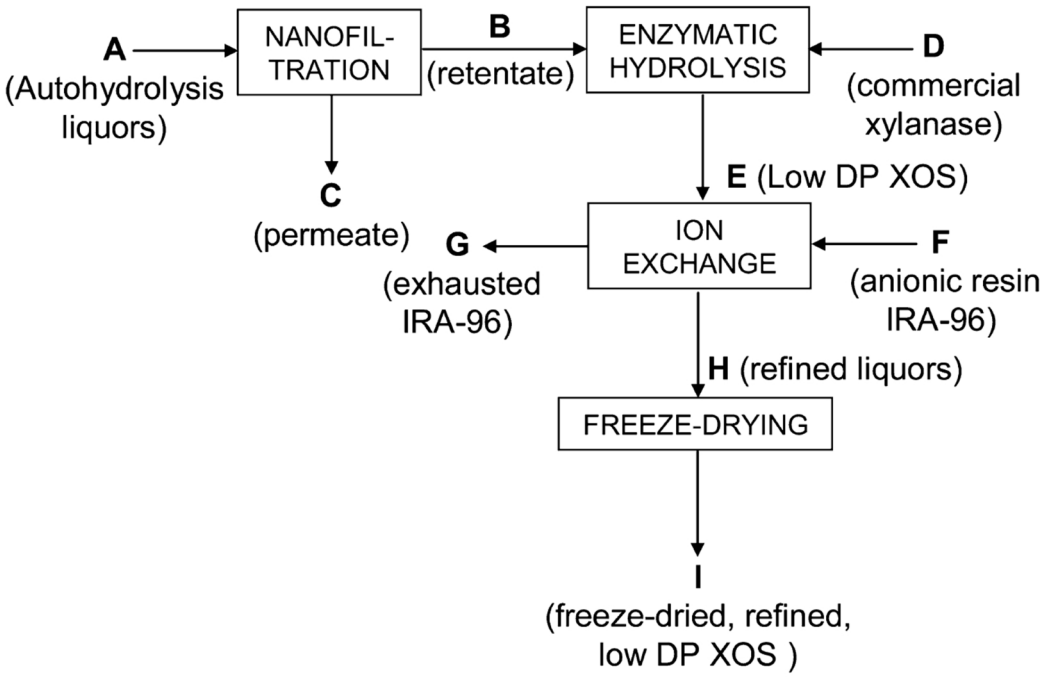

Fig. 7.9. Comparison of XOS purification procedure with published reports (Gullón et al., 2008).

Table 7.6. Comparison of XOS end product with other published reports.

Raw material	TSOS[a] % of DM	DP1 % of DM	Main purification strategy	Source
Miscanthus x giganteus	89.3	1.7	Carbon adsorption, ethanol elution, ion exchange chromatography	This study
Eucalyptus globulus	70.6 to 82.6	2.8	Vacuum evaporation, precipitation, solvent extraction,	Vázquez et al. (2005)
Rice husks	90.7	2.0	Nanofiltration, solvent extraction, ion exchange chromatography	Vegas et al. (2006)
Eucalyptus globulus	72.8	16.3	Evaporation, solvent extraction, ion exchange chromatography	Vázquez et al. (2007)
Rice husks	74.9	1.2	Nanofiltration, enzymatic hydrolysis, ion exchange chromatography	Gullón et al. (2008)
Rice husks	90.7	0.6	Diafiltration, concentration, ultrafiltration, ion exchange chromatography	Gullón et al. (2010)

[a]TSOS, total substituted oligosaccharides.
TSOS%= % of (glucooligosaccharides + xylooligosaccharides + arabinooligosaccharides + acetyl groups + uronic acids).

7.4 Conclusions

MxG harvested in 2012 had similar cell wall composition and XOS production kinetics as 2011. The carbon adsorption and ethanol elution steps were successfully scaled up to 2 L. An XOS purification procedure combined with ion exchange resin treatments following carbon adsorption and ethanol elution was investigated. During three stages of resin treatments, the oligomer composition remained similar. The colorants of XOS solution were removed as OD declined during purification. The end product MxG XOS was composed of 76.6% xylose oligomer, 1.5% arabinose oligomer, 4.4% glucose oligomer and 6.9% acetyl groups. MxG XOS had 1.7% X1, 8.9% X2, 11.3% X3, 8.8% X4, 9.0% X5 and 5.8% X6 and were different from commercial Wako XOS product, which was consisted of X2 and X3.

Chapter 8. Pure culture fermentations of xylooligosaccharides from *Miscanthus x giganteus* by *Bifidobacterium adolescentis* and *Bifidocbacterium catenulatum*

8.1 Introduction

Xylooligosaccharides (XOS) are classified as nondigestible oligosaccharides (NDO) because they cannot be digested by gastrointestinal enzymes and are instead utilized gut microorganisms. Ingestion of NDO stimulates growth of beneficial gut bacteria such as *Bifidobacterium* spp. and *Lactobacillus* spp. Because of composition and structure differences, prebiotic effects of NDO vary with sources and processing methods. Some substituted XOS are reported to be minimally utilized by beneficial bacteria (Aachary and Prapulla, 2011).

Bifidobacterium spp. is a primary bacteria genus naturally present in the human colon. They represent up to 25% of the cultivable bacteria in adult fecal samples. Since the early 20th century, researchers have evidence that *Bifidobacterium* spp. was beneficial to health and are grouped along with *Lactobacillus* spp. as probiotics. *Bifidobacteria* functions in the gut as a barrier against infectious microbes, inhibits pathogens, simulates the immune response, and generates short chain fatty acid (SCFA). There are usually $10^{9.4}$ cell/g of *Bifidobacterium* genus in human feces including species such as *B. adolescentis* ($10^{9.1}$ cell/g), *B. angulatum* ($10^{6.6}$ cell/g), *B. bifidum* ($10^{8.3}$ cell/g), *B. breve* ($10^{7.3}$ cell/g), *B. catenulatum* ($10^{8.9}$ cell/g), *B. longum* ($10^{8.1}$ cell/g) and *B. infantis* ($10^{6.9}$ cell/g) (Picard et al., 2005). *B. adolescentis* and *B. catenulatum* are two prelevent species within the population (Palframan et al., 2003); therefore, these two strains were selected as model bacteria for pure culture growth experiments using MxG XOS.

The objective was to elucidate the utilization of MxG XOS by *Bifidobacterium* spp. The purified MxG XOS from Chapter 7 was cultured with *B. adolescentis* and *B. catenulatum in vitro* for 24 h. Cell growth (OD), specific growth rate (μ, h^{-1}), total xylose consumption (% w/w) and oligomers preference were monitored.

8.2 Material and Methods

8.2.1 Substrates and chemicals

MxG XOS, prepared as described in Chapter 7, powder had 76.6% (w/w) XOS and 89.3% (w/w) total substituted oligosaccharides (TSOS), 1.5% ash and 12.1% moisture. A commercial XOS (Wako XOS) sample was purchased from Wako Chemicals USA (Richmond, VA) for comparison. The Wako XOS had 77.8% (w/w) XOS and 93.4% TSOS, 0.03% ash and 4.9% moisture. High purity xylobiose (X2), xylotriose (X3), xylotetraose (X4), xylopentaose (X5) and xylohexaose (X6) were purchased from Megazyme International (Wicklow, Ireland) as standards for quantating XOS using a high performance anion exchange chromatography with pulsed amperometric detection(HPAEC-PAD) system. All chemicals and laboratory reagents, unless stated otherwise, were of analytical quality and purchased from Fisher Scientific (Springfield, NJ).

8.2.2 Bacteria strains and media preparations

B. adolescentis DSM 20083 and *B. catenulatum* DSM 16922 were obtained from the DSMZ culture collection (DSMZ, Braunschweig, Germany). Strain selection was based on previous results of xylan utilization (Palframan et al., 2003). Strains were cultured anaerobically in a modified RGM medium (mRGM) which was supplemented with 0.5% (w/v) XOS sample as the carbon source. The mRGM removed short chain volatile fatty acid (VFA) from the formula, and the yeast extract and trypticase were reduced to half amount (Hespell et al., 1987; Cotta et al., 1993). The composition of mRGM medium is shown in Table 8.1. XOS samples were dissolved in boiled dH_2O to form 20% (w/v) stock solutions. Stock solutions were cooled under N_2 gas, filtered-sterilized and stored in sterile anaerobic bottles that were flushed with N_2. To prepare culture medium with 0.5% substrates, 0.25 mL of stock solution was added into 10 mL mRGM medium.

Table 8.1. Composition of modified RGM medium (Hespell et al., 1987).

Components	Amt/100 mL
Trypticase	0.15 g
Yeast extract	0.1 g
Mineral solution no. 1[a]	5.0 mL
Mineral solution no. 2[b]	5.0 mL
Trace mineral solution (R1 salts)[c]	0.1 mL
Resazurin (0.1% w/v)	0.1 mL
L-Cysteine hydrochloride-sodium sulfide•9 H_2O (2.5% w/v)	1.0 mL
Sodium carbonate (8% w/v)	2.0 mL
Hemin-naphthoquinone (0.01% w/v)	1.0 mL
Distilled water	81.0 mL

[a]Composition: 0.3% K_2HPO_4; [b]Composition: 0.3% KH_2PO_4, 0.6% $(NH_4)_2SO_4$, 0.6% NaCl, 0.06% $MgSO_4$ and 0.06% $CaCl_2$. [c]Composition: 75 mL of salt solution with tetrasodium ethylenediamine tetraacetate, 1 g; $CaCl_2$•$2H_2O$, 3.75 g; $MgCl_2$•$6H_2O$, 12.5 g; $FeSO_4$•$7H_2O$, 0.5 g was added with 25 mL of trace element solution. Trace element solution was prepared by $SnCl_2$•$2H_2O$, 0.30 g; $BaCl_2$•$2H_2O$, 0.30 g; $CoCl_2$•$6H_2O$, 1.0 g in 3600 mL.

8.2.3 *In vitro* fermentation

The bacteria were cultured at 37°C for 24 h with 0.5% respective XOS substrate. Each culture tube was then inoculated with 0.5 mL of the overnight growth. Three replicates were prepared for each combination of bacterium and XOS sample. Fermentation was carried on at 37°C in an aerobic chamber and sampled at 0, 1, 2, 3, 4, 5, 6, 7, 8 and 24 h. At each sampling point, one mL aliquot was divided into 0.75 mL and 0.25 mL for total xylose determination and HPAEC-PAD analysis, respectively. Cells were removed by centrifugation; supernatant was stored at -20°C until analyzed.

8.2.4 Measurement of bacteria growth

Bacterial growth was determined by monitoring optical density (OD) at 660 nm using a Vis spectrophotometer (Spectronic 21, Milton-Roy Co., Rochester, NY). The maximum specific

growth rate (μ_{max}) was calculated based on logarithm values recorded of OD during bacterial exponential growth stage.

8.2.5 Determination of XOS utilization

Total XOS utilization during fermentation was determined by orcinol assay. Orcinol reagent was prepared by one gram of orcinol dissolved in 100 mL of concentrated HCl containing 0.5 g of $FeCl_3$ (Schneider, 1957). The colorimetric assay was quantified at OD 660 nm, and a standard curve was developed using xylose (Hespell et al., 1987; Cotta et al., 1993).

8.2.6 HPAEC-PAD analysis of oligomer degradation

Filtered culture media were analyzed for oligomer consumption by high performance anion exchange chromatography with a pulsed amperometric detection system. (HPAEC-PAD, Dionex ICS 3000, Sunnyvale, CA). Twenty five mL diluted filtrate (diluted 1:20 with milliQ water) were analyzed by HPAEC-PAD utilizing a Dionex PA-100 column (22 x 30 mm, Dionex) (Chapter 7).

8.3 Results and Discussion

8.3.1 Growth of *B. adolescentis* and *B. catenulatum* with MxG XOS and Wako XOS

Both strains, *B. adolescentis* and *B. catenulatum*, were able to grow on mRGM media with 0.5% (w/v) MxG XOS (Fig.8.1). *B. adolescentis* grew faster and reached a maximum OD of 0.55 within 24 h and a maximum specific growth rate (μ_{max}) at 0.69 h^{-1} (Table 8.2). *B. catenulatum* growth was slower and the final OD less than for *B. adolescentis*. The maximum OD of 0.29 was reached at 24 h and the net specific growth rate from 2 to 4 h of fermentation was 0.33 h^{-1} (Table 8.2).

Similarly, *B. adolescentis* grew faster than *B. catenulatum* when cultured with Wako XOS (Fig. 8.2). *B. adolescentis* reached OD 0.73 at 24 h and has a maximum specific growth rate (μ_{max}) of 0.63 h^{-1} (Table 8.2). Unlike cultured with MxG XOS, *B. catenulatum* attained

stationary phase at 8 h; the OD value reached 0.56 at 24 h and maximum specific growth rate was 0.68 h^{-1} (Table 8.2).

B. adolescentis and *B. catenulatum* have been reported to utilize XOS and xylose for proliferation. Palframan et al. (2003) tested *B. adolescentis* DSM 20083 and *B. catenulatum* DSM 20103 for growth on glucose, xylose, XOS and xylan. *B. adolescentis* DSM 20083 preferred glucose, but had similar growth on XOS and xylose; *B. catenulatum* DSM 20103 preferred xylose over glucose and had high cell growth in XOS. Moura et al. (2007) cultured *B. adolescentis* DSM 20083 with commercial XOS (Xylo-Oligo95P, Suntory, Osaka, Japan) and attained a maximum growth of OD 0.7 at substrate concentration of 0.5% (w/v) that was similar to Wako XOS fermentation in this study. Pastell et al. (2009) used Wako XOS and arabinoxylan derived oligosaccharides to culture with *B. adolescentis* ATCC 15703 (DSM 20083). *B. adolescentis* ATCC 15703 was not able to grow in arabinose but could grow in XOS. However, the growth rate became slow with the presence of xylose monomers. Our results were similar to Palframan et al. (2003), the slower growth of *B. catenulatum* may indicate strain differences in XOS utilization among species.

Table 8.2. Maximum absorbances (A_{max}) and maximum specific growth rate (μ) determined for *B. adolescentis* and *B. catenulatum* growing in media containing XOS.

		Bifidobacterium aldolescentis		*Bifidobacterium catenulatum*	
Substrate	Amount	Max OD	μ_{max}, h^{-1}	Max OD	μ_{max}, h^{-1}
MxG XOS	0.5%	0.55 ± 0.01	0.69 ± 0.08	0.29 ± 0.05	0.33 ± 0.06[a]
Wako XOS	0.5%	0.73 ± 0.05	0.63 ± 0.03	0.56 ± 0.02	0.68 ± 0.05

[a]Calculated as μ_{net} from 2 to 4 h of fermentation.

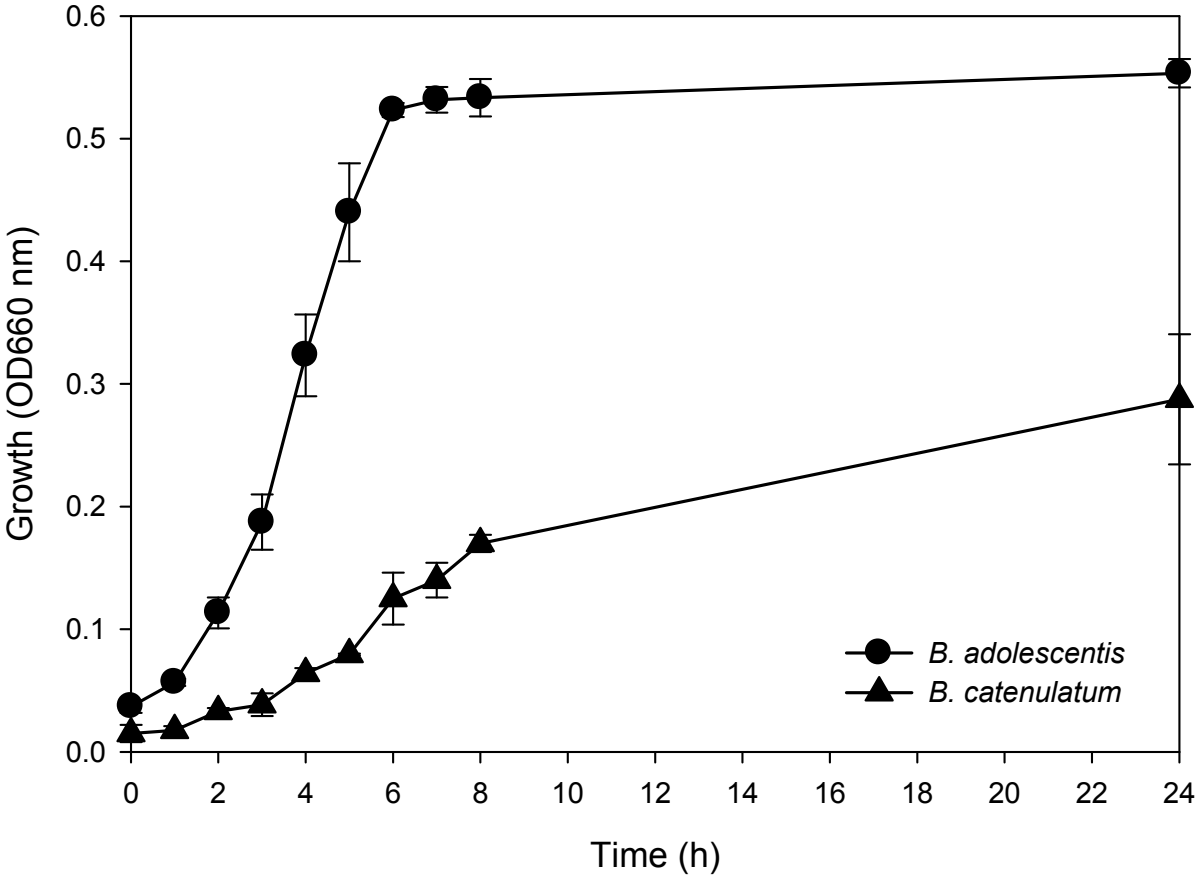

Fig. 8.1. Growth of *Bifidobacterium adolescentis* and *Bifidobacterium catenulatum* in nutrient base medium supplemented with MxG XOS.

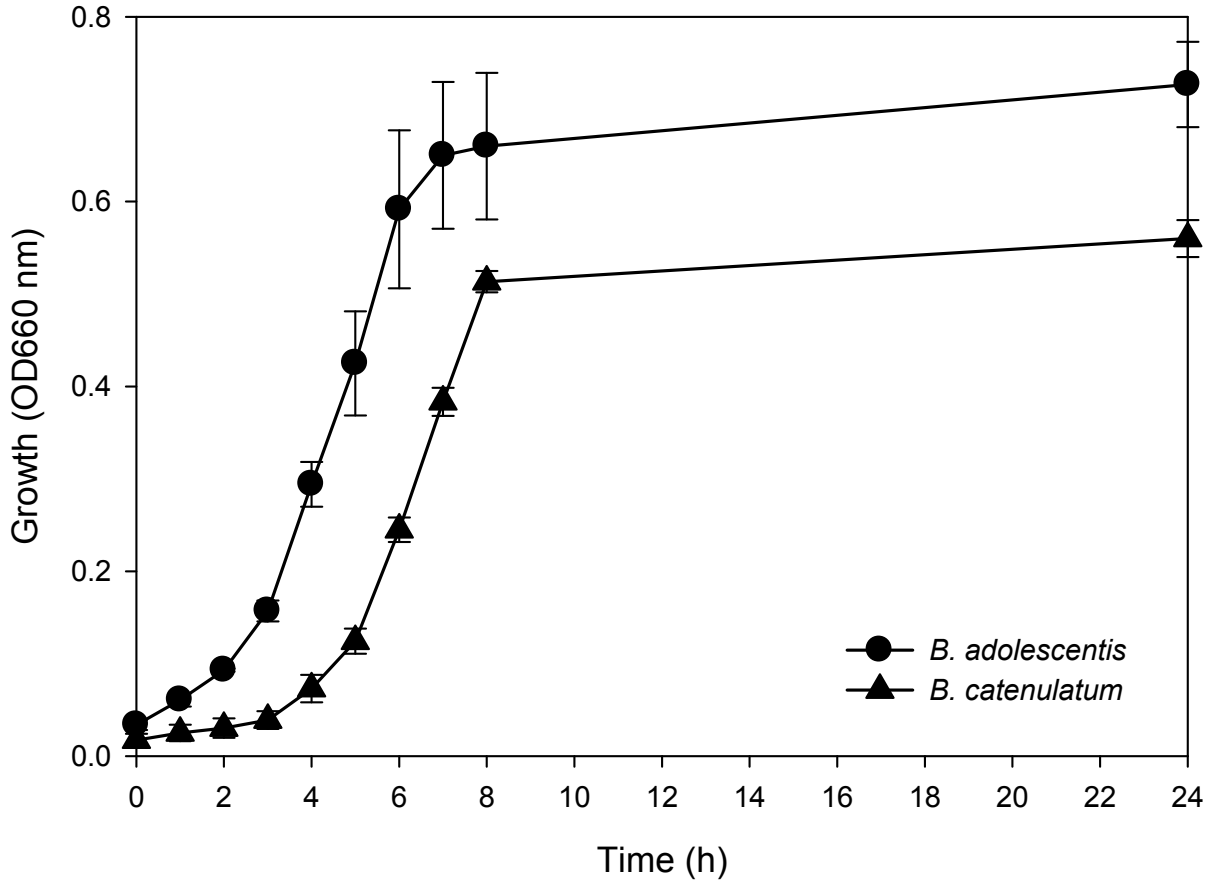

Fig. 8.2. Growth of *Bifidobacterium adolescentis* and *Bifidobacterium catenulatum* in nutrient base medium supplemented with Wako XOS.

8.3.2 Substrate consumption during culture

Total XOS consumption for the *B. adolescentis* culture is shown in Fig. 8.3. The residual XOS concentration in the medium was determined by reaction with orcinol reagent and expressed as total xylose based upon a xylose calibration curve. Beginning with 5.5 mg/mL of xylose in MxG XOS, the total xylose concentration decreased rapidly from 2 to 6 h corresponding to exponential growth of cell mass. At the end of fermentation, 0.9 mg/mL of xylose (15.9% of the initial amount) was remained in the medium. The Wako XOS culture started with a lower initial xylose at 4.5 mg/mL and decreased from 3 to 8 h. At the end of fermentation, 0.7 mg /mL of xylose (15.2% of the initial amount) was remained in the medium.

Total XOS utilization, cultured with *B. catenulatum*, is shown in Fig. 8.4. Starting from 4.9 mg/mL of initial xylose, the total xylose concentration decreased continuously from 0 to 24 h. At the end of fermentation, 1.2 mg/mL of xylose (23.4% of the initial amount) was remained in the medium. The Wako XOS medium started with a lower concentration of 4.4 mg/mL and decreased from 4 to 8 h. At 24 h, 1.1 mg/mL of xylose (26.4% of the initial amount) was remained in the medium.

The orcinol reagent includes concentrated HCl that dehydrates pentose (e.g. xylose) into furfural. The furfural can react with two molecules of orcinol to form color substance. With the presence of ferric ion, the solution resulted in green and blue color. The assay also reacted with hexose and formed a muddy brown solution. Though the oricinol assay has been used in xylose determination, results were overestimated. The reagent reacted with other pentoses such as arabinose equally. However, the results were parallel to actual xylose concentration (Hespell et al., 1987; Cotta et al., 1993).

From the growth and substrate consumption during fermentation, *B. adolescentis* produced more cell mass in theWako XOS than the MxG XOS cultures. The specific growth rate was similar for both XOS samples. The growth of *B. adolescentis* in MxG XOS entered stationary phase earlier at 6 h than 8 h in Wako XOS. Total xylose consumption corresponded to the growth curve. *B. catenulatum* grew slowly in the MxG XOS but appeared to grow well on the Wako XOS. The total sugar utilizations were similar between two XOS samples but this was

not reflected in cell growth either because of the presence of non-pentose growth factors and or growth on MxG required the cell to expend further energy for non-growth related activities.

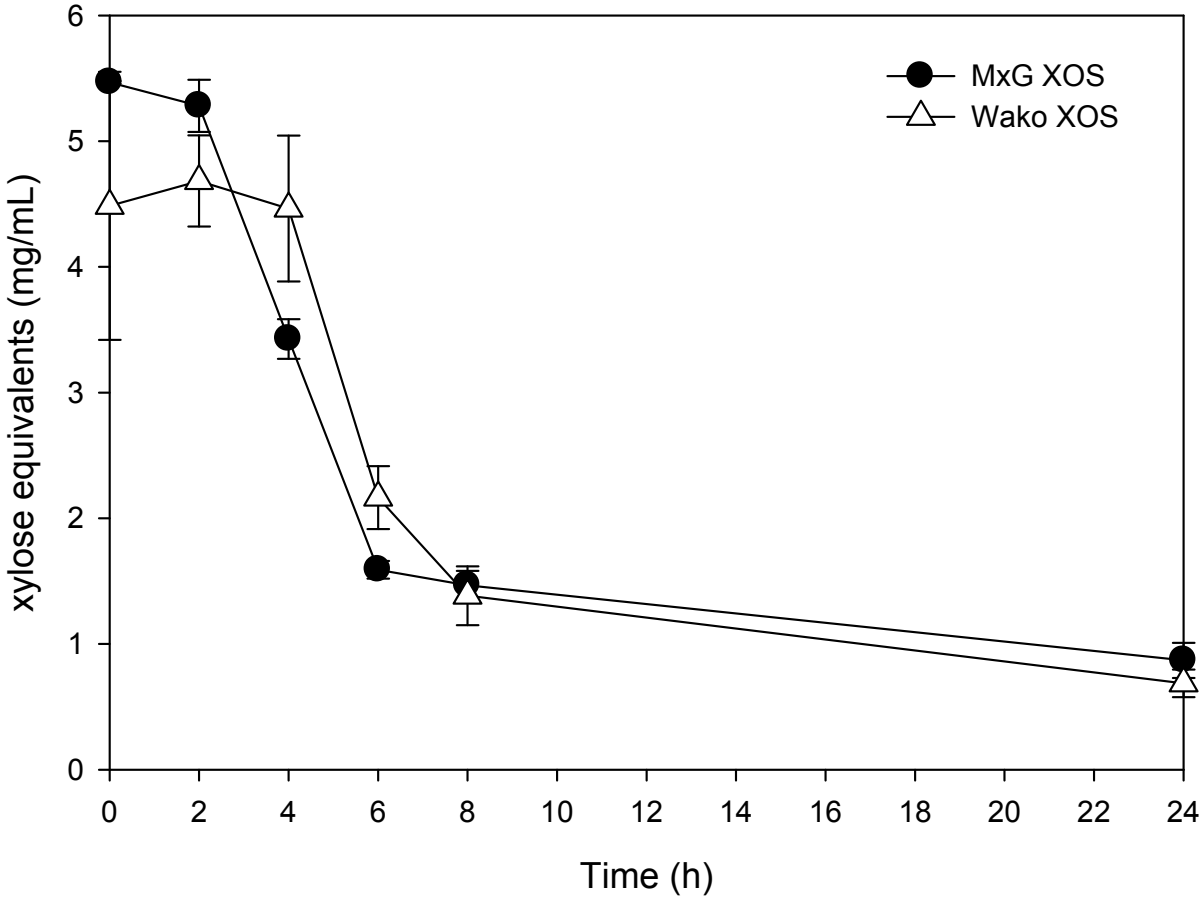

Fig. 8.3. Total xylose consumption during culture with *B. adolescentis.*

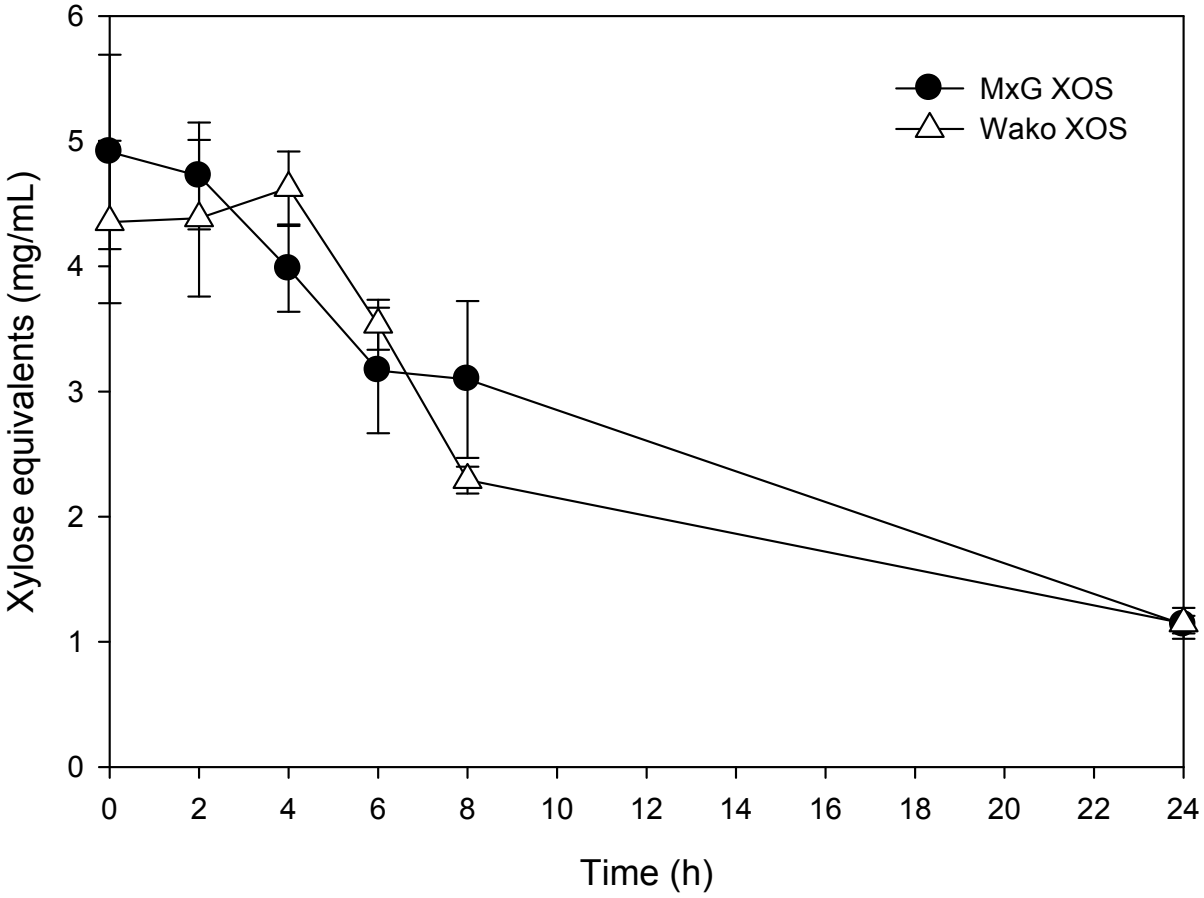

Fig. 8.4. Total xylose consumption during culture with *B. catenulatum*.

8.3.3 Time profile of XOS oligomers in *B. adolescentis* and *B. catenulatum* growth cultures.

Oligomer consumption during fermentation of MxG XOS is shown in Figs. 8.5 and 8.6. For *B. adolescentis*, the concentration of X2, X3 and X4 decreased rapidly at the beginning of fermentation and was almost depleted at 8 h. The concentration of X1 increased from 200 to 309 µg/mL from 0 to 6 h and decreased to 96 µg/mL at 24 h. X5 and X6 concentrations were slower decreasing compared with X2 to X4 oligomers. At the end of fermentation, the concentrations of XOS were 94.9% X2, 97.5% X3, 95.0% X4, 39.9% X5 and 34.1% X6 lower than at the beginning. The HPAEC-PAD chromatogram further validated that X2, X3 and X4 were depleted at 24 h but for higher DP, X5, X6, X7 and X8, the utilizations were slower (Fig. 8.7). For *B. catenulatum*, X3 concentration decreased rapidly and was followed by X2 and X4. X1 kept accumulating in the medium after 2 h and reached 886.9 µg/mL at 24 h. X5 and X6 were slower decreasing compared with X2 to X4 oligomers. At the end of fermentation, 90.4% X2, 97.7% X3, 87.2% X4, 50.4% X5 and 52.8% X6 lower than at the beginning. The HPAEC-PAD chromatogram revealed the depletion of X2, X3 and X4 with residual concetrations of X5, X6, X7 and X8 and the accumulation of X1 (Fig. 8.8).

Oligomer consumption during fermentation of Wako XOS is shown in Figs. 8.9 and 8.10. Unlike MxG XOS, the Wako XOS was mainly composed of X2 (899.5 to 948.1 µg/mL) and X3 (300.2 to 348.8 µg/mL) and only minor amounts of X4 and X5. For *B. adolescentis*, the concentration of X2 and X3 decreased rapidly after 2 h, which corresponded to exponential cell growth. X2 and X3 were depleted at 8 h. Accumulation of X1 was observed for 0 to 6 hr and then decreased to 73.8 µg/mL at 24 h. At the end of fermentation, 97.7% X2 and 95.6% X3 were utilized. Unexpected increases in X5 and X6 concentrations were observed at the end of fermentation; by comparison with HPAEC-PAD chromatogram, the X5 and X6 peaks appeared after 8 h of fermentation (Fig. 8.11). For *B. catenulatum*, the concentration of X2 decreased immediately after inoculation. The utilization of X2 and X3 slowed at 8 h. At the end of fermentation, 96.0% X2 and 96.2% X3 were utilized. Accumulation of X1 was observed and maintained at high concentration to the end of fermentation. Increases of X4, X5 and X6 concentrations were found at 24 h (Fig. 8.12).

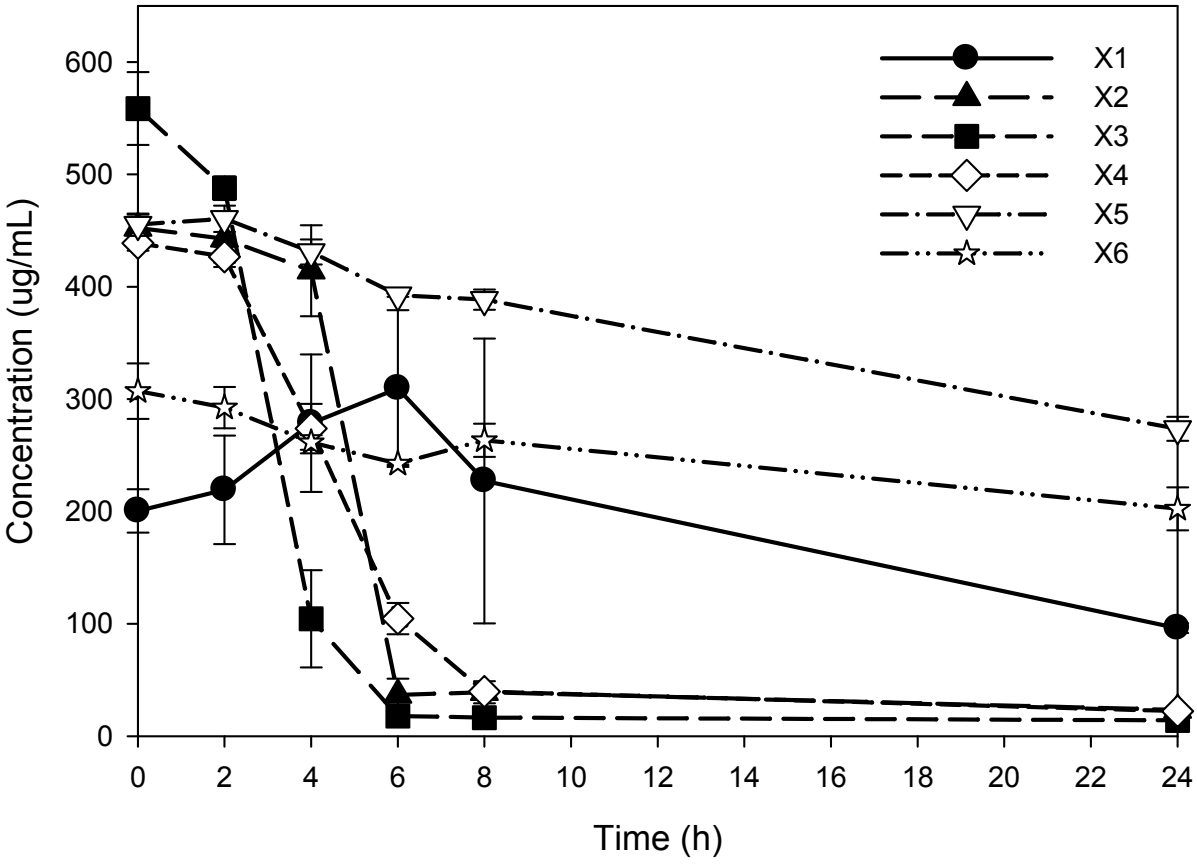

Fig. 8.5. Time course of MxG XOS oligomers consumed during fermentation with *B. adolescentis*.

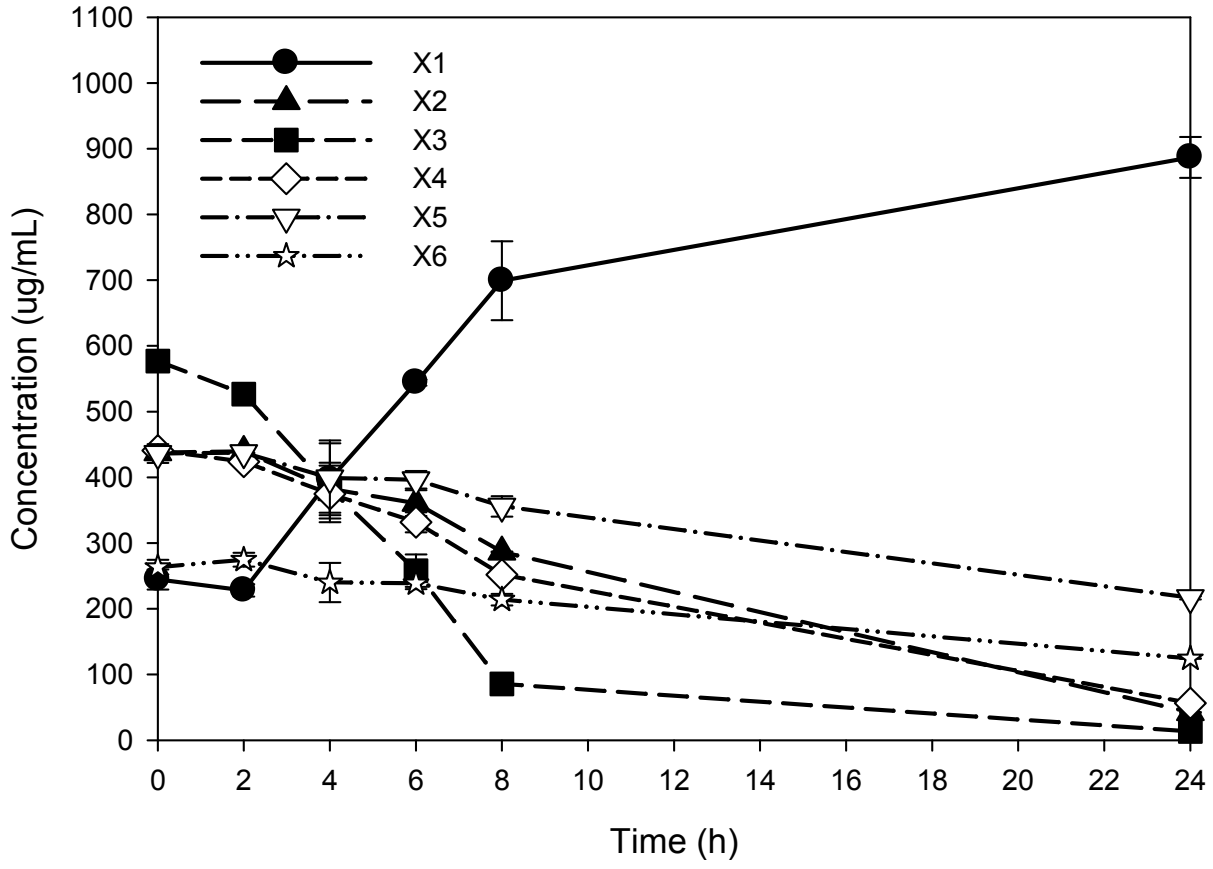

Fig. 8.6. Time course of MxG XOS oligomers consumed during fermentation with *B. catenulatum*.

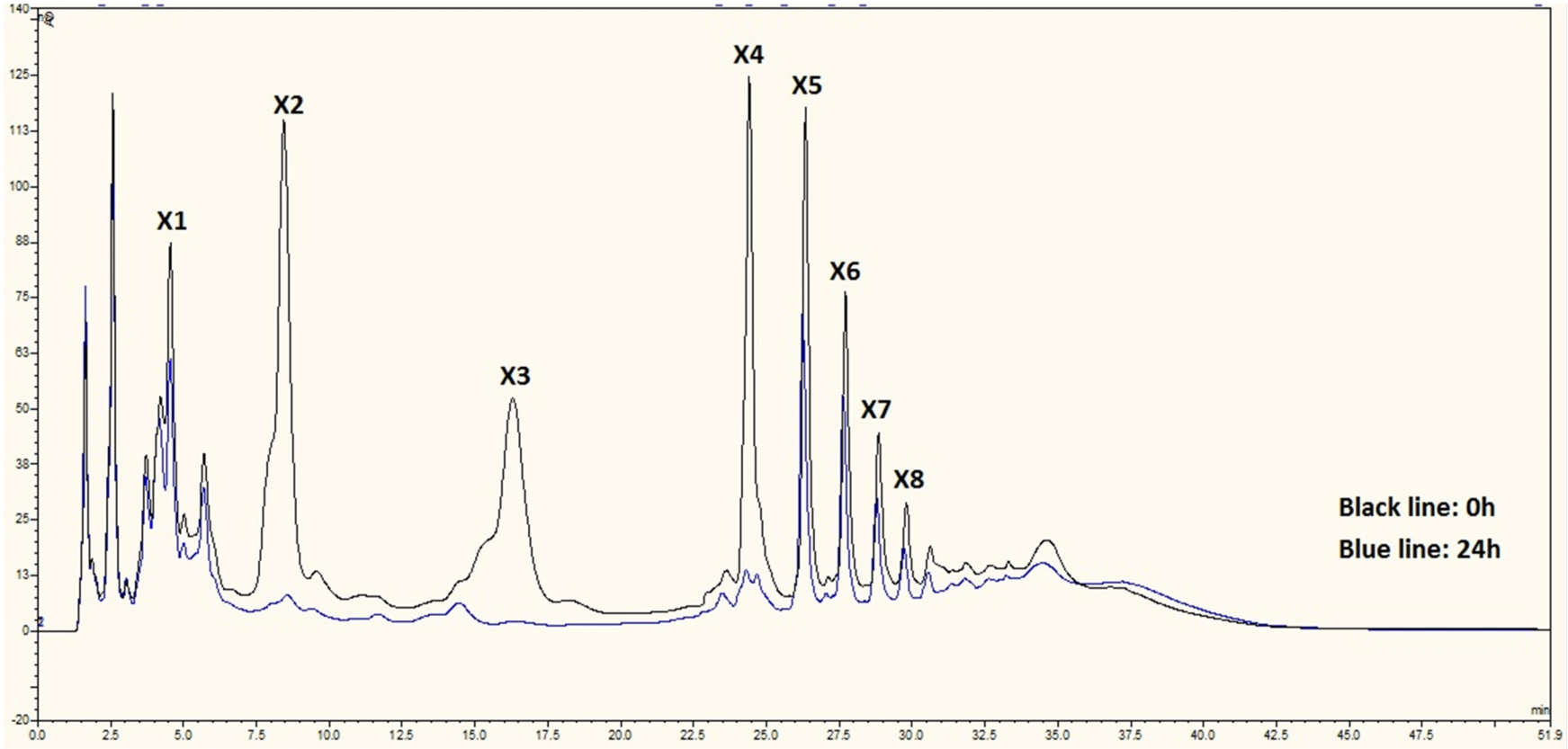

Fig. 8.7. HPAEC-PAD chromatograms of MxG XOS containing media fermented with *B. adolescentis* used to determine which DP of XOS were unutilized.

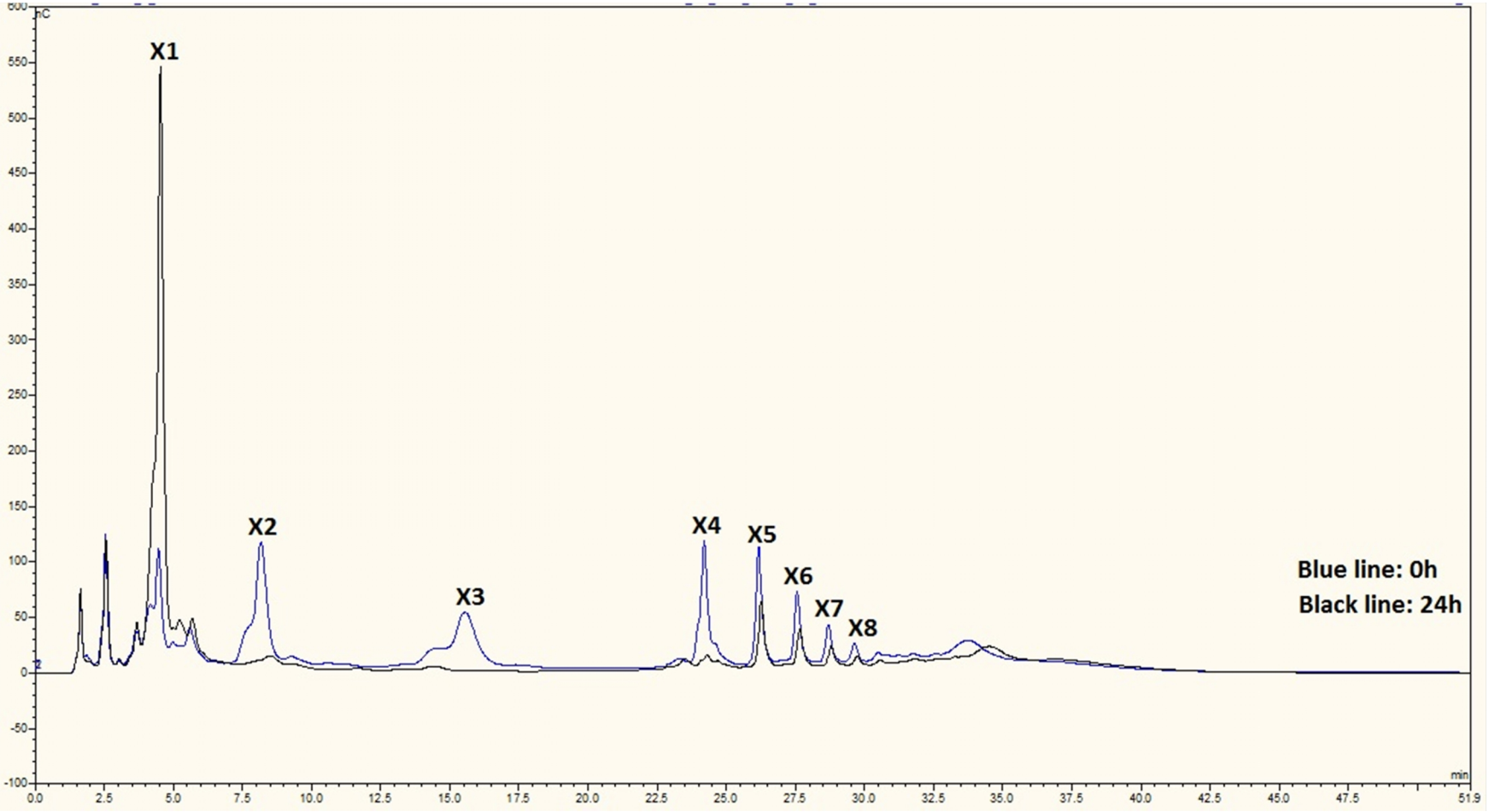

Fig. 8.8. HPAEC-PAD chromatograms of MxG XOS containing media fermented with *B. catenulatum* used to determine which DP of XOS were unutilized.

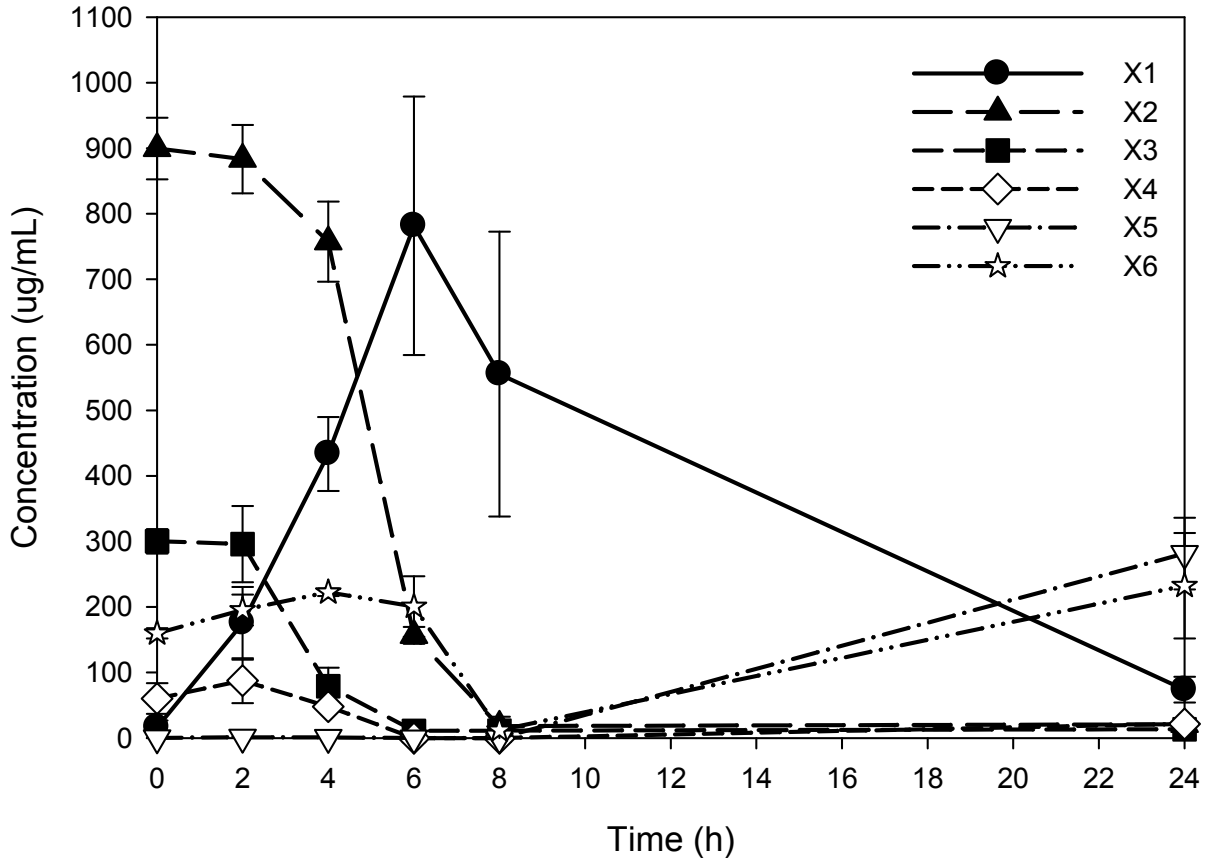

Fig. 8.9. Time course of Wako XOS oligomers consumed during fermentation with *B. adolescentis*.

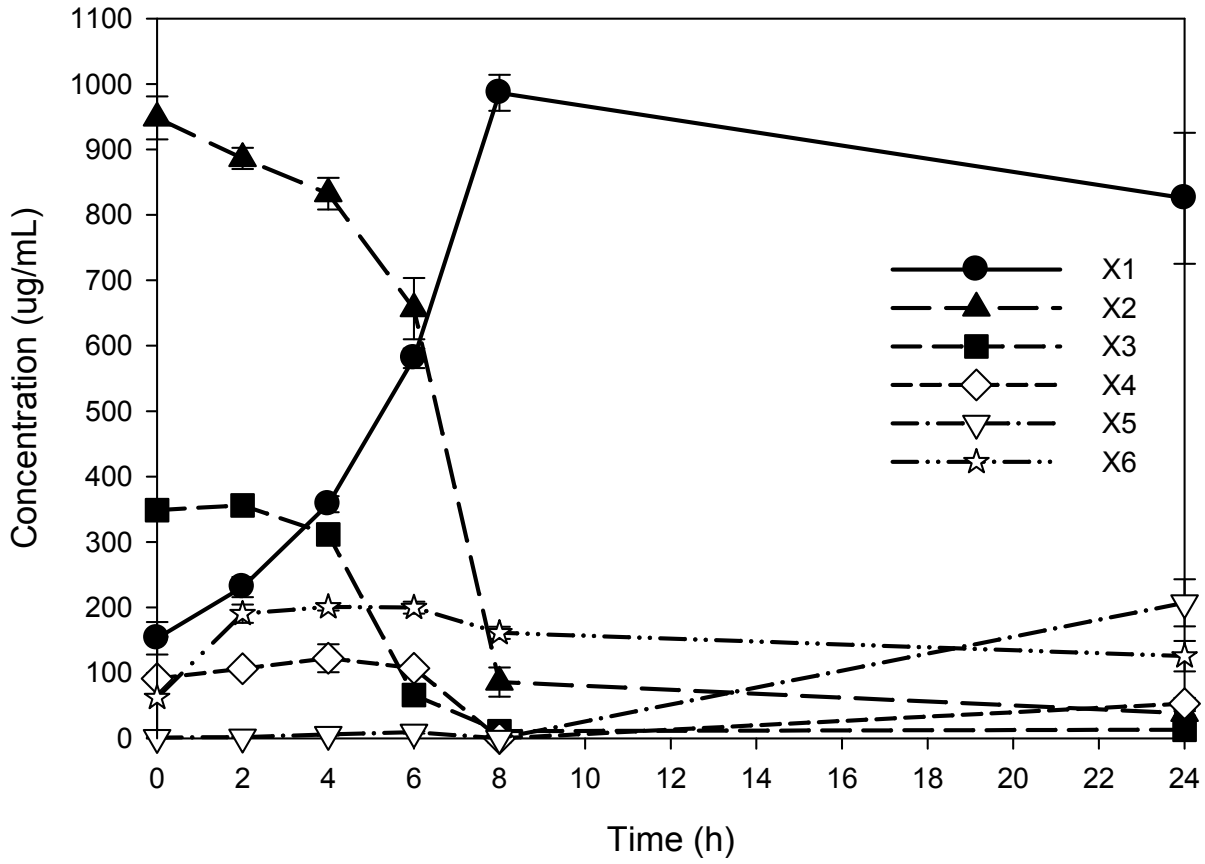

Fig. 8.10. Time course of Wako XOS oligomers consumed during fermentation with *B. catenulatum*.

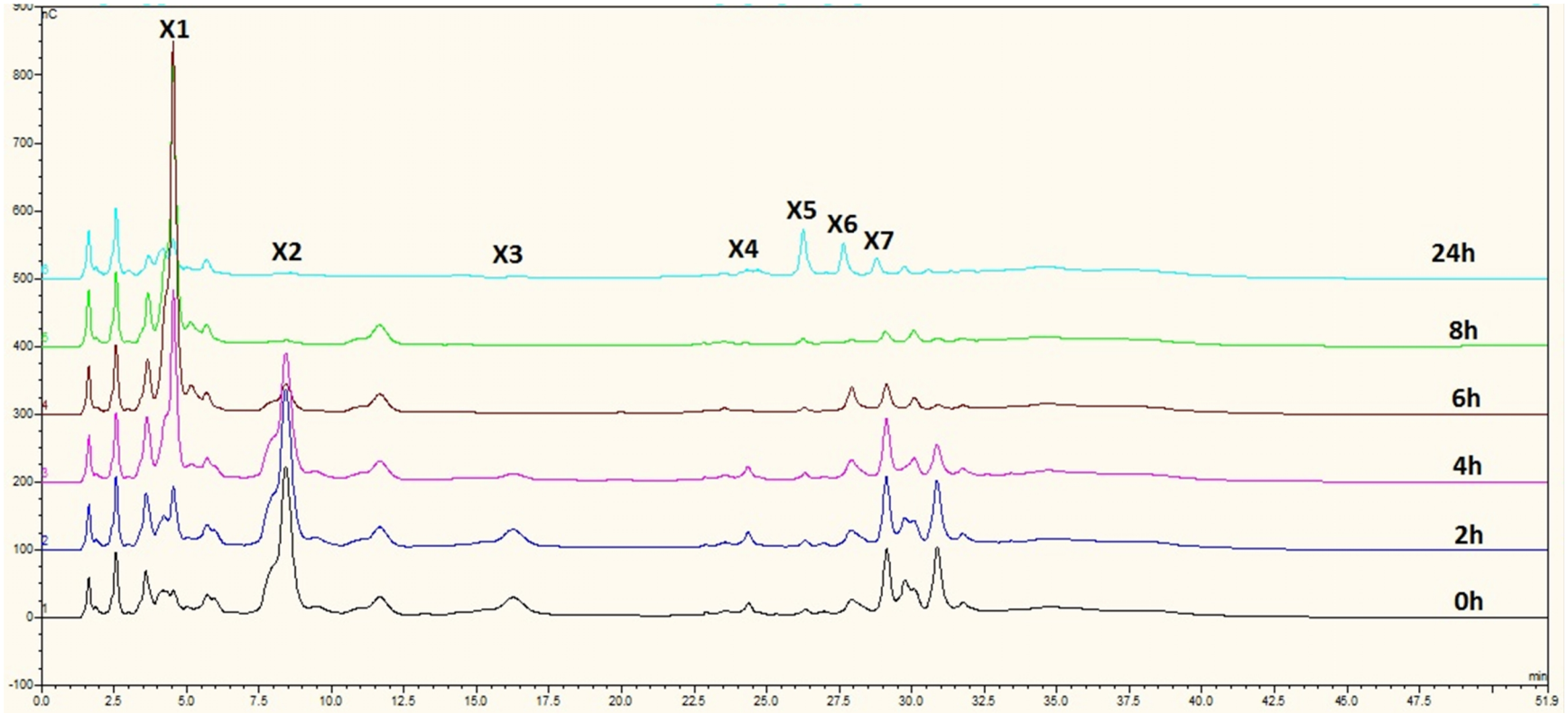

Fig. 8.11. HPAEC-PAD chromatograms of Wako XOS containing media fermented with *B. adolescentis*.

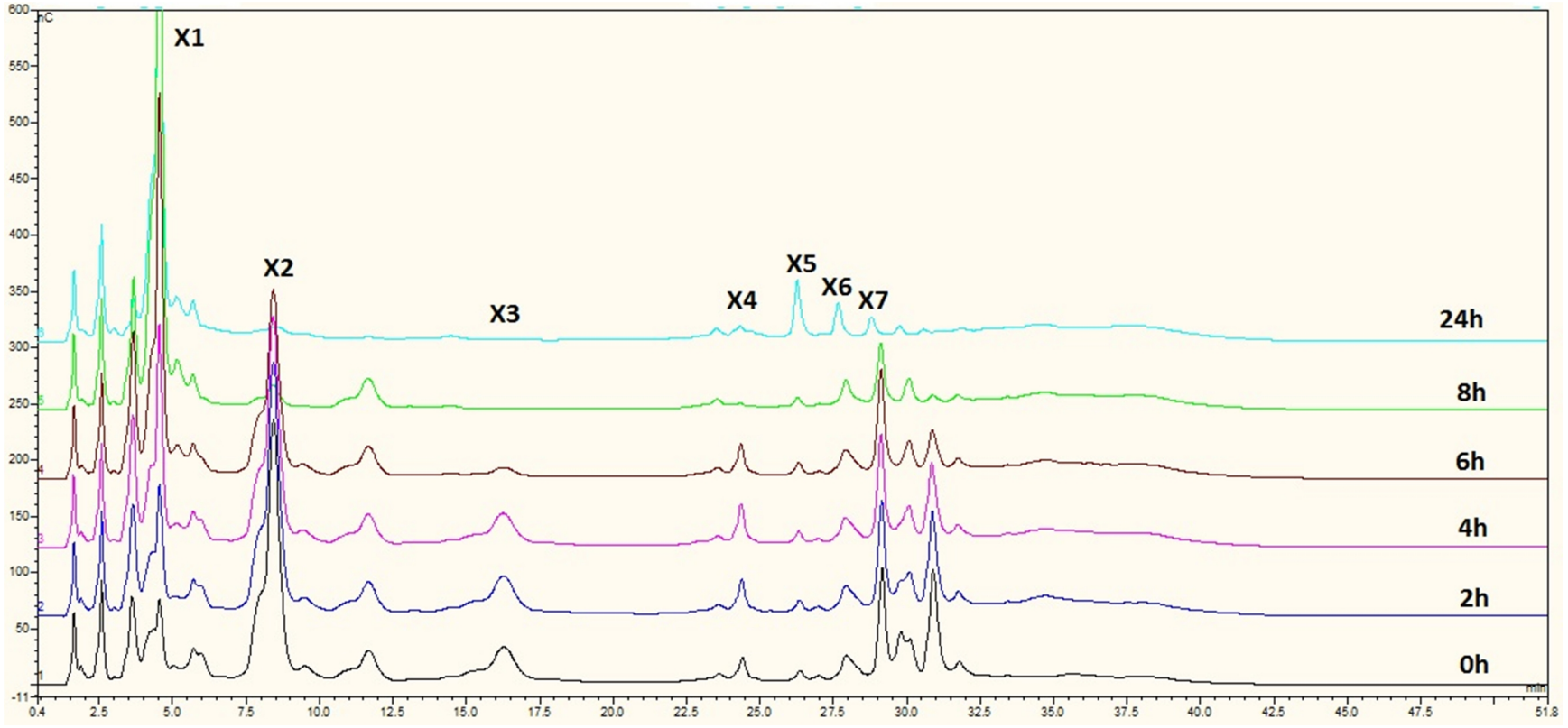

Fig. 8.12. HPAEC-PAD chromatograms of Wako XOS containing media fermented with *B. catenulatum*.

With HPAEC-PAD to monitor oligomer consumption, X2, X3 and X4 were favored by two tested *Bifidobacteria* strains. In MxG XOS, the consumption of X3 was faster than X2 (Figs 8.5 and 8.7). Gullón et al. (2008) assessed the fermentability of XOS from rice husk by *B. adolescentis* CECT5781. A rapid decrease of DP2 and DP3 and slower degradation of DP4 and DP5 were found. Due to the increase of xylose concentration, they suggested xylose was not a prefered sugar by *B. adolescentis* because monosaccharides are absent inthe colon. Pastel et al. (2009) tested utilization of arabinoxylan derived XOS by *B. adolescentis* ATCC 15703 (DSM 20083); quick consumption of X2, X3 and X4 were reported. Pastel et al. (2009) hypothesized the rapid use of X2, X3 and X4 may have been because *B. adolescentis* was able to transport low DP XOS into cell; the slowdown of growth in higher DP XOS may have been due to the requirement to hydrolyze longer XOS into shorter XOS before utilization. Pastel et al. (2009) claimed xylose was a possible substrate for *B. adolescentis*; but this was in disagreement with Gullón et al. (2008.) Wang et al. (2010) cultured *B. adolescentis* with wheat bran derived XOS. Consumptions of 88.0% DP3, 79.4% DP2, 75.0% DP4, 73.5% DP5, 59.5% DP6 and 50.9% DP7 were recorded. They stated DP3 was the preferred substrate for comsumption by *B. adolescentis*.

Our results were in agreement with previous reports. As MxG XOS had 29% X2, X3 and X4; *B. adolescentis* grew faster at the beginning of the fermentation. Growth decreased at 6 h when the smaller DP XOS were depleted. The xylose was produced and released in the medium. Xylose concentration was decreased, which implied *B. adolescentis* was able to utilize xylose. Lagaert et al. (2011) characterized two β-xylosidases from *B. adolescentis*; however, it was not clear if the XOS hydrolyzing enzyme existed in extracellular or intracellular. A hypothesis was accepted that *B. adolescentis* had membrane transporters for XOS but not for xylose. *B. catenulatum* had a slower growth with MxG XOS, which implied the lack of efficient enzymatic system to utilize xylose.

8.4 Conclusions

Two XOS samples were cultured with pure cultures of *Bifidobacterium adolescentis* and *Bifidobacterium catenulatum*. *Bifidobacterium adolescentis* was observed to grow faster on both MxG XOS and Wako XOS; total xylose consumptions were 84.1 and 84.8%, respectively. The rates of disappearance of XOS were from faster to slower: X3, X2, X4, X5 and X6.

Bifidobacterium catenulatum grew slower in MxG XOS but utilized 76.9% of pentose during fermentation compared with 73.6% in Wako XOS. An accumulation of xylose was observed in both MxG XOS and Wako XOS. MxG XOS could be utilized by *Bifidobacterium* spp. as the carbon source. The results indicated that the XOS purification in Chapter 7 was effective to remove toxic reaction derivatives. The preference of X3 by *Bifidobacterium* spp. could be used to optimize XOS production with predominant oligomer in DP3.

Chapter 9. Effects of xylooligosaccharides from *Miscanthus x giganteus* on human gut microbiota

9.1 Introduction

The human gastrointestinal (GI) tract harbors more than 1000 species of microorganisms and over a trillion (10^{14}) cells. Most GI microbes colonize the colon and the the makeup of the population is affected by diet. The colon is anaerobic and numerically dominated by *Bacteroides* spp., *Bifidobacterium* spp., *Eubacterium* spp., *Clostridium* spp., *Lactobacillus* spp. and *Fusobacterium* spp. and includes *Enterococcus* spp. *Enterobacteriaceae* spp. in lower numbers (Wallace et al., 2011). Health disorders such as allergy, gastric cancer and obesity were reported to associate with an imbalance of gut microbiota (Clemente et al., 2012). Based on the bacterial physiology and metabolic characteristics, gut microbiota can be classified into health promoting or potential pathogens. *Bifidobacterium* spp. and *Lactobacillus* spp. are representative of beneficial bacteria; whereas, certain *Escherichia coli*, *Clostridium perfringens* and *Staphylococcus aureus* represent potential pathogens. The population of beneficial bacteria can be selected for by feeding prebiotics such as fructooligosaccharides (FOS) or xylooligosaccharides (XOS). Oligosaccharide fermentation results in production of short chain fatty acid (SCFA) such as acetic, propionic and butyric acids. SCFA can promote health through metabolism, acetic acid is the energy source for muscle cells and can be used in cholesterol synthesis; propionic acid can be used in hepatic gluconeogenesis and butyric acid can be used as an energy source for enterocytes (Brüssow and Parkinson, 2014).

In the previous chapter, MxG XOS were cultured with two pure *Bifidobacteria* cultures to elucidate the bacterial growth and substrate utilization. The pure culture study provides evidence that the XOS supports gut associated microbial growth, but for using the substrate in diet, the situation is more complex. Microbes may have mutual effects; for examples various species produce different hydrolyzing enzymes and secreted metabolites from one strain could be nutrients for another strain.

Our objective was to subject the purified MxG XOS to human gut microbiota using *an in vitro* fermentation system. Commercial Wako XOS and pectin were used as a comparison and

positive control, respectively. Medium pH change, SCFA production and population change of *Bifidobacterium* spp, *Lactobacillus* spp., *Escherichia coli* and *Clostridium perfringens* were monitored through the study.

9.2 Material and Methods

9.2.1 Substrates and chemicals

MxG XOS was prepared as described in Chapter 7. The MxG XOS powder had 76.6% (w/w) XOS and 89.3% (w/w) total substituted oligosaccharides (TSOS; TSOS represented total amount of arabinose, glucose, xylose oligomers and substituted acetyl groups in XOS rich solution), 1.5% ash and 12.1% moisture. Commercial XOS (Wako XOS) sample was purchased from Wako Chemicals USA (Richmond, VA) for comparison to an exisiting commercial product. The Wako XOS had 77.8% (w/w) XOS and 93.4% TSOS, 0.03% ash and 4.9% moisture. Pectin (pectin HM rapid, Tic Gums, Belcamp, MD) was used as a positive control in fermentation.

9.2.2 Donors and microbiota solution

Three human fecal samples were collected and homogenized to provide the microbiota solution. All donors were adult males, free of gastrointestinal disease, and had no antibiotic treatment within three months before initiation. The experimental protocol was approved by the University of Illinois at Urbana-Champaign Institutional Review Board. All subjects signed an informed consent form before start of the experiment. Fresh fecal samples were delivered in a Commode Specimen Collection System (Sage Products, Crystal Lake, IL) at early morning. Samples were mixed with anaerobic dilution solution at the ratio of 1:10 and blended for 15 sec in a Waring blender with CO_2 injection. The diluted solution was filtered through four layers of cheesecloth into 125 mL serum bottles under stable and continuous CO_2 injection. The microbiota solution was used immediately for inoculum.

9.2.3 *In vitro* fermentation cultures

Culture medium was prepared one day before inoculation. The detailed composition of the medium followed the description in Hernot et al. (2009). All components (Table 9.1), except vitamin solution and hemin solution, were mixed and autoclaved at 121°C for 20 min. The vitamin solution and hemin solution were filter sterilized using a 0.22 μm membrane and added before dispensing medium.

Table 9.1. Composition of medium used in *in vitro* fermentations (Hernot et al., 2009).

Component	Concentration in medium, mL/L
Solution A[a]	330.0
Solution B[b]	330.0
Trace mineral solution[c]	10.0
Water soluble vitamin solution[d]	20.0
Folate:biotin solution[e]	5.0
Riboflavin solution[f]	5.0
Hemin solution[g]	2.5
Short chain fatty acid mix[h]	0.4
Resazurin[i]	1.0
Yeast extract	0.5
Na_2CO_3	4.0
Cysteine HCl-H_2O	0.5
Trypticase	0.5
Distilled H_2O	296.1

[a]Composition (g/L): NaCl, 5.4; KH_2PO_4, 2.7; $CaCl_2•H_2O$, 0.16; $MgCl_2•6H_2O$, 0.12; $MnCl_2•4H_2O$, 0.06; $CoCl_2•6H_2O$, 0.06; $(NH_4)_2SO_4$, 5.4. [b]Composition (g/L): K_2HPO_4, 2.7. [c]Composition (mg/L): ethylenediaminetetraacetic acid (disodium salt), 500; $FeSO_4•7H_2O$, 200; $ZnSO_4•7H_2O$, 10; $MnCl_2•4H_2O$, 3; H_3PO_4, 30; $CoCl_2•6H_2O$, 20; $CuCl_2•2H_2O$, 1; $NiCl_2•6H_2O$, 2; $Na_2MoO_4•2H_2O$, 3. [d]Composition (mg/L): thiamin•HCl, 100; D-pantothenic acid, 100; niacin, 100; pyridoxine, 100; p-aminobenzoic acid, 5; vitamin B12, 0.25. [e]Composition (mg/L): folic acid, 10; D-biotin, 2; NH_4HCO_3, 100. [f]Composition: riboflavin, 10 mg/mL in 5 mmol/L of Hepes. [g]Composition: hemin, 500 mg/mL in 10 mmol/L of NaOH. [h]Composition: 250 mL/L each of n-valerate, isovalerate, isobutyrate, and DL-α-methylbutyrate. [i]Composition: resazurin, 1 g/L in distilled H_2O.

Anaerobic cultures were conducted using 1% (w/v) substrate in 50 mL culture tubes capped with butyl rubber stopper. Either 300 mg of of MxG XOS, Wako XOS or pectin were mixed with 26 mL medium in culture tubes; blanks were prepared without substrate. The tubes were stored at 4°C for 12 h to improve substrate hydration and then incubated in 37°C water bath, 30 min prior to inoculation.

Each culture tube was inoculated with 4 mL microbiota solution and incubated at 37°C for 12 h. Every 4 h, tubes were removed from the incubator for periodic mixing and immediate sampled; sampled tubes were scarficed. The pH of the medium was measured using a standard pH meter (Denver Instrument Co., Arvada, CO); 2 mL of medium was collected for SCFA analysis, and 1 mL culture was collected for bacteria population analysis.

9.2.4 Short chain fatty acid quantification

A volume of 0.5 mL 25% (w/v) metaphosphoric acid was added to the 2 mL aliquot. The solution was incubated for 30 min at room temperature and centrifuged at 20,000 x *g* for 20 min and the supernatant recovered. Short chain fatty acid (SCFA, acetic, propionic, butyric acids) present in the supernatants were analyzed by a Hewlett-Packard 5890A series II gas chromatography (Palo Alto, CA) with a glass column packed with 10% SP-1200/1% H_3PO_4 on 80/100+ mesh Chromosorb-WAW (Supelco Inc., Bellefonte, PA). Parameters were injection temperature 175°C, nitrogen flow 50, oven temperature 125°C, FID temperature 180°C and running time 20 min.

9.2.5 Quantitative polymerase chain reaction (qPCR)

The microbial population was quantified by qPCR using bacterial DNA as template. DNA was extracted from sampled medium using PowerLyzer™ PowerSoil® DNA Isolation Kit (MO BIO Laboratories, Inc., Carlsbad, CA, USA) and quantified by a Qubit® 2.0 Fluorometer (Life TechnologiesTM, InvitrogenTM, Grand Island, NY, USA).

The qPCR was performed to monitor the population of *Bifidobacterium* spp., *Lactobacillus* spp., *Escherichia coli* and *Clostridium perfringens*. The 10 µL reaction mixture

had 5 μL of 2x SYBR Green PCR Mater Mix (Applied Biosystems, Foster City, CA, USA), 15 pmol of the forward and reverse primers and 10 ng of extracted bacterial DNA (DePlancke et al., 2002). The standard curve for each bacterium was prepared by single strain culture sampled in exponential growth phase. Bacterial cells were collected by centrifugation and serial diluted. DNA was extracted from each pure strain dilution and used for qPCR. Colony forming units in each dilution were determined by plating on the specific medium in lactobacilli MRS (Difco, BD, Franklin Lakes, NJ, USA), reinforced clostridial medium and Luria Bertani medium. Standard curves were plotted by log cfu per mL vs cycle threshold (Ct) values from qPCR.

9.3 Results and Discussion

9.3.1 Observation of medium pH during fermentation

Due to multiple organic acids and CO_2 produced during anaerobic metabolism, culture pH became more acidic with time (Table 9.1). Starting at pH 6.98, pectin as the positive control revealed rapid pH drop during the first 4 h of fermentation. The pH decrease in MxG XOS and Wako XOS became faster from 4 to 8 h. At the end of fermentation, pH values for pectin, Wako XOS and MxG XOS were 5.26, 5.01 and 5.04, respectively. The two XOS samples had similar pH decline trend (Fig. 9.1).

Increased acidity during fermentation is an indicator of substrate utilization and organic acid production. When Flickinger et al. (2000) tested fructooligosaccharides (FOS) and glucooligosaccharides (GOS) with fecal microbiota, the pH of FOS tubes decreased more rapidly compared with GOS, which was taken as evidence that FOS was utilized faster. Hernot et al. (2009) tested several commercial fructans, galactooligosaccharides and polydextrose with human fecal microbiota; during 12 h of culture, fructans had the largest pH decrease from 0.9 to 1.32. Compared with our results, the pH drop was 1.72 for pectin, 2.11 for Wako XOS and 2.05 for MxG XOS. The decline in pH demonstrated the substrates were utilized well by fecal microbiota. The overlapped pH decreasing curve of MxG XOS and Wako XOS indicated both XOS samples suggest similar metabolic rates in colon (Fig 9.1).

Table. 9.2. pH change in media during *in vitro* fermentation of XOS and pectin.

	pH measurement			
Substrate[a]	0 h	4 h	8 h	12 h
Pectin	6.98 ± 0.01	5.80 ± 0.06	5.34 ± 0.03	5.26 ± 0.03
Wako XOS	7.12 ± 0.05	6.20 ± 0.04	5.16 ± 0.01	5.01 ± 0.05
MxG XOS	7.09 ± 0.04	6.12 ± 0.03	5.15 ± 0.10	5.04 ± 0.02

[a]Values were the average of triplicates.

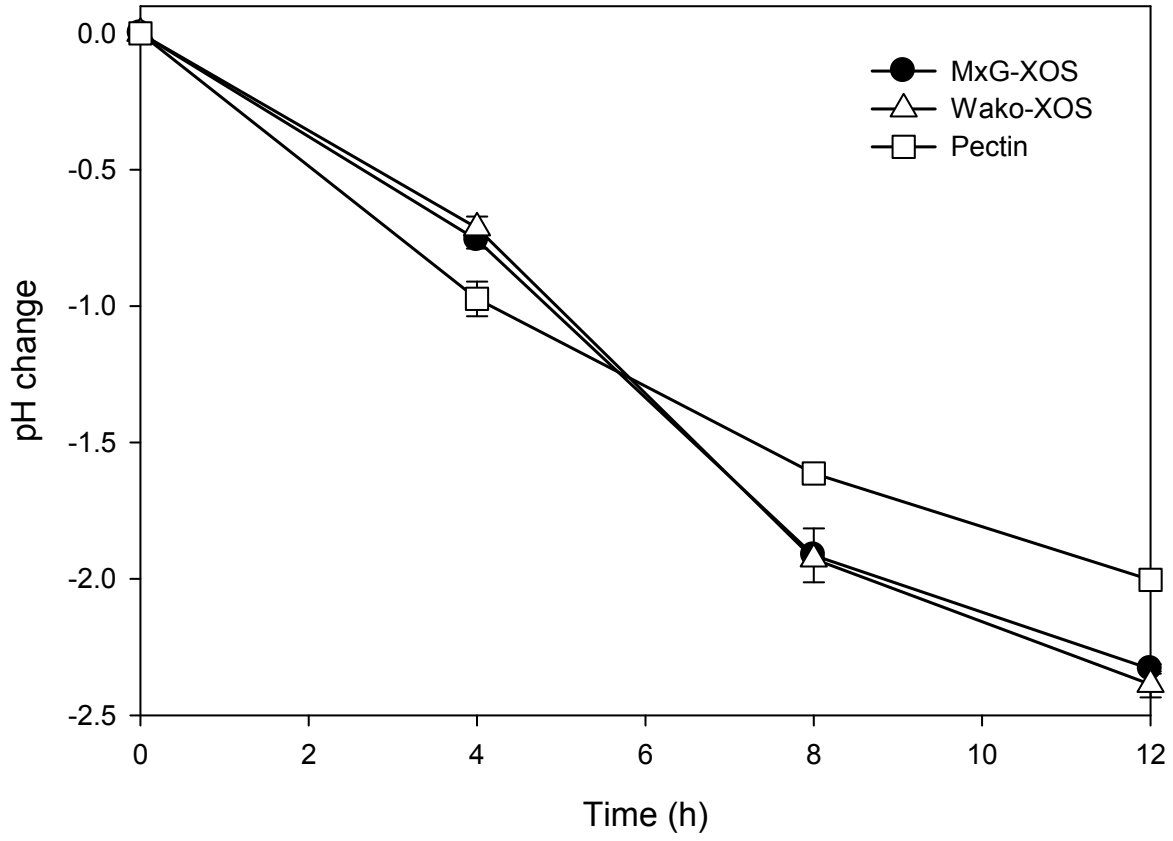

Fig. 9.1. pH change after 4, 8 and 12 h of *in vitro* fermentation of MxG XOS, Wako XOS and pectin.

9.3.2 Short chain fatty acid (SCFA) production

Concentrations of acetic, propionic and butyric acids produced during fermentation were quantified by gas chromatography (Table 9.2). MxG XOS were converted into 466.2 mg/g acetic acid, 74.6 mg/g propionic acid and 84.2 mg/g butyric acid at 12 h of fermentation, compared with 383.6 mg/g acetic acid, 49.0 mg/g propionic acid and 80.9 mg/g butyric acid from pectin and 400.2 mg/g acetic acid, 80.7 mg/g propionic acid and 110.4 mg/g butyric acid from Wako XOS. Total SCFA was highest for MxG XOS with 259.4, 545.1 and 625.0 mg/g SCFA at 4, 8 and 12 h, respectively (Fig 9.2).

In the colon, SCFA are produced through metabolism of nondigestible carbohydrates. The pentose substrate (present in both xylan and pectin) is metabolized through the pentose phosphate pathway into pyruvate. Pyruvate can be converted into acetyl-CoA and then into acetate and butyrate, or converted into succinate and then into propionate. The ratio of acetatic, propionic and butyric acids produced varies withsubstrate. Rycroft et al. (2001) evaluated commercial XOS (Suntory, Osaka, Japan) with human fecal microflora with 26.7 mM of acetatic, 7.21 mM of propionic and 1.75 mM of butyric acids were produced. Hughes et al. (2007) fermented wheat arabinoxylan with human fecal microflora with 28.7 mM acetatic, 6.5 mM propionic, and 14.7 mM butyric acids being produced from 66 kDa arabinoxylan. Pastell et al. (2009) used Wako XOS to culture with human fecal microflora with 16.7 mM acetatic, 4.3 mM propionic and 4.0 mM butyric acids produced. From our results, the Wako XOS had a higher acetate ratio produced compared with Pastell et al. (2009) which may have been due to a variance of mixing strains fermentation. The higher acetate production from MxG XOS can be explained by 6.7 % (w/w) bound acetyl groups on the XOS,which are enzymatically released by acetyl esterase (EC 3.1.1.6).

Table 9.3. Acetatic, propionic, butyric acids and total short chain fatty acid (SCFA) production during *in vitro* fermentation of XOS and pectin.

	Acetic acid			Propionic acid			Butyric aicd			Total SCFA		
Substrate[a]	4 h	8 h	12 h	4 h	8 h	12 h	4 h	8 h	12 h	4 h	8 h	12 h
	mg/g of dry mater in sample											
Pectin	192.7	338.6	383.6	20.3	46.0	49.0	23.5	55.8	80.9	236.6	440.4	513.4
Wako XOS	154.3	358.9	400.2	23.7	61.1	80.7	24.5	76.9	110.4	202.5	496.8	591.3
MxG XOS	211.6	419.1	466.2	25.3	63.6	74.6	22.5	62.5	84.2	259.4	545.1	625.0

[a]Values are the average of triplicates.

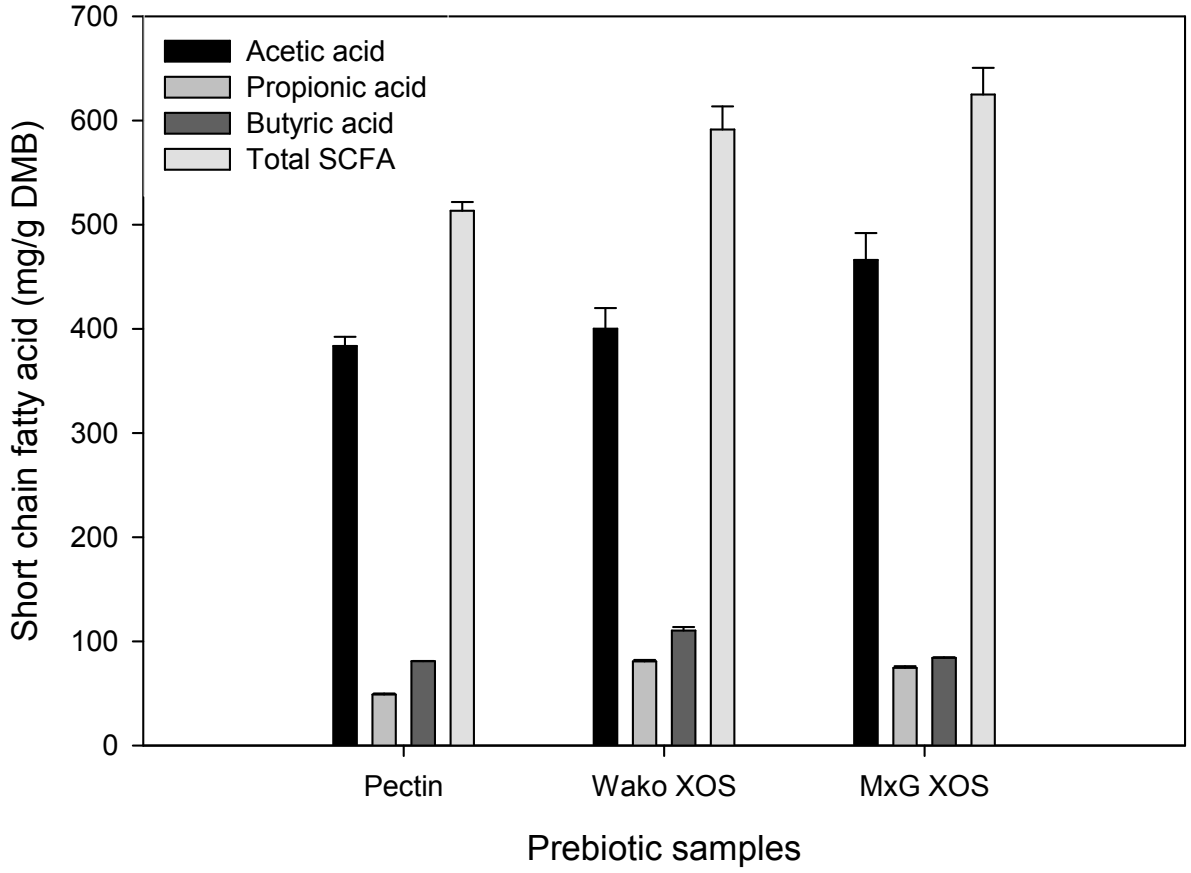

Fig. 9.2. Production of short chain fatty acid during *in vitro* fermentation of pectin, Wako XOS and MxG XOS.

9.3.3 Bacteria population changes during fermentation

The bacterial populations were monitored by qPCR using extracted microbiota DNA (Table 9.3). Both beneficial bacteria genera increased during fermentation in both XOS samples. For *Bifidobacterium* spp., the total cell number started with an average of $10^{10.12}$ (CFU/tube) and then increased to $10^{10.97}$ (CFU/tube) for pectin, to $10^{11.62}$ (CFU/tube) for Wako XOS and to $10^{11.54}$ (CFU/tube) for MxG XOS. For *Lactobacillus* spp., the total cell number started with an average of $10^{11.18}$ (CFU/tube) and increased to $10^{12.17}$ (CFU/tube) for pectin, to $10^{12.08}$ (CFU/tube) for Wako XOS and to $10^{12.12}$ (CFU/tube) for MxG XOS. A mild increase of *E.coli* population was observed, there was no difference in *E.coli* population among three substrates. The trend for *Clostridium perfringens* populations were not impacted over time for all substrates.

For culture with fecal microbiota, Rycroft et al. (2001) observed an increase of *Bifidobacterium* spp. and *E.coli* population in XOS tubes. Hughes et al. (2007) reported an increase in total cells including *Bifidobacterium* spp., *Clostridium* spp. and *Lactobacillus* spp. populations. Moura et al. (2008) tested XOS from *Eucalyptus* (EUC), corn cobs (CC) and brewery's spent grain (BSG); the *Bifidobacterium* spp. population was increased in EUC and CC but not in BSG. In our study, the qPCR results validated that XOS were able to improve beneficial bacteria population growth. The increased number of potential pathogens may have been due to the expanding of total cell numbers in the medium. The prebiotic function of MxG XOS was comparable to Wako XOS, based on the increase cell number of probiotics.

Table 9.4. Microbiota concentration (log10 cfu/tube) in batch culture fermentation with MxG XOS, Wako XOS and pectin.

	Bifidobacterium spp.[†]				*Lactobacillus* spp.				*Escherichia coli*				*Clostridium perfringens*			
Substrates	0 h	4 h	8 h	12 h	0 h	4 h	8 h	12 h	0 h	4 h	8 h	12 h	0 h	4 h	8 h	12 h
	CFU[2], log10/tube of *in vitro* fluid															
Pectin	10.04^{a}	10.90^{b}	10.97^{Ab}	10.97^{Ab}	11.11^{a}	11.92^{b}	12.07^{b}	12.17^{b}	8.98^{a}	9.86^{b}	9.93^{b}	9.89^{b}	7.89	8.17	8.28	8.34
Wako XOS	10.15^{a}	11.18^{b}	11.13^{ABbc}	11.62^{Bc}	11.25^{a}	11.98^{b}	12.28^{b}	12.08^{b}	9.25^{a}	9.83^{b}	9.80^{b}	9.83^{b}	7.79	8.25	8.20	7.98
MxG XOS	10.18^{a}	11.15^{b}	11.50^{Bb}	11.54^{Bb}	11.20^{a}	11.95^{b}	12.18^{c}	12.12^{bc}	9.01^{a}	9.84^{b}	9.83^{b}	9.65^{b}	8.02	8.13	8.40	7.81
Pooled SEM[3]	0.10				0.06				0.07				0.23			

[1]Mean values ± SD for the 0 h tubes are 10.12 ± 0.10 for *Bifidobacterium* spp., 11.18 ± 0.10 for *Lactobacillus* spp., 9.08 ± 0.16 for *Escherichia coli*, and 7.90 ± 0.15 $\log_{10}$ cfu/tube for *Clostridium perfringens*.
[2]Colony-forming unit.
[3]Standard error of the means.
The interaction of substrate and time of fermentation for *Bifidobacterium* spp. was significant ($P < 0.05$).
[a-c]within a row, means without a common letter differ (effect of substrate at specific time point; $P < 0.05$).
[A-B]within a column, means without a common letter differ (effect of time within substrate; $P < 0.05$).
[†]Substrate effect ($P < 0.05$).

9.4 Conclusions

MxG XOS was cultured with human fecal microbiota along with Wako XOS and pectin as comparisons. A culture medium pH decrease from 7.1 to 5.0 was observed during fermentation, indicating the utilization of MxG XOS. Change in pH was similar for the MxG and Wako XOS cultures. MxG XOS produced 466.2 mg/g acetic acid, 74.6 mg/g propionic acid and 84.2 mg/g butyric acid; total SCFA was highest among the substrates. The beneficial bacteria *Bifidobacterium* spp. and *Lactobacillus* spp. population increased during the fermentation of MxG XOS. Compared with Wako XOS, MxG XOS had similar *Bifidobacterium* spp., *Lactobacillus* spp., *Escherichia coli* and *Clostridium perfringens* cell titers. The results substantiated MxG XOS as a prebiotic candidate could be utilized by fecal microbiota, be converted into beneficial metabolites and stimulate probiotics growth.

Chapter 10. Conclusions and recommendations for future work

The goal of this dissertation was to evaluate xylooligosaccharides (XOS) production as a potential coproduct with cellulosic ethanol production. Specific objectives regarding XOS production, characterization, purification, separation, biological activity were listed in the Introduction and the major conclusions are:

1. Xylooligosaccharides (XOS) could be produced efficiently from *Miscanthus x giganteus* (MxG) through autohydrolysis. The optimal yield could be obtained at various temperatures provided the reaction time was adjusted accordingly. The optimal autohydrolysis reaction conditions were: 160°C, 60 min , 180°C, 20 min , and 200°C, 5 min. High extraction of 13.5% (w/w) of initial dry biomass and 69.2% (w/w) of initial xylan were obtained.
2. The produced XOS were characterized by gel permeation chromatography (GPC) and high performance anion exchange chromatography with pulsed amperometric detection system (HPAEC-PAD). The XOS produced were in the molecular weight range of 100 to 2000 Da. The results from HPAEC-PAD validated the reaction conditions at 160°C, 180°C and 200°C. XOS compositions from all three reaction conditions were similar.
3. The XOS in crude hydrolyzate could be recovered by activated carbon adsorption. By addition of 10% (w/v) carbon, 98.3% of the XOS in the liquid was adsorbed. The capacity of carbon to adsorb XOS was 0.14 g XOS/g carbon powder. With the sequential elution, most of the XOS were eluted in 30 and 50% ethanol/water solutions; the highest recovery of initial XOS obtained was 47.9% . The carbon refined XOS was analyzed by HPAEC-PAD for degree of polymerization (DP). The highest recoveries of X2 and X3 were 91.8% and 86.9% , respectively.
4. Xylose oligomers from MxG hydrolyzate were separated by centrifugal partition chromatography (CPC) to produce fractions with single DP molecules. The separation was based on a solvent system of butanol:methanol:water in 4:1:4 ratio. Using CPC, 230 mg of DP2 to DP6 oligomers could be recovered from 1 g of MxG hydrolyzate. XOS at each DP were recovered at 90.2% DP2, 64.5% DP3, 71.2% DP4, 61.9% DP5 and 68.9% DP6. Purities of DP2 to DP6 fractions were 61.9, 63.2, 44.5, 31.5 and 51.3%, respectively. DP2 and DP3

were validated by mass spectrometry; pentobiose and pentotriose were the primary components of each fraction.

5. A XOS purification procedure following carbon adsorption/ethanol solution was investigated. We used a combination of ion exchange resin treatments to remove impurities and colorants in XOS solution. The end product MxG XOS was composed of 76.6% xylose oligomers, 1.5% arabinose oligomers, 4.4% glucose oligomers and 6.9% bounded acetyl groups. Total substituted oligosaccharides were 89.3% (w/w). Using HPAEC-PAD analysis, we found the MxG XOS had 1.7% xylobiose (X1), 8.9% xylobiose (X2), 11.3% xylotriose (X3), 8.8% xylotetraoase (X4), 9.0% xylopentaose (X5) and 5.8% xylohexaose (X6).
6. Purified MxG XOS was used in fermentation with *Bifidobacterium adolescentis* and *Bifidobacterium catenulatum*. *B. adolescentis* grew fast in MxG XOS and had maximum specific growth rate at 0.69 (h^{-1}). Total sugar consumption was 84.1% at 24 h of culture, and the substrate preference was X2, X3, and X5. *B. catenulatum* grew slower on MxG XOS and had maximum specific growth rate of 0.33 (h^{-1}). Though *B. catenulatum* may lack an efficient system to utilize MxG XOS, total sugar utilization was 76.9% at 24h of culture.
7. Purified MxG XOS was used in an *in vitro* fermentation with human fecal microbiota. A pH drop was observed during 12 h of fermentation from 7.1 to 5.0. MxG XOS was converted by fecal microorganisms into short chain fatty acid (SCFA): 466.2 mg/g acetate, 74.6 mg/g propionate and 84.2 mg/g butyrate. MxG XOS resulted in high SCFA production among three tested substrates. The qPCR was used to monitor bacterial population migration. The number of beneficial bacteria *Bifidobacterium* spp. and *Lactobacillus* spp. increased with MxG XOS as substrate. MxG XOS had potential to develop into a prebiotic product and a coproduct for cellulosic ethanol plant.

Based on the current results and conclusions, there are several topics recommended for future research focus:

1. Optimization of carbon refining to improve XOS recovery.
   Though carbon adsorption and ethanol elution was effective in removing impurities, the step also was responsible for 50% of initial XOS loss. Further improvement methods could be investigated to improve XOS recovery and simplify the adsorption steps.
2. Investigation of a food grade MxG XOS production procedure.

The XOS purification process is currently laboratory grade. The produced MxG XOS is suitable only to use for *in vitro* research. To make the purification procedure more applicable for industry, a similar purification process designed for food grade could be evaluated.

3. Processing of XOS produced MxG into fuel.
   The optimum condition for XOS production from MxG does not match with the pretreatment condition used for enzymatic hydrolysis and fermentation. The pretreatment conditions that favor maximum XOS production are lower than those that favor enzymatic cellulose conversion. As such, it might be worthwhile to explore a two-stage pretreatment process for (1) production of XOS and (2) optimal pretreatment of cellulose for enzymatic conversion to glucose.
4. Evaluation of a model plant with XOS and fuel production with technoeconomic analysis.
   With information in XOS purification and fuel conversion, it would be relevant to evaluate the process feasibility. A processing facility could be modelled using SuperPro Designer™ software and used for assessing the effect of each parameter.

References

Aachary, A.A., Prapulla, S.G., 2011. Xylooligosaccharides (XOS) as an emerging prebiotic: microbial synthesis, utilization, structural characterization, bioactive properties, and application. Compr. Rev. Food Sci. F. 10, 2-16.

Agbor, V.B., Cicek, N., Sparling, R., Berlin, A., Levin, D.B., 2011. Biomass pretreatment: fundamentals toward application. Biotechnol. Adv. 29, 675-685.

Alexandratos, S.D., 2009. Ion-exchange resins: a retrospective from Industrial and Engineering Chemistry Research. Ind. Eng. Chem. Res. 48, 388-398.

Alvira, P., Tomas-Pejo, E., Ballesteros, M., Negro, M.J., 2010. Pretreatment technologies for an efficient bioethanol production process based on enzymatic hydrolysis: a review. Bioresourc. Technol. 101, 4851-4861.

Aureli, P., Capurso, L., Castellazzi, A.M., Clerici, M., Giovannini, M., Morelli, L., Poli, A., Pregliasco, F., Salvini, F., Zuccotti, G.V., 2011. Probiotics and health: an evidence-based review. Pharmacol. Res. 63, 366-376.

Balat, M., Balat, H., 2009. Recent trends in global production and utilization of bio-ethanol fuel. Appl. Energ. 86, 2273-2282.

Bals, B., Wedding, C., Balan, V., Sendich, E., Dale, B., 2011. Evaluating the impact of ammonia fiber expansion (AFEX) pretreatment conditions on the cost of ethanol production. Bioresour. Technol. 102, 1277-1283.

Berthod, A., Armstrong, D.W. 1988. Centrifugal partition chromatography. I. General features. J. Liq. Chromatogr. Relat. Technol. 11, 547-566.

Bowman, M.J., Dien, B.S., O'Bryan, P.J., Sarath, G., Cotta, M.A., 2011. Selective chemical oxidation and depolymerization of switchgrass (*Panicum virgatum* L.) xylan with oligosaccharide product analysis by mass spectrometry. Rapid Commun. Mass Spectrum. 25, 941-950.

Broekaert, W.F., Courtin, C.M., Verbeke, K., de Wiele, T.V., Verstraete, W., Delcour, J.A., 2011. Prebiotic and other health-related effects of cereal-derived arabinoxylans, arabinoxylan-oligosaccharides, and xylooligosaccharides. Crit. Rev. Food Sci. 51, 178-194.

Brosse, N., Dufour, A., Meng, X., Sun, Q., Ragauskas, A. 2012. Miscanthus: a fast-growing crop for biofuels and chemicals production. Biofuels, Bioprod. Bioref. 6, 580-598.

Brosse, N., Sannigrahi, P., Ragauskas, A., 2009. Pretreatemnt of *Miscanthus x giganteus* using the ethanol organosolv process for ethanol production. Ind. Eng. Chem. Res. 48, 8328-8334.

Brown, T.R., Brown, R.C., 2013. A review of cellulosic biofuel commercial-scale projects in the United States. Biofuels, Bioprod. Biorefin. 7, 235-245.

Brüssow, H., Parkinson, S.J., 2014. You are what you eat. Nat. Biotechnol. 32, 243-245.

Cara, C., Ruiz, E., Carvalheiro, F., Moura, P., Ballesteros, I., Castroa, E., Gírio, F., 2012. Production, purification and characterisation of oligosaccharides from olive tree pruning autohydrolysis. Ind. Crops Prod. 40, 225-231.

Carrasco, F., Roy, C., 1992. Kinetic study of diluted-acid prehydrolysis of xylan-containing biomass. Wood Sci. Technol. 26, 189-208.

Carroll, A., Somerville, C., 2009. Cellulosic biofuels. Annu. Rev. Plant Biol. 60, 165-182.

Carvalheiro, F., Esteves, M.P., Parajó, J.C., Pereira, H., Girio, F.M., 2004. Production of oligosaccharides by autohydrolysis of brewery's spent grain. Bioresour. Technol. 91, 93-100.

Carvalho, A.F.A., Neto, P.D.O., da Silva, D.F., Pastore, G.M., 2013. Xylo-oligosaccharides from lignocellulosic materials: chemical structure, health benefits and production by chemical and enzymatic hydrolysis. Food Res. Int. 51, 75-85.

Chum, H.L., Warner, E., 2013. A comparison of commercial ethanol production systems from Brazilian sugarcane and US corn. Biofuels, Bioprod. Biorefin. 8, 205-223.

Chundawat, S.P.S., Beckham, G.T., Himmel, M.E., Dale, B.E., 2011. Deconstruction of lignocellulosic biomass to fuels and chemicals. Annu. Rev. Chem. Biomol. Eng. 2, 121-145.

Clemente, J.C., Ursell, L.K., Parfrey, L.W., Knight, R., 2012. The impact of the gut microbiota on human health: an integrative review. Cell 148, 1258-1270.

Cook, S.I., Sellin, J.H., 1998. Review article: short chain fatty acid in health and disease. Aliment. Pharmacol. Ther. 12, 499-507.

Cosgrove, D.J., 2005. Growth of the plant cell wall. Nat. Rev. Mol. Cell Biol. 6, 850-861.

Cotta, M.A., 1993. Utilization of xylooligosaccharides by selected ruminal bacteria. Appl. Environ. Microbiol. 59, 3557-3563.

Dias de Oliveira, M.E., Vaughan, B.E., Rykiel JR. E.J., 2005. Ethanol as fuel: energy, carbon dioxide balances, and ecological footprint. Bioscience 55, 593-602.

Eitzinger, J., Kossler, C., 2002. Microclimatological characteristics of a Miscanthus (Miscanthus cv. giganteus) stand during stable conditions at night in the nonvegetative winter period. Theor. Appl. Climatol. 71, 254-257.

El Hage, R., Chrusciel, L., Desharnais, L., Brosse, N., 2010. Effect of autohydrolysis of *Miscanthus x giganteus* on lignin structure and organosolv delignification. Bioresour. Technol. 101, 9321-9329.

Filbakk, T., Skjevrak, G., Høibø, O., Dibdiakova, J., Jirjis, R., 2011. The influence of storage and drying methods for Scots pine raw material on mechanical pellet properties and production parameters. Fuel Process Technol. 92, 871-878.

Finneran, K.T., Lovley, D.R., 2001. Anaerobic degradation of methyl *tert*-butyl ether (MTBE) and *tert*-butyl alcohol (TBA). Environ. Sci. Technol. 35, 1785-1790.

Flickinger, E.A., Wolf, B.W., Garleb, K.A., Chow, J., Leyer, G.J., Johns, P.W., Fahey Jr., G.C., 2000. Glucose-based oligosaccharides exhibit different *in vitro* fermentation patterns and affect *in vivo* apparent nutrient digestibility and microbial populations in dogs. J. Nutr. 130, 1267-1273.

Fujikawa, S., Sasaki, H., Ishizuka, T. (Suntory Limited, JP; Hokkaido Sugar Co., JP). High-purity xylooligosaccharide compositions. US 2009/0062232, Mar 5, 2009.

Fujiya, M., Kohgo, Y., 2010. Novel perspectives in probiotic treatment: the efficacy and unveiled mechanisms of the physiological functions. Clin. J. Gastroenterol. 3, 117-127.

Garrote, G., Falqué, E., Domínguez, H., Parajó, J, C., 2007. Autohydrolysis of agricultural residues: Study of reaction byproducts. Bioresour. Technol. 98, 1951-1957.

Gibson, G.R., Roberfroid, M., 1995. Dietary modulation of the human colonic microbiota: introducing the concept of prebiotics. J. Nutr. 125, 1401-1412.

Girio, F.M., Fonseca, C., Carvalheiro, F., Duarte, L.C., Marques, S., Bogel-Lukasik, R., 2010. Hemicellulose for fuel ethanol: a review. Bioresour. Technol. 101, 4775-4800.

Gullón, P., González-Múñoz, M.J., van Gool, M.P., Schols, H.A., Hirsch, J., Ebringerová, A., Parajó, J.C., 2010. Production, refining, structural characterization and fermentability of rice husk xylooligosaccharides. J. Agric. Food Chem. 58, 3632-3641.

Gullón, P., Moura, P., Esteves, M.P., Girio, F.M., Domínguez, H., Parajó, J.C., 2008. Assessment on the fermentability of xylooligosaccharides from rice husks by probiotic bacteria. J. Agric. Food Chem. 56, 7482-7487.

Gupta, R., Sharma, K.K., Kuhad, R.C., 2009. Separate hydrolysis and fermentation (SHF)of Prosopis juliflora, a woody substrate, for the production of cellulose ethanol by Saccharomyces cerevisiae and Pichia stipites-NCIM3498. Bioresour. Technol. 100, 1214-1220.

Heaton, E.A., Dohleman, F.G., Long, S.P., 2008. Meeting US biofuel goals with less land: the potential of Miscanthus. Glob. Change Biol. 14, 2000-2014.

Hendricks, A.T., Zeeman, G., 2009. Pretreatments to enhance the digestibility of lignocellulosic biomass. Bioresourc. Technol. 100, 10-18.

Hernot, D.C., Boileau, T.W., Bauer, L.L., Middelbos, I.S., Murphy, M.R., Swanson, K.S., Fahey, G.C. Jr., 2009. *In vitro* fermentation profiles, gas production rates, and microbiota modulation as affetcted by certain fructans, galactooligosaccharides, and polydextrose. J. Agric. Food Chem. 57, 1354-1361.

Hespell, R.B., Wolf, R., Bothast, R.J., 1987. Fermentation of xylans by *Butyrivibrio fibriolvens* and other ruminal bacteria. Appl. Environ. Microbiol. 53, 2849-2853.

Hill, J., 2007. Environmental costs and benefits of transportation biofuel production from food- and lignocellulose-based energy crops. A review. Agron. Sustain. Dev. 27, 1-12.

Hopkins, M.J., Cummings, J.H., Macfarlane, G.T., 1998. Inter-species differences in maximum specific growth rates and cell yields of bifidobacteria cultured on oligosaccharides and other simple carbohydrate sources. J. Appl. Microbiol. 85, 381-386.

Huang, H.J., Ramaswamy, S., Al-Dajani, W., Tschirner, U., Cairncross, R.A., 2009. Effect of biomass species and plant size on cellulosic ethanol: A comparative process and economic analysis. Biomass Bioenerg. 33, 234-246.

Hughes, S.A., Shewry, P.R., Li, L., Gibson, G.R., Sanz, M.L., Rastall, R.A., 2007. *In vitro* fermentation by human fecal microflora of wheat arabinoxylans. J. Agric. Food Chem. 55, 4589-4595.

Humbird, D., Davis, R., Tao, L., Kinchin, C., Hsu, D., Aden, A., Schoen, P., Lukas, J., Olthof, B., Worley, M., Sexton, D., Dudgeon, D., 2011. Process design and economics for biochemical conversion of lignocellulosic biomass to ethanol. Technical report no.NREL/TP-5100-47764. National Renewable Energy Labratory, May 2011. http://www.nrel.gov/biomass/pdfs/47764.pdf

Izumi, Y., Sugiura, J., Kagawa, H., Azumi, N. (Oji Paper Co., JP). Process for producing xylooligosaccharide from lignocellulose pulp. US patent 6,942,754, B2, Sep 13, 2005.

Jayapal, N., Samanta, A.K., Kolte, A.P., Senani, S., Sridhar, M., Suresh, K.P., Sampath, K.T., 2013. Value addition to sugarcane bagasse: Xylan extraction and its process optimization for xylooligosaccharides production. Ind. Crops Prod. 42, 14-24.

Kabel, M.A., Kortenoeven, L., Schols, H.A., Voragen, A.G.J., 2002. *In vitro* fermentability of different substituted xylooligosaccharides. J. Agric. Food Chem. 50, 6205-6210.

Kaylen, M., Van Dyne, D. L., Choi, Y., Blasé, M., 2000. Economic feasibility of producing ethanol from lignocellulosic feedstocks. Bioresour. Technol. 72, 19-32.

Kazi, F.K., Fortman, J.A., Anex, R.P., Hsu, D.D., Aden, A., Dutta, A., Kothandaraman, G., 2010. Techno-economic comparison of process technologies for biochemical ethanol production from corn stover. Fuel 89, 20-28.

Khanna, M., Dhungana, B., Clifton-Brown, J., 2008. Costs of producing miscanthus and switchgrass for bioenergy in Illinois. Biomass Bioenerg. 32, 482-493.

Khullar, E., Dien, B.S., Rausch, K.D., Tumbleson, M.E., Singh, V., 2013. Effect of particle size on enzymatic hydrolysis of pretreated Miscanthus. Ind. Crop Prod. 44, 11-17.

Kontula, P., von Wright, A., Mattila-Sandholm, T., 1998. Oat bran beta-gluco- and xylo-oligosaccharides as fermentative substrates for lactic acid bacteria. Int. J. Food Microbiol. 45, 163-169.

Kovarik, B., 1998. Henry Ford, Charles Kettering and the "fuel of the future". Automot. Hist. Rev. 32, 7-27.

Kubista, M., Andrade, J.M., Bengtsson, M., Forootan, A., Jonák, J., Lind, K., Sindelka, R., Sjöback, R., Sjögreen, B., Strömbom, L., Ståhlberg, A., Zoric, N., 2006. The real-time polymerase chain reaction. Mol. Asp. Med. 27, 95-125.

Kuhn, R.C., Filho, F.M., 2010. Purification of fructooligosaccharides in an activated charcoal fixed bed column. New Biotechnol. 27, 862-869.

Lagaert, S., Pollet, A., Delcour, J.A., Lavigne, R., Courtin, C.M., Volckaert, G., 2011. Characterization of two β-xylosidases from *Bifidobacterium adolesscentis* and their contribution to the hydrolysis of prebiotic xylooligosaccharides. Appl. Microbiol. Biotechnol. 92, 1179-1185.

Lau, C-S., Bunnell, K.A., Clausen, E.C., Thoma, G.J., Lay, J.O., Gidden, J., Carrier, D.J., 2011. Separation and purification of xylose oligomers using centrifugal partition chromatography. J. Ind. Microbiol. Biotechnol. 38, 363-370.

Lau, C-S., Clausen, E.C., Lay, J.O., Gidden, J., Carrier, D.J., 2013. Separation of xylose oligomers using centrifugal partition chromatography with a butanol-methanol-water system. J. Ind. Microbiol. Biotechnol. 40, 51-62.

Lau, M.W., Gunawan, C., Balan, V., Dale, B.E., 2010. Comparing the fermentation performance of *Escherichia coli* KO11, *Saccharomyces cerevisiae* 424A (LNH-ST) and *Zymomonas mobilis* AX101 for cellulosic ethanol production. Biotechnol. Biofuels 3, 11.

Le Ngoc Huyen, T., Rémond, C., Dheilly, R.M., Chabbert, B. 2010. Effect of harvesting date on the composition and saccharification of *Miscanthus x giganteus*. Bioresour. Technol. 101, 8224-8231.

Lewandowskia, I., Clifton-Brownb, J.C., Scurlockc, J.M.O., Huismand, W., 2000. Miscanthus: European experience with a novel energy crop. Biomass Bioenerg. 19, 209-227.

Ligero, P., van der Kolk, J.C., de Vega, A., van Dam, J.E.G., 2011. Production of xylo-oligosaccharides from *Miscanthus x giganteus* by autohydrolysis. Bioresur. 6, 4417-4429.

Lozupone, G.A., Stombaugh, J.I., Gordon, J.I., Jansson, J.K., Knight, R., 2012. Diversity, stability and resilience of the human gut microbiota. Nature 489, 220-230.

MacFarlane, S., MacFarlane, G.T., Cummings, J.H., 2006. Review article: prebiotics in the gastrointestinal tract. Aliment. Pharmacol. Ther. 15, 1139-1145.

Maloney, M,T., Chapman, T.W., Baker, A.J.,1985. Dilute acid hydrolysis of paper birch: kinetics studies of xylan and acetyl-group hydrolysis. Biotechnol. Bioeng. 27, 355-361.

Marchal, L., Legrand, J., Foucault, A., 2003. Centrifugal partition chromatography: A survey of its history, and our recent advances in the field. Chem. Rec. 3, 133-143.

Morales, V., Sanz, M.L., Olano, A., Corzo, N., 2006. Rapid separation on activated charcoal of high oligosaccharides in honey. Chromatographia 64, 233-238.

Moura, P., Barata, R., Carvalheiro, F., Girio, F., Loureiro-Dias, M.C., Esteves, M.P., 2007. *In vitro* fermentation of xylo-oligosaccharidesnfrom corn cobs autohydrolysis by *Bifidobacterium* and *Lactobacillu*s strains. LWT-Food Sci. Technol. 40, 963-972.

Moura, P., Cabanas, S., Lourenco, P., Girio, F., Loureiro-Dias, M., Esteves, M.P., 2008. *In vitro* fermentation of selected xylo-oligosaccharides by piglet intestinal microbiota. LWT-Food Sci. technol. 41, 1952-1961.

Moure, A., Gullo´n, P., Domínguez, H., Parajó, J.C., 2006. Advances in the manufacture, purification and applications of xylooligosaccharides as food additives and nutraceuticals. Process Biochem. 41, 1913-1923.

Mumtaz, S., Rehman, S.U., Huma, N., Jamil, A., Nawaz, H., 2008. Xylooligosaccharides enriched yogurt: physiochemical and sensory evaluation. Pak. J. Nutr. 7(4), 566-569.

Nabarlatz, D., Farriol, X., Montané, D., 2004. Kinetic modeling of the autohydrolysis of lignocellulosic biomass for the production of hemicellulose derived oligosaccharides. Ind. Eng. Chem. Res. 43, 4124-4131.

Nabarlatz, D., Farriol, X., Montané, D., 2005. Autohydrolysis of almond shells for the production of xylo-oligosaccharides: product characteristics and reaction kinetics. Ind. Eng. Chem. Res. 44, 7746-7755.

Nabarlatz, D., Torras, C., Garcia-Valls, R., Montané, D., 2007. Purification of xylo-oligosaccharides from almond shells by ultrafiltration. Sep. Purif. Technol. 52, 235-243.

Otieno, D.O., Ahring, B.K., 2012. A thermochemical pretreatment process to produce xylooligosacchatrides (XOS), arabinooligosacchorides (AOS) and mannooligosaccharides (MOS) from lignocellulosic biomasses. Bioresour. Technol. 112, 285-292.

Palframan, R.J., Gibson, G.R., Rastall, R.A., 2003. Carbohydrate preference of *Bifidobacterium* species isolated from human gut. Curr. Issues Interst. Microbiol. 4, 71-75.

Pandey, M.P., Kim, C.S., 2011. Lignin depolymerization and conversion: a review of thermochemical methods. Chem. Eng. Technol. 34, 29-41.

Pastell, H., Westermann, P., Meyer, A.S., Tuomainen, P., Tenkanen, M., 2009. *In vitro* fermentation of arabinoxylan-derived carbohydrates by bifidobacterium and mixed fecal microbiota. J. Agri. Food Chem. 57, 8598-8606.

Perlack, R.D.,Wright, L.L., Turhollow, A.F., Graham, R.L., Stokes, B.J., Erbach, D.C., 2005. Biomass as feedstock for a biomass and bioproducts industry: the technical feasibility of a 1 billion ton annual feedstock supply. ORNL/TM-2005/66. Oak Ridge, TN: Oak Ridge Natl. Lab./US DOE/USDA

Picard, C., Fioramonti, J., Francois, A., Robinson, T., Neant, F., Matuchansky, C., 2005. Review article: bifidobacteria as probiotic agents- physiological effects and clinical benefits. Aliment. Pharmacol. Ther. 22, 495-512.

Qing, Q., Yang, B., Wyman, C.E., 2010. Xylooligomers are strong inhibitors of cellulose hydrolysis by enzymes. Bioresour. Technol. 101, 9624-9630.

Rantanen, H., Virkki, L., Tuomainen, P., Kabel, M., Schols, H., Tenkanen, M., 2007. Preparation of arabinoxylobiose from rye xylan using family 10 *Aspergillus aculeatus* endo-1,4-β-D-xylanase. Carbohyd. Polym. 68(2), 350-359.

Rastall, R.A., Gibson, G.R., 2002. Prebiotic oligosaccharides: evaluation of biological activities and potential future developments. Probiot. Prebiot., 107-148.

Rycroft, C.E., Jones, M.R., Gibson, G.R., Rastall, R.A., 2001. A comparative *in vitro* evaluation of the fermentation properties of prebiotic oligosaccharides. J. Appl. Microbiol. 91, 878-887.

Saha, B.C., 2003. Hemicellulose bioconversion. J. Ind. Microbiol. Biotechnol. 30, 279-291.

Sánchez, Ó.J., Cardona, C.A., 2008. Trends in biotechnological production of fuel ethanol from different feedstocks. Bioresour. Technol. 99, 5270-5295.

Scheppach, W., Luehrs, H., menzel, T., 2001. Beneficial health effects of low digestible carbohydrate consumption. Br. J. Nutr. 85, S23-S30.

Schneider, W.C., 1957. Determination of nucleic acids in tissues by pentose analysis. Methods Enzymol. 3, 680-684.

Solomon, B.D., Barnes, J.R., Halvorsen, K.E., 2007. Grain and cellulosic ethanol: history, economics, and energy policy. Biomass Bioenerg. 31, 416-425.

Sluiter, A., Hames, B., Ruiz, R., Scarlata, C., Sluiter, J., Templeton, D., 2008. Determination of ash in biomass. In: NREL Laboratory Analytical Procedure (TP-510-42622), National Renewable Energy Laboratory, Golden, Colorado.

Sluiter, A., Hames, B., Ruiz, R., Scarlata, C., Sluiter, J., Templeton, D., Crocker, D., 2010. Determination of structural carbohydrates and lignin in biomass. In: NREL Laboratory Analytical Procedure (TP-510-42618), National Renewable Energy Laboratory, Golden, Colorado.

Sluiter, A., Ruiz, R., Scarlata, J., Sluiter, J., Templeton, D., 2008. Determination of extractives in biomass. In: NREL Laboratory Analytical Procedure (TP-510-42619), National Renewable Energy Laboratory, Golden, Colorado.

Somerville, C., Bauer, S., Brininstool, G., Hamann, F.M., et al., 2004. Toward a systems approach to understanding plant cell walls. Science 306, 2206-2211.

Somerville, C., Youngs, H., Taylor, C., Davis, S.C., Long, S.P., 2010. Feedstock for lignocellulosic biofuels. Science 329, 790-792.

Sørensen, A., Teller, P.J., Hilstrom, T., Ahring, B.K., 2008. Hydrolysis of *Miscanthus* for bioethanol production using dilute acid presoaking combined with wet explosion pretreatment and enzymatic treatment. Bioresour. Technol. 99, 6602-6607.

Subramani, V., Gangwal, S.K., 2008. A review of recent literature to search for an efficient catalytic process for the conversion of syngas to ethanol. Energ. Fuel 22, 814-839.

Sullivan, Å., Nord, C.E., 2005. Probiotics and gastrointestinal diseases. J. Intern. Med. 257, 78-92.

Sun, Y., Cheng, J., 2002. Hydrolysis of lignocellulose materials for ethanol production: a review. Bioresour. Technol. 83, 1-11.

Thammasouk, k., Tandjo, D., Penner, M.H., 1997. Influence of extractives on the analysis of herbaceous biomass. J. Agri. Food Chem. 45, 437-443.

Timilsena, Y.P., Abeywickrama, C.J., Rakshit, S.K., Brosse, N., 2013. Effect of different pretreatments on delignification pattern and enzymatic hydrolysability of miscanthus, oil palm biomass and typha grass. Bioresour. Technol. 135, 82-88.

Tuomela, M., Vikman, M., Hatakka, A., Itavaara, M., 2000. Biodegradation of lignin in a compost environment: a review. Bioresourc. Technol. 72, 169-183.

Vasan, P.T., Piriya, P.S., Prabhu, D.I., Vennison, S.J., 2011. Cellulosic ethanol production by *Zymomonas mobilis* harboring an endoglucanase gene from *Enterobacter cloacae*. Bioresour. Technol. 102, 2585-2589.

Van Laere, K.M.J., Hartemink, R., Bosveld, M., Schols, H.A., Voragen, A.G.J., 2000. Fermentation of plant cell wall derived polysaccharides and their corresponding oligosaccharides by intestinal bacteria. J. Agric. Food Chem. 48, 1644-1652.

Vázquez, M.J., Alonso, J.L., Domínguez, H., Parajó, J.C., 2000. Xylooligosaccharides: manufacture and applications. Trends Food Sci. Technol. 11, 387-393.

Vázquez, M.J., Garrote, G., Alonso, J.L., Domínguez, H., Parajó , J.C., 2005. Refining of autohydrolysis liquors for manufacturing xylooligosaccharides: evaluation of operational strategies. Bioresour. Technol. 96, 889-896.

Vázquez, M.J., Alonso, J.L., Domínguez, H., Parajó, J.C., 2007. Production and refining of soluble products from *Eucalyptus globulus* glucuronoxylan. Collect. Czech. Chem. Commun. 72 (3), 307-320.

Vegas, R., Alonso, J.L., Domínguez, H., Parajó, J.C., 2005. Manufacture and refining of oligosaccharides from industrial solid wastes. Ind. Eng. Chem. Res. 44,614-620.

Vegas, R., Luque, S., Alvarez, J.R., Alonso, J.L., Domínguez, H., Parajó, J.C., 2006. Membrane-assisted processing of xylooligosaccharide-containing liquors. J. Agri. Food Chem. 54, 5430-5436.

Wallace, T.C., Guarner, F., Madsen, K., Cabana, M.D., Gibson, G., Hentges, E., Sanders, M.E., 2011. Human gut microbiota and its relationship to health and disease. Nutr. Rev. 69(7), 392-403.

Wang, J., Sun, B., Cao, Y., Wang, C., 2010. *In vitro* fermentation of xylooligosaccharides from wheat bran insoluble dietary fiber by Bifidobacteria. Carbohydr. Polym. 82, 419-423.

Wyman, C.E., Dale, B.E., Elander, R.T., Holtzapple, M., Ladisch, M.R., Lee, Y.Y., 2005. Coordinated development of leading biomass pretreatment technologies. Bioresourc. Technol. 96, 1959-1966.

Wyman, C.E., 2007. What is (and is not) vital to advancing cellulosic ethanol. Trends Biotechnol. 25, 153-157.

Yang, C.H., Yang, S.F., Liu, W.H., 2007. Production of xylooligosaccharides from xylans by extracellular xylanase from *Thermobifida fusca*. J. Agric. Food Chem. 55, 3955-3959.

Zhou, W., Hao, Z.Q., Xu, Y., Schutter, H.B., 2009. Cellulose hydrolysis in evolving substrate morphologies II: numerical results and analysis. Bitechnol. Bioeng. 104, 275-289.

Zhu, Y., Kim, T.H., Lee, Y.Y., Chen, R., Elander, R.T., 2006. Enzymatic production of xylooligosaccharides from corn stover and corn cobs treated with aqueous ammonia. Appl. Biochem. Biotech. 129-132, 586-598.

Zhu, J.Y., Pan, X., Ronald, S., Zalesny, J., 2010. Pretreatment of woody biomass for biofuel production: energy efficiency, technologies, and recalcitrance. Appl. Microbiol. Biotechnol. 87, 847-857.